UNIVERSITÀ DEGLI STUDI DI PADOVA

UNIVERSITA' DEGLI STUDI DI PADOVA

Dipartimento di Ingegneria Industriale DII

Corso di Laurea Magistrale in Ingegneria dell'Energia Elettrica

Design of Renewable Energy Systems for ECUSTA's University Campus in Addis Ababa

Relatore: Prof. Arturo Lorenzoni

Correlatore: Prof. Piergiorgio Sonato

Andrea Corrà 1105110

Anno Accademico 2016/2017

ABSTRACT

In this thesis, three installations powered by renewable energy sources are proposed for the Campus of the Ethiopian Catholic University St Thomas Aquinas. A forced circulation solar thermal system is designed to produce hot water for the showers of the dormitory; a drain-back configuration is suggested to protect the system from overheating. A photovoltaic system with electrochemical storage is designed, to protect from power outages the sensible equipment of the International School of Perinatal Medicine for Africa. A natural circulation solar thermal system is proposed to produce hot water for the Medical Center. It is then evaluated the feasibility of the installation of a pump-as-turbine for energy recovery from the water distribution system of the Campus.

CONTENTS

LIST OF FIGURES

LIST OF TABLES

1 INTRODUCTION

1.1 ENERGY IN ETHIOPIA

The estimated population of Ethiopia is 103 million of people (2017, [1]), whose 80% is represented by rural households. With a primary energy demand of 45 Mtoe per year, energy use per capita in Ethiopia is less than one-third of the world average. The prevalent primary energy source is by far represented by biomass, which covers the 89% of the total energy demand. Biomass is traditionally used for cooking. It is used by almost the totality of the rural population, and by the 80% of the urban population; the average fuel wood consumption per day is 1kg per capita[1]. The balance of the energy demand is mainly met by fossil fuel consumption (8%) and hydropower, which is the main source exploited to produce electricity. Geothermal and wind have neglectable influence on the balance.

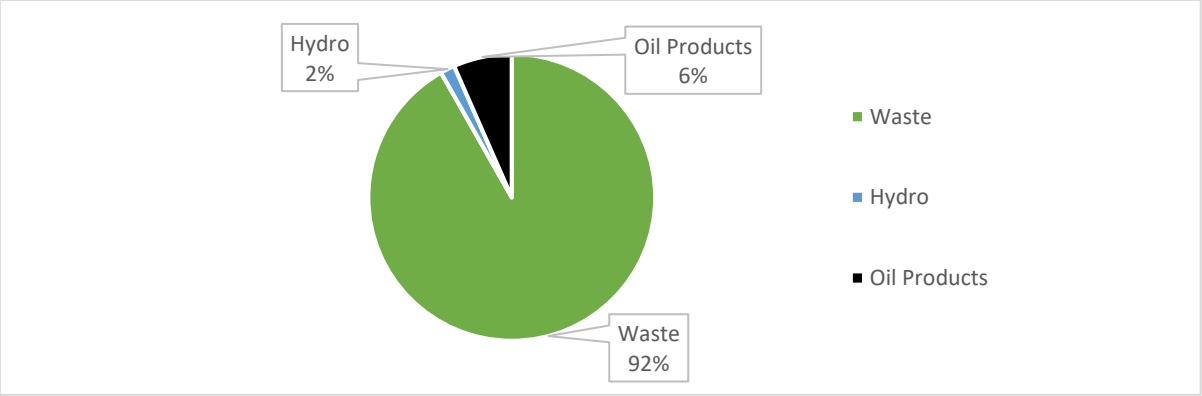

Figure 1 *Primary energy consumption in Ethiopia. Elaboration from IEA-Statistics, 2014*

Ethiopia has the world's second largest population without access to electricity, with 70 million people in rural areas lacking access to it. The electrification rate of the country (23% in 2012) is planned to be extended up to 60% by 2040, by means of combined grid-extension programs and off-grid solutions[1].

Currently, electricity in Ethiopia is highly subsidized: the average cost of generation is about 110 $/MWh, while the end-use price for commercial users is the equivalent of 30 $/MWh. Electricity consumption is 0,07 MWh per capita [2]. The distribution grid is characterized by frequent power outages, whose duration is estimated to be almost 600 hours per year; power outages are mainly due to planned load shedding, as the actual generation capacity is not enough to meet the fast-increasing demand of electric energy.

1.1.1 Actual and planned electric energy production

Electric power generation mainly relies on hydropower plants; the balance is mainly met by wind farms, thermoelectric plants, cogeneration plants and geothermal. Currently 12 hydropower plants are operating in the country, for a total capacity of 1900 MW, which represents the 76% of the total electric power generation capacity installed in Ethiopia. Three wind farms are found in the country: two of them are in Adama area, 99 km south-east from Addis Ababa, and one is in the northern side of the country in Ashegoda; a total capacity of 320 MW is installed, generating 1091 GWh per year. Being the dry season also a windy season, wind power represents

a valid complement to hydropower in Ethiopia [2]. Three cogeneration plants, for a total capacity of 59 MW, are installed in correspondence of sugar cane processing factories.

A geothermal power plant, Aluto Langano, is located in correspondence of the Aluto volcanic complex, about 200 km south-east of Addis Ababa. The construction of the plant began on 1997; two generation units each rated about 4 MW gross are installed in the plant. The plant has been inoperative for several years for technical issues, then was successfully re-commissioned in 2007 [3].

Source	Capacity installed [MW]	Energy Production [GWh]
Hydro	1939	7916
Wind	324	1091
Geothermal	7,3	19
Oil	112,3	9
total	**2441,3**	**9383**

Table 1 *Electricity production in Ethiopia. Sources: IEA-Statistics, 2014;* [2]

The expansion of solar energy has lagged behind hydro and wind energy. Currently no large solar plants result to be operative. More than for large power generating plants, solar energy has importance in the supply of off-grid communities; it is reported in [3] that more than 2 million Solar Home Systems have been distributed during the period 2010-2015.

As per the intentions of the National Planning Commission[3], the following order of priority will be given to exploitation of Renewable Resources: hydropower projects, geothermal energy, wind power, solar energy. Biomass and diesel generators will be used as standby energy sources.
Several large hydropower projects are currently under construction; the completion of this projects will increase the installed hydroelectric capacity from 1940 MW to 8124 MW. Among these projects, it is worth to note the Grand Ethiopian Renaissance Dam along the Blue Nile, whose estimated production is 15000 GWh per year. Four geothermal projects have been committed, for a total capacity of 605 MW; many other geothermal projects are planned, for a total capacity of 4,256 GW. Regarding wind energy, as per a medium-term plan of the Ministry of Water, Irrigation and Energy a new capacity of 1750 MW is planned to be installed. It is reported in the same source [2] that three photovoltaic plant are planned to be constructed, for a total capacity of 300 MW.

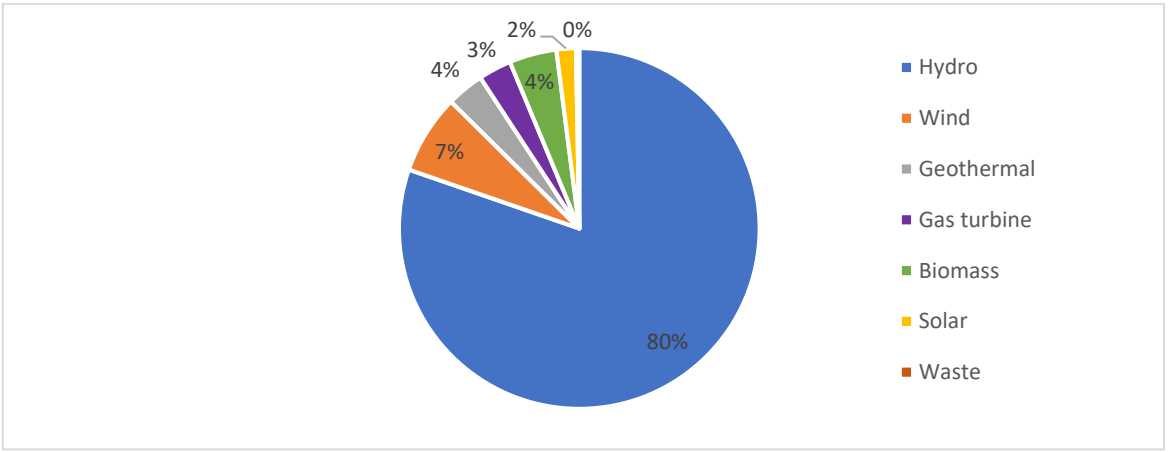

Figure 2 *Planned generation mix capacities. Short term plan, data eleborated from* [2]

1.2 A NEW CAMPUS FOR ETHIOPIAN CATHOLIC UNIVERSITY OF ST. THOMAS AQUINAS

The establishment of the Catholic University of Ethiopia dates back to 2005, when the Federal Democratic Republic of Ethiopia and the Catholic Bishops Conference of Ethiopia signed a formal agreement for the institution of a University open to students and teachers of all backgrounds and beliefs. In 2006, the University was officially named Ethiopian Catholic University of St. Thomas Aquinas (ECUSTA). At the time of the study, Ecusta was hosted in the Catholic Cathedral Compound in Addis Ababa, where courses of Medical Laboratory Technology, Social Word, Clinical Social Work and Information Technology are offered.

The Ethiopian Government granted land to the Catholic Bishop Conference of Ethiopia for the construction of a Campus for the University. The site is located in South-West of the Addis Ababa urban area, in proximity of the sub-center of Lebu. A new road connection will link the area of the Campus to the Ring Road, one of the major traffic way of the Capital, leading to the city center and to Bole International Airport. The area consists of sixty hectares of land, characterized by a nearly rectangular shape whose longest edge runs from east to west. The site is characterized by a slope from north to south, for a total elevation difference of 74 m from the northern to the southern end.

Figure 3 *Rendering of the Campus. View from the central core looking West. From* [4]

According to the Master Plan, the construction of ECUSTA's Campus is divided into four phases. During the first phase two faculties will be built: the School of Medicine and Health Science and the School of Technology; in the second construction phase, the extension of the School of Technology and the School of Social Science will be established; the School of Agriculture and Agroprocessing and the School of Education are planned for the third construction phase, while the schools of Natural and Computational Science will be established in the fourth phase.

At the time of the study, the first part of the first phase was under construction; Figure 4 represents a satellite view dated February 2017 where the five buildings which were nearly completed are represented. The two central buildings in the picture represent the didactical structures of the School of Technology; the structure below in the right is the dormitory, to which Chapter 2 of this work is dedicated; below the dormitory, a multi-purpose hall; on the left corner of the picture, a Maternal and Infant Care Center (ISPEMA), to which Chapter 3 and Chapter 4 are dedicated.

Figure 4 *Satellite view of the Campus at the time of the study*

1.3 THE INTERNATIONAL SCHOOL OF PERINATAL MEDICINE FOR AFRICA

The picture below represents the headquarter of the International School of Perinatal Medicine for Africa. Within the building, both a Maternal-Infant Care Medical Center and a School of Perinatal Medicine are located. Chapter 3 is dedicated to the design of a PV solution to increase the reliability of the electrical supply for the building.

Picture 1 *View of the southern facade of ISPEMA Center*

The realization of the building represented in the picture is a result of the collaboration between ECUSTA and Matres Mundi International, with the support of the major societies of Perinatology. Matres Mundi is an international organization based in Barcelona, specialized in Maternal and Infant Health; it developed the Life for Africa Program, an international cooperation program, supported by the participation of the major

international societies of Perinatal Medicine, whose aim is to improve maternal and child health in sub-Saharan Africa. To reach the goal of the Program, Matres Mundi intends to provide formal education and training to reproductive health professionals. For this purpose, a Maternal and Infant Special Medical Center, and an International School of Perinatal Medicine have been established, and are physically located in the building represented in the picture above.
The first floor of the building is the Maternity Hospital section, which provides services in Obstetrics, Pediatrics, Gynecology, Internal Medicine and a Nutritional Science. On the ground floor, the School of Perinatal Medicine is settled, which is intended to become a reference for the whole Africa. The International School of Perinatal Medicine for Africa (ISPEMA), as association, was founded in Barcelona in December 2012.

The main objectives of ISPEMA Center are[5]:

- to be a Center of Training in Maternal and Infant Health, representing a reference point for the whole continent, with specialization in medico-chirurgical problems specific to Africa, such as malaria, obstetric fistulae, etc.;
- to assist the neighboring population with clinical services;
- to do healthcare research for the whole continent, realizing a "health map of Africa";
- to offer a residence for teaching staff and for scholars from the whole Africa.

The education of health professionals would shorten the way to reach the main medium/long-term objective, meaning the reduction of the percentage of maternal, perinatal and infant mortality in Africa.

1.4 PURPOSE OF THE STUDY

The purpose of this work is to develop several proposals for the integration of Renewable Energy Systems in Ecusta's Campus. The analyses are focused on two buildings located in the Campus' area: the Dormitory and the Maternal and Infant Medical Center. Regarding the Dormitory of the Campus, a solar thermal system to supply hot water for showering is designed. For what concerns the Medical Center, a proposal for a photovoltaic with electrochemical storage system is developed, to guarantee continuous power supply in the event of power failure from the main grid, and to reduce the hours of operation of the diesel generator; a solar thermal system is then designed, to provide hot water to the building without the need to use electrical water heaters. Finally, the feasibility of the installation of a Pump-as-Turbine in the water distribution system of the Campus is analyzed. The analysis carried on in this work are intended to provide a basis for future executive design of the renewable energy powered plans of the Campus.

2 DESIGN OF A SOLAR THERMAL PLANT FOR THE DORMITORY OF THE CAMPUS

2.1 INTRODUCTION TO THE CHAPTER

2.1.1 The building

The first phase of construction of the Campus, beside didactical structures, foresees also a dormitory to provide accommodation to the students. The construction of the building started during year 2012; it is supposed to become operative by the end of year 2017.

The building consists of two floors (G+1). In the ground floor there are different facilities, such as: a gym (36,88 m^2), TV room (59,76 m^2), Internet point (14.44 m^2), a laundry (23,77 m^2), 12 bedrooms (varying from 18 to 21 m^2), a study hall (40 m^2), an office (13,43 m^2), proctor bedroom, janitor room, common toilets and showers. The first floor is mainly dedicated to the bedrooms (22 rooms); there are also washrooms, common toilets and showers.

The solar thermal system should provide hot water to the showers located both at the first and at the ground floor; we find 27+1 showers in the dorm, distributed as follows: 16 at the first floor, equally divided at the western and eastern ends of the floor; 11 showers at the ground floor, located at the eastern end. One shower is located within the proctor bedroom at the ground floor; it will be supplied by electrical boiler and is not part of the study.

2.1.2 Local experience with solar thermal installations

The most common solar thermal system configuration encountered in Addis was passive water heaters coupled with evacuated tubes collectors. No installations adopting flat plate collectors have been recognized. A local professional reported that flat plate technology, even if constructively simpler, has a higher price in the local market, being this kind of collector usually imported from Europe [1]. A reason for the high level of penetration of evacuated tubes collectors (ETC) in local solar thermal market could be found in the strong economic relationships between China and Ethiopia. Beside the market shrank of the last four years, whit a decline rate of 17%, China still detain a percentage above the 70% of the globally installed capacity of solar thermal systems[6].

Considering that the ratio between evacuated tubes and flat plate collectors in Chinese installations is greater than 12:1%[6], the great availability of ETC collectors in the Chinese market led to the adoption of this technology, even though, from a technical point of view, flat pate collectors represents a valuable choice considering the weather of the area.

It has been reported from a local company that several closed loop forced-circulation systems have been installed in Addis and are currently running since approximatively 5 years without having encountered major operational issues.

2.1.3 Climatic features of the site

The climatic features of the site have significant impact in the design of a solar thermal system. Typical values of air temperature and irradiance levels for the site are hereby presented. Maximum values of air temperature of approximatively 25°C are found in February at noon, while usual mean temperatures drop below 10°C.

Jan	Feb	Mar	Apr	Maj	Jun	Jul	Aug	Sept	Oct	Nov	Dec
15°C	16°C	17,0°C	17,5°C	17,5°C	16,0°C	15,5°C	15,5°C	15,5°C	15,5°C	14,5°C	14,0°C

Table 2 *Monthly average air temperature for Addis Ababa's area. Data from https://www.ncdc.noaa.gov/cdo-web/orders*

For what concerns the design of a solar thermal system, it is of primary importance to determine the probability of having freezing temperatures in the site. Various strategies are adopted to protect solar systems from damages occurring by frozen water in the piping of the system, such as use of water-glycol solution in the primary circuit, drainage of the fluid from collectors, night recirculation of hot water from the storage. To avoid increased complexity of the system it is auspicial not to have a need for frost protection.

The analysis of weather data about Addis Ababa area shows that since 1990 no temperatures below 0°C have been registered. The minimum temperature registered in the period taken into consideration is 0,6 °C in the month of November 1990. Hence, frost protection is considered unnecessary.

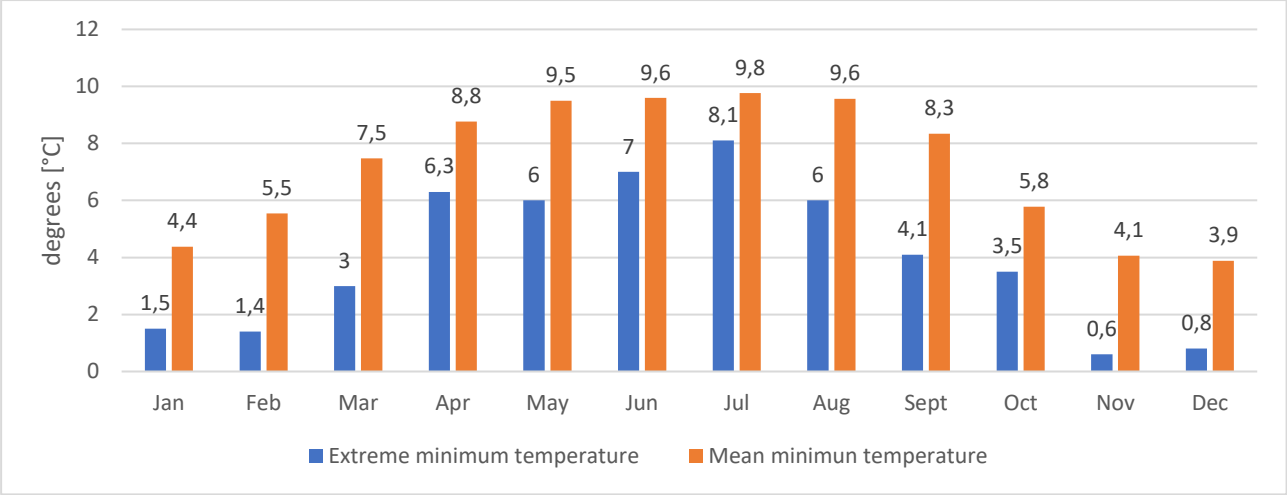

Table 3 *Extreme minimum and Monthly mean minimum temperature in Addis Ababa. Data range: Jan 1990 - Jan 2015. Data from https://www.ncdc.noaa.gov/cdo-web/orders*

On the other side, overheating prevention is considered of primary relevance because of the high radiation characteristic of the latitude. Figure 5 gives a comparison between irradiation values for Addis' area and a southern European locality, Padua. The values reported refer to an optimally[1] inclined fixed surface.

[1] 14° for Addis, 36° for Padua. Values from PV-GIS.

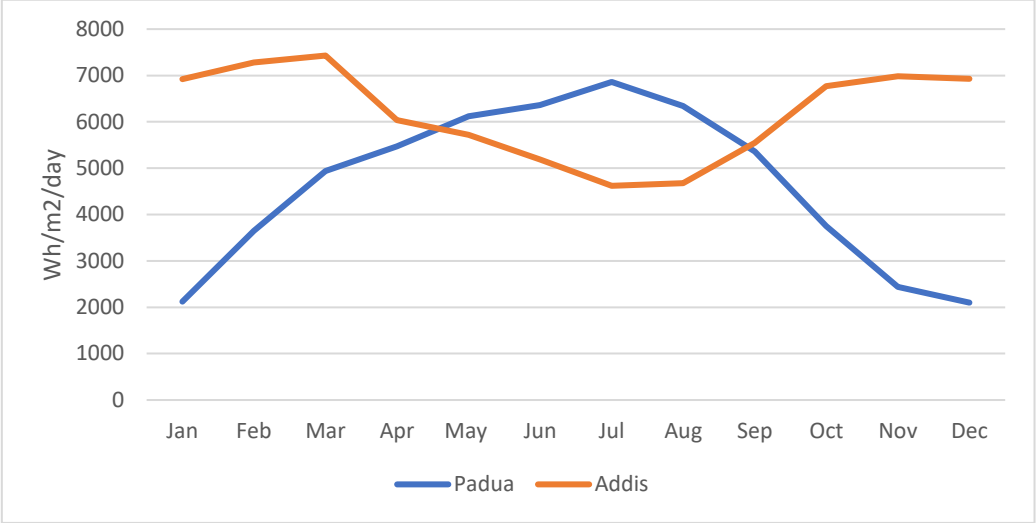

Figure 5 *Comparison between monthly irradiation levels for Addis and Padua*

The yearly average irradiance level in Addis is 6170 $Wh\,/\,m^2day$, while for Padua is 4630 $Wh\,/\,m^2day$. It is underlined how irradiance levels for Addis are much more constant during the year. As it will be shown in further sections, solar thermal systems can be designed to stand occasional stagnation. In the case of Addis, high levels of radiation encountered in most part of the year can lead to frequent events of stagnation, that might damage the system even if it has been properly designed. For this reason, considerable attention is given to overheating prevention in the design of the system.

2.2 BRIEF REVIEW OF SOLAR THERMAL TECHNOLOGIES

In this section an overview of the most common solar systems for hot water production is presented; the main typologies of solar thermal collectors are described, and some important topics regarding solar thermal installations are introduced. The purpose of this section is to give to the reader some basic notions on solar thermal systems to facilitate the comprehension of further sections.

2.2.1 System typologies

The basic elements in solar water heating systems (solar collectors, storage tank, heat exchangers, pump and relative controller, piping and valves, expansion vessels) can be arranged in different configurations to obtain the most appropriate system with respect to load requirements, climatic features of the site, physical and economic constraints. Different system typologies have been developed.

A first classification is between **active** and **passive** systems, where in passive systems water circulates in the collectors by natural convection, while active (or forced circulation) systems require a pump to circulate the fluid within the collectors. Active and passive systems can either be **direct** or **indirect** systems, meaning systems where potable water is directly circulated through the collector or systems that adopt heat exchangers to transfer heat from the primary (collectors') loop and the utilization loop.

2.2.1.1 Direct and Indirect Systems

In a direct circulation system, potable water is directly headed through the collector. Water from the bottom of the storage is circulated through the collector by the pump, and delivered to the storage in such a way not to disturb stratification. An auxiliary system provides further heating if needed. Direct circulation systems are attractive because they offer a considerable simplification of the system; in addition, the efficiency of the system is higher as no heat exchanger between primary and secondary circuits is present.

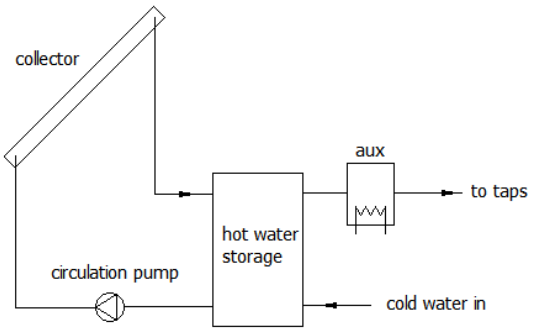

Figure 6 *Schematic diagram of a direct circulation system*

The adoption of a direct circulation system is subjected to the quality of the water circulating in the system. Unsuitable water conditions can lead to scaling issues that compromise the functionality of the system. A concern regarding direct circulation systems is the potential to deliver too high temperatures at the distribution point in case of failure of the tempering valve downstream the auxiliary heater.

2.2.1.2 Thermosyphon systems

In **passive** water heaters**,** the fluid inside the collector circulates by natural convection. Whenever solar energy adds energy to the fluid, varying its temperature, a density difference is established. The driving force for the fluid is the pressure difference established by such density difference. Thus, hot water rises towards the tank, which is located above the collector. Such kind of system, also referred as thermosyphon, is represented in the picture below. Thermosyphon systems can either be closed-coupled (schematic on the left), where a horizontal tank is placed just above the collector, or with a larger storage located in an upper position than the collectors (schematic on the left), whose inlet can be supplied by multiple collectors.

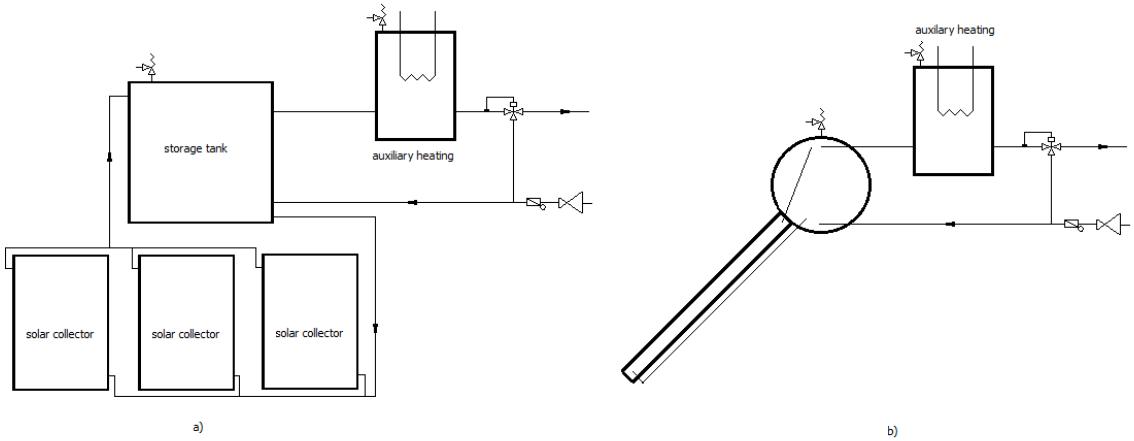

Figure 7 *Schematic configurations of direct thermosyphon systems: with separate storage (left, frontal view) and closed-coupled (right, section)*

Thermosyphon systems can be attractive for their economical convenience and simple configuration; the natural phenomena of thermosyphon effect is exploited to circulate water within them, instead of adopting circulating pumps.

The major drawback of these systems is the requirement for the storage tank to be located above the collectors; therefore, the possibility to install such systems, in the case of need for a large storage, depends on the structural features of the building, in particular on the possibility to install a big tank on the top of collectors.

Scaling can be particularly detrimental to these systems as it both increases the thermal resistance (leading to lower heat transfer rates) and the hydraulic resistance, reducing the fluid circulation. It is therefore necessary to evaluate the quality of water that circulates in the collector's loop. If quality of water is good enough, these systems can be of direct type, meaning potable water is directly circulated in the collectors; simplicity and efficiency of the system is then at maximum. Alternatively, a tank-in-tank storage configuration is adopted in indirect systems, where treated water is circulated in the collectors and in the inner jacket of the tank, while potable water surrounds the inner mantel.

During the night reverse circulation can happen: collector's surface is colder than the fluid within it, heat is wasted to the surroundings; density of water increases, establishing pressure differences and leading further hot water from the top of the storage to flow to collector's surface. It has been experimented [7] that a height difference of at least 30 cm from the bottom of the tank to the top of collectors is sufficient to prevent night reverse circulation. Adopting check-valves to block reverse flow is not recommended as valves introduce resistance to fluid circulation, decreasing the efficiency of the system.

2.2.1.3 Closed-loop pressurized system

In a closed-loop pressurized systems, the heat transfer fluid is pumped through the primary loop by a circulation pump; the power required by the pump is just that needed to compensate hydraulic losses.

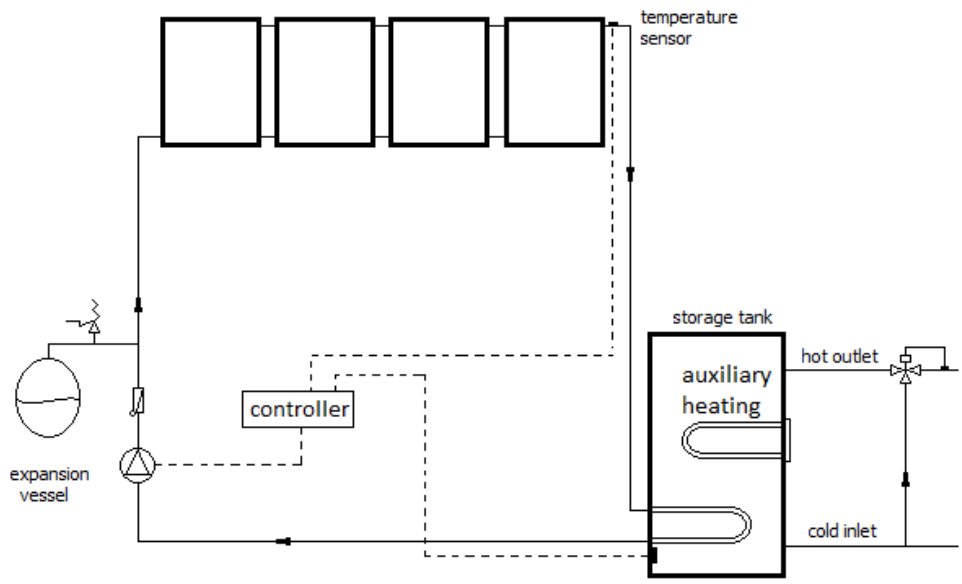

Figure 8 *Schematic diagram of a closed-loop pressurized system*

The pump is activated by a controller which receives information about the temperature of the fluid at the top of the collectors and at the bottom of the storage from temperature sensors. A usual control strategy consists of activating the pump when the temperature difference between the fluid in the collectors and the bottom of the storage is above a fixed value. Pumps are then switched off either when this temperature difference drops below a certain value (irradiance is low), or when a maximum temperature in the storage tank is reached.

The heat transfer fluid is usually a water-glycol mixture to prevent freezing of the liquid within the collectors; this is not necessary if temperatures below 0° do not occur in the site, as it is the case for Ecusta's Campus.

The controller stops the circulation pump when the maximum heat storage capacity has been reached (meaning a maximum temperature has been reached in the tank). These situations can lead to stagnation of the system if radiation is further available. Closed-loop pressurized systems handle stagnation by means of oversized expansion vessels that accommodates the fluid in its expanded state. In addition, heat dumps can be installed to facilitate the condensation of the vapor. Beside this precautions, good emptying behavior of collectors and collectors array is of primary importance not to encounter too high pressure and temperature that put the systems under heavy stress.

2.2.1.4 Drain-back systems

Drain-back systems (DBS) were developed in the Netherlands in the 1980's because of governmental regulations regarding drinking water quality that restricted the use of antifreeze solutions in solar thermal systems[8]. These systems are spread in different areas of the world with different degrees of popularity. It is estimated that in the USA they represent the twenty percent of solar thermal installations; in France and Spain drain-back design covers almost 15% of the local market, whereas in Portugal and Italy about 10% [9].

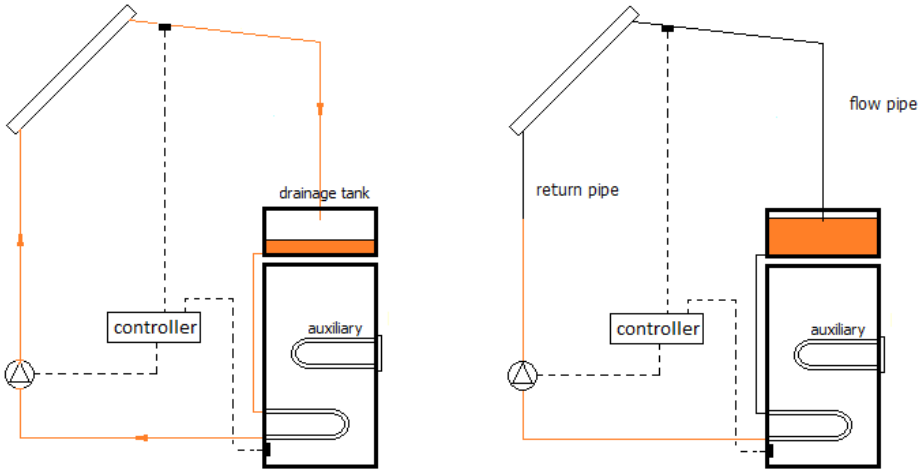

Figure 9 *Operating principle of a drain-back system. System in operation on the left; system not in operation on the right.*

A major difference regarding closed-loop pressurized systems is that drain-back systems do not present pressurized circuits, and air is present in the primary circuit; these systems are closed-loop, as air venting must be avoided to protect the system from corrosion and bacterial growth. The air within the system is always the same since commissioning, and its percentage of oxygen is tied to the piping [8]. The crucial point in drain-back configurations is the automatic drainage of the fluid from the collectors when the pumps stop circulating. This makes the system to be inherently safe and protected against both overheating and freezing of the fluid. To have a proper drainage, the pumps must allow a backflow; no check-valves must be installed in the hydraulic circuit, and piping must be properly sloped.

The operation of a drain-back system can be divided into four different phases[10], which are encountered with the following order: system not in operation; filling of the collectors; operating mode; draining of the collectors. When the system is not operating (the pumps are switched off) collectors are filled with air. The thermal fluid is gathered in the drainage tank, which is positioned above the heat storage tank. All the parts of the system located above the level of water within the drainage tank are filled with air. The pumps are positioned so that they are constantly in contact with thermal fluid. The filling of the collectors begins when the controller switches on the pumps; this phase begins when a pre-set temperature difference between collector's plates and water in the bottom of the tank is recognized by the controller. Values of the duration of the filling phase can be in the order of less than a minute for small experimental setup up to 10 minutes for much larger systems[8]. During the operation mode, thermal energy is collected by the thermal fluid and delivered to the water in the storage tank through a coil within it (in the case of an indirect configuration), as it happens for closed-loop pressurized systems. When the pumps are switched off by the controller, or in consequence of a power failure, the fluid automatically drains from the collectors. This phase lasts up to 5 minutes for large installations.

A recent (2014) investigation on the filling and draining processes of the drain back system clarified the functioning of this kind of installations: it has been shown as for such systems a siphon effect is crucial both for filling and draining processes[10].

During the experimental investigation, static pressure was measured by manometers behind the pumps and at the uppermost point of the hydraulic circuit. After the fluid reached the top of the hydraulic circuit during the filling phase, the establishment of a syphon was shown by negative values of hydrostatic pressure at the top of the circuit. By application of Bernoulli's equation, it is explained that the reduction of pressure at the top is proportional to the height from the air gap in the drain-back reservoir to the top of the circuit. The appearance of a syphon allows to continue the operation of the circuit with a single pump, as it cancels out the initial lifting

head. It has been shown that a reverse flow occurs during the draining phase; the reason for this reverse flow is found in the difference of hydrostatic pressure in flow and return pipe. The syphon is crucial in this phase: water falling in the return pipe pulls up the water in the flow pipe; the part of the solar loop above the bottom of the air gap in the draining reservoir can be thought as a syphon, while the lowest part of the circuit as communicating vessels.

Beside its simple configuration, there is the need for a proper installation, as little mistakes in the installation phase could endanger the functioning of the system. This implies the need for instructing local technicians about the proper functioning of the system.

2.2.2 Solar collector typologies

Different typologies of collectors are available in the market. The choice of the most suitable collector for a system mainly depends on the climatic features of the site and the temperature of hot water required by the user. In this section the most common typologies adopted for hot water production for domestic use are described.

2.2.2.1 Flat Plate collectors

Flat plate collectors are the simplest kind of thermal collector; this typology represents the most common one for space heating and hot water production in Europe[11]. Flat-plate collectors use both beam and diffuse solar radiation. The risers can have either a harp or meander shape. Flat plate collectors essentially consist of:

- glazing, or covering: one or more sheets of glass or other material, whose transmittance at typical wavelengths of solar radiation must be as high as possible
- fluid conduits, or fins, or risers: copper tubes that represent the conduits for the fluid of the primary circuit;
- Absorber plate: usually a flat sheet of copper, where the risers are welded;
- Headers, or manifolds: to admit and discharge the fluid;
- Insulation: to minimize heat losses from the back and sides of the collector;
- Collector box, or casing: to envelope the aforementioned components and protect them from the environment.

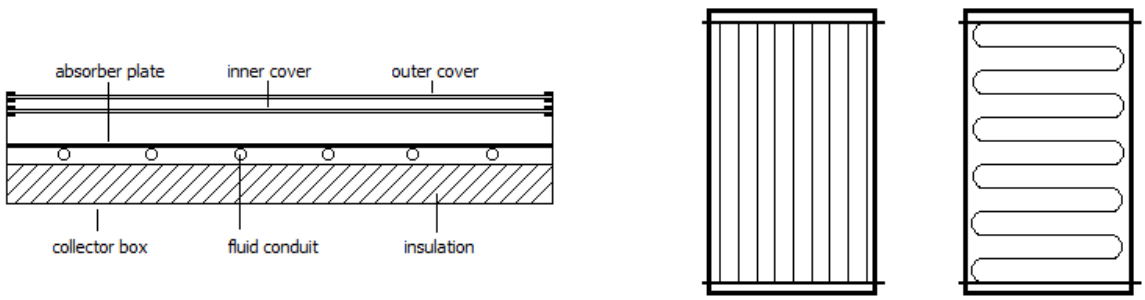

Figure 10 *Schematic representation of a flat plate collector. From left to right: frontal view; harp risers collector; meander absorber collector*

2.2.2.2 Evacuated tubes collector

The benefits of conventional flat plate collectors are greatly reduced when weather conditions are those of cold, cloudy or windy days[12].

These collectors present a sealed copper pipe inside a vacuum-sealed tube; a high efficient heat transfer is obtained exploiting a liquid–vapor phase change process. The heat pipe contains a small amount of fluid that undergoes an evaporating-condensing cycle: solar heat evaporates the liquid, and the vapor releases its latent heat in the heat pipe condenser; the condensed fluid returns to the bottom of the pipe, and the process is repeated. Heat pipes offer inherent protection against freezing and overheating, as no evaporation nor condensation is possible above the phase-change temperature[12].

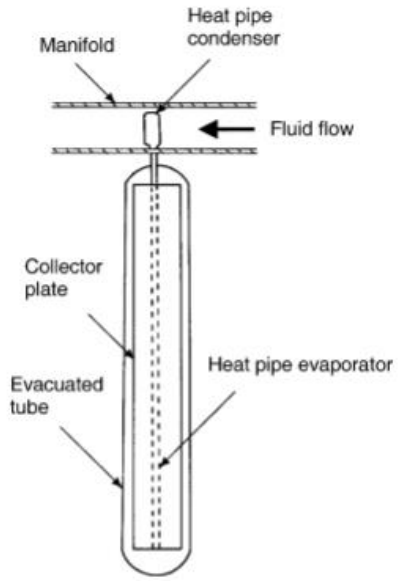

Figure 11 *Representation of a heat pipe evacuated tube. Adapted from* [12].

The advantages of this design are that here is only one seal, at one end of the tube; the fin (collector plate in the picture) and heat pipe are free to expand inside the evacuated space. On the other hand, this typology is characterized by a higher cost compared to flat plate collators.

2.2.3 Overheating prevention and stagnation handling

Among the causes that can lead to increased repairing and maintenance requirements for solar thermal systems, there is the undesired condition of *stagnation*. Stagnation occurs when the flow in the collector loop is interrupted, while solar irradiance is still available: energy is further absorbed by the collector, and its temperature rises until the absorbed radiation equals the energy given to the surroundings.

2.2.3.1 The dynamic of stagnation

The sequence of events encountered during stagnation can be divided into five different phases[13]:

1. Expansion of the fluid
   The fluid inside the collector gains energy and the evaporation process begins in the upper part of the collector. During this phase, there is a modest increment of the system pressure.
2. Pushing the fluid out of the collector

The saturated steam pushes back the fluid to the expansion vessel; this phase goes on until the steam finds a continuous path from the inlet to the outlet of the collector. High thermal and pressure stress on system components is found in this phase. Residual liquid remains in the collector.

3. Emptying of the collectors by boiling
   The residual liquid in the collectors evaporates. Steam penetrates further into the system and the energy transported via steam condensates at cold sections within the solar loop. At the end of this phase, steam volume and system pressure reach their maximum values.
4. Emptying of collectors by superheated steam
   The collector becomes increasingly dry; the steam volume further decreases and the solar loop is slowly filled with liquid although there is still solar irradiation. This phase can take a few hours on cloudless days and ends when irradiance is on decline.
5. Refilling of collector.

2.2.3.2 Damages due to stagnation

If a system which has been properly designed might withstand *occasional* events of stagnation without being damaged, the situation might be different in case of frequent and prolonged period of stagnation; considering that high levels of radiation in Addis Ababa are typical for the major part of the year, enhanced protection against stagnation must be provided to thermal systems installed in this area.

As it is outlined in different references ([14], [15]), stagnation can have detrimental effects on the thermal plant both at collector and system levels. Damages can occur to:

- the rubber seals, or other non-metallic components (e.g. expansion vessel's membrane): prolonged exposure to high temperature can imply the deterioration of these components and leaks can appear in the system;
- the absorber coating, which resists up to a specific temperature; above that temperature the coating starts to degenerate[14];
- absorber mountings and the absorber structure itself: they might be subjected to excessive stresses due to thermal expansion.

Furthermore, because of evaporation of the thermal fluid, pressure in the primary loop can reach values above the limit of pressure-release safety valves, resulting in venting of vapor to the atmosphere. When the system cool down, the lack of heat transfer fluid can lead to further overheating issues, or pumping and circulation problems[15]. In addition, there is the need to refill the loss of fluid, hence increased maintenance costs are encountered.

Different strategies are adopted to prevent stagnation, and overheating is handled in different ways depending on the typology of the system. Two strategies can be identified: on one hand, stagnation and evaporation of the fluid can be accepted as a normal operational incident; the other strategy consists in preventing stagnation as much as possible.

2.2.3.3 Stagnation handling and overheating prevention strategies

Accepting stagnation as a normal operational incident, and consequently accepting the evaporation of the fluid in the primary loop, implies that care must be taken in the planning and design phases to prevent collectors and solar loop components from exposure to high temperatures and pressures. In other words, stagnation handling capabilities must be provided to the system. In the case of a closed-loop indirect system, evaporation of the fluid is usually handled with oversized expansion vessels, so that fluid expansion is accommodated as temperature increases. It is also necessary to reduce the steam volume and the maximum pressure in the primary loop during stagnation with good emptying behavior of the collectors. In case of stagnation, overheated fluid starts boiling

in the collector and, while expanding, pushes back the fluid both to the feeding and return leg. Good emptying behavior is provided when the fluid is easily pushed back by steam, without being trapped in collector's piping and tubes.

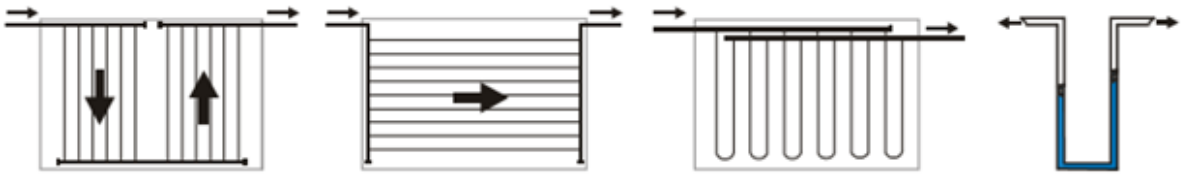

Figure 12 *Collector circuits with poor emptying behavior. From IEA SHC - Task 26 - Solar combisystems*

In the case of flat plate collectors, connections to be avoided are such those in figures 2a and 2b; in the case of evacuated tubes, connections to be avoided are those where flow and return lines are at the top of collector.

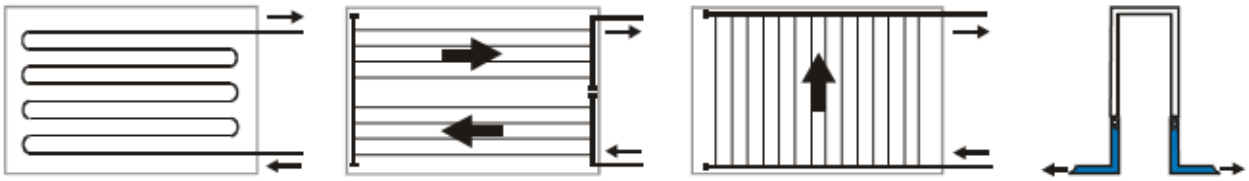

Figure 13 *Collector circuits with good emptying behavior. From IEA SHC - Task 26 - Solar combisystems*

Figure 8 represents collector's circuits with good emptying behavior, where steam can easily push back the residual fluid.

If evaporation of the fluid in the primary circuit must to be avoided, then overheating prevention measures must be taken. Overheating prevention implies that the maximum temperature the solar fluid can reach is limited to a temperature quite below the corresponding evaporation temperature at the maximum system pressure that is determined by the safety valve.

Another approach to overheating prevention consists in finding a way to keep the fluid circulating when the maximum heat storage capacity of the tank has been reach. Usual control strategies would stop the circulator not to collect heat anymore. Thermal energy cannot further be given to the tank, but could be deviated to another load. Heat dumps are a possibility, and several systems have been proposed. As an instance, Apricus Solar adopts a scheme where a fin and tube heat dissipater is connected downstream to the collectors; an electrically powered controller and a solenoid valve operated by the controller deviates the flow to the heat waster when excessive temperatures of the fluid are recognized. Heat is given to the ambient, and thermal fluid's temperature drops sufficiently low not to give further energy to the tank.

Another system which has been recently patented[16] is represented in the schematic below. In this system, a solar DC pump operated by a PV collector guarantees the circulation of the fluid in the collectors even in case of a power failure of the main supply; the flow is directed to a heat waster by a thermostatic valve, and the flow rate (hence the heat given to the ambient) is proportional to the irradiance level.

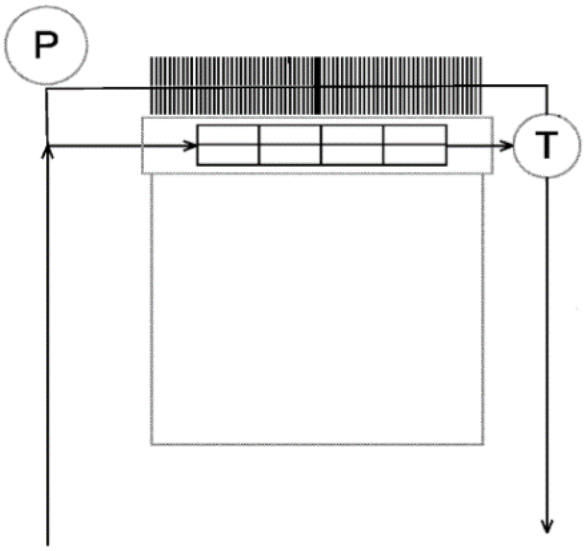

Figure 14 *Schematic representation of a recent proposal for overheating prevention. From* [16]

These systems can effectively protect the system from overheating, but require more components (thermostatic diverter, additional solar pump): the complexity and the cost of the installation is augmented.

2.2.4 Other topics

2.2.4.1 Stratification in storage tanks

An important aspect regarding the efficiency of the solar thermal system is the stratification of the temperature within the heat storage tank. A high level of stratification in the storage tank enhance the performance of the system. In fact, water in the bottom of a stratified tank is at lower temperature compared to a fully mixed tank; sudden water thus enters the collector at a lower temperature, the efficiency of the collector is higher, and more energy gained passing through it. The degree of stratification in a heat storage tank depends on: the design of the tank; the size, location and design of the inlet and outlet manifolds; flow rates of the entering and leaving streams.
The adoption of a low-flow rate has a positive influence on the degree of stratification in the tank.

2.2.4.2 Flow rate in the primary loop

While typical values of flow rate for pumped systems are in the range of 0,01 to 0,02 kg/m^2s, systems with considerably lower flow rates in the range of 0,002 to 0,007 kg/m^2s have been studied.
The adoption of a low flow rate can result in a net improvement in system performance[17]. From one hand, lower collectors heat removal factors must be accepted, but this negative aspect is balanced by increased stratification levels in the tank. Several other advantages are encountered with low flow systems, such as: the reduction of installation cost by the adoption of piping of smaller diameter; the reduction of operating costs thanks to lower electric energy required to operate the pump.

2.3 HOT WATER DEMAND ESTIMATION

2.3.1 Daily hot water requirements

For what concerns the volume of hot water required for every shower, the amount of 50 liters was chosen. This values is suggested in [18] and is consistent with Normative 9182. After discussion with the contractor responsible of the construction of the building, the value of temperature of 39° for the shower was chosen. This amount of water is obtained by mixing cold water at approximatively 17°C with hot water produced by the solar thermal plant and delivered at a maximum temperature of 45°C; to obtain 50 liters at 39°C, 39 liters of hot water are mixed with 11 liters of cold water.

It has been assumed a percentage of 0,4 showers per person per day for week days, while for weekends it has been assumed a percentage of 0,6 showers per person per day. Multiplying these percentages by the maximum number of students residing in the dorm, we obtain a maximum hot water demand of 2,1 $m^3$of hot water at 45°C for a week day, and a value of $3{,}2\ m^3$ for Saturdays and Sundays.

Therefore, two standard daily load profiles have been created: a week-day profile, to represent the estimated hot water demand for a day from Monday to Friday, when students are busy for academic purposes; a weekend profile, for Saturdays and Sundays. From Monday to Friday, it its supposes that most of the students do not require hot water for showering during the central hours of the day, as they are busy for didactical purposes; hot water withdrawal is gathered at early hours in the morning, and in the late afternoon. It is supposed that the 30% of the students have shower in the morning and the remaining 70% in the evening. The peak load duration in the morning is 2 hours, from 7 to 9 am. In the evening, 3 hours from 5 to 8 pm. These assumptions lead to the load profile represented in the graph below.

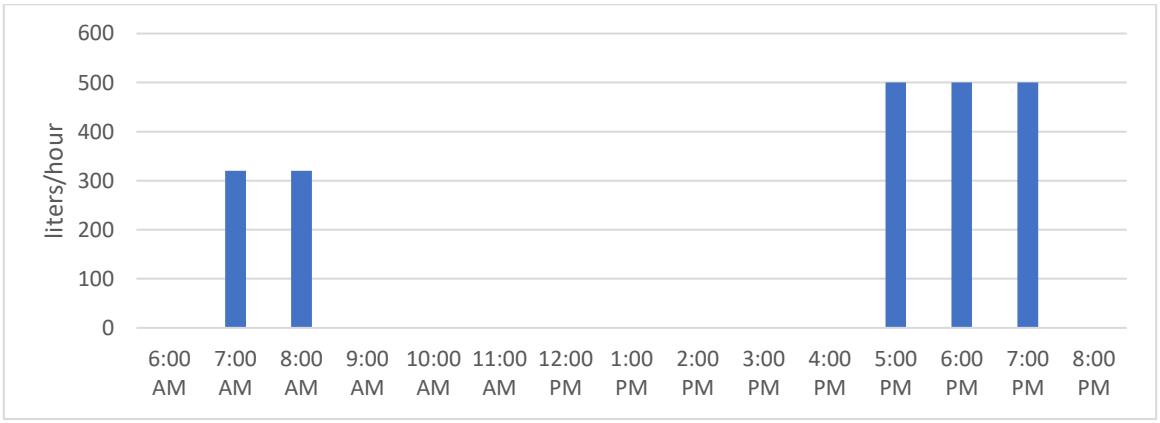

Figure 15 *Week-day hot water hourly consumption*

During weekends, when students do not have academic duties, it is supposed that more students take advantage of showers, with a withdraw pattern nearly constant during daytime. It is assumed that from 8 to 12 am, and from 1 to 5 pm showers are equally used. The load profile is represented in the picture below.

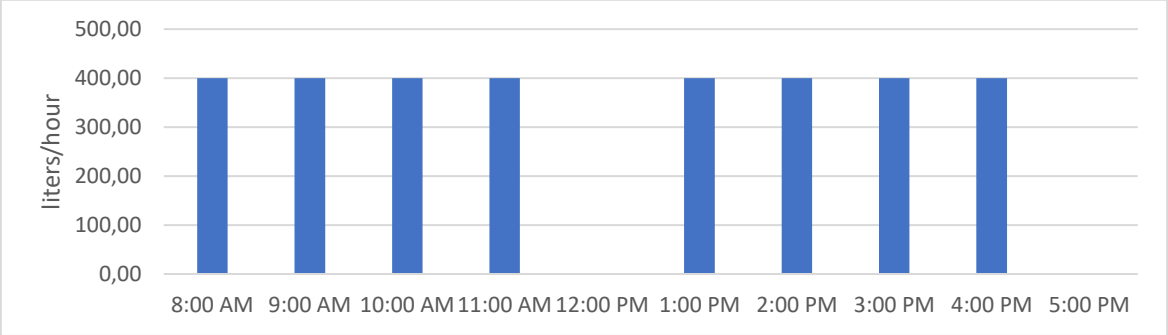

Figure 16 *Hourly hot water consumption for Saturdays and Sundays*

These simplistic load profiles represent a conservative choice for the sizing of the system, in particular for the weekday load profile: if showers are used either early in the morning or in the late afternoon, hence when solar radiation is either low or absent, then the required thermal energy should have been previously stored in the tank; thus, a storage tank of bigger capacity is required to meet the load.

In terms of thermal energy, the estimated consumption for a week day of 2,1 m^3 corresponds to $Q_t = 2{,}1 \cdot 4186 \cdot (45 - 17{,}5) \cdot \frac{1}{3600} = 67{,}15\ kWh_t/day$, while for weekends $Q_t = 102{,}3\ kWh_t/day$. To get awareness of the order of magnitude of these values, it might be interesting to note that, considering the maximum value of average daily radiation of 7,4 kWh/m^2day (February) and the minimum of 4,6 kWh/m^2day (July), the energy required for the showers during the week is collected by a surface respectively of 9 m^2 and 14,4 m^2 for February and July, while for showers during the weekend respectively by a surface of 13,8 m^2 and 22,2 m^2.

2.3.2 Monthly thermal load

The creation of a yearly load profile must consider the presence of the students in the dorm, which varies during the year depending on the didactical period (lectures period, examinations or vacation). To estimate the number of students residing in the dorm each month, the total number has been multiplied by a monthly coefficient. The chart below resumes the occurrences for every month, and the coefficients that were assigned.

Month	**Occurrences**	**Coefficient**
January	Christmas and Epiphany Holiday	0,75
February	2 weeks of examinations	0,7
March	1 week of vacation	0,75
April	Easter	0,8
May	Easter holiday; mid-term examinations	0,9
June	lectures	0,95
July	Final examinations; graduation week	0,7
August	holidays	0,5
September	Meskal	0,5
October	One week of vacation	0,75
November	lectures	0,9
December	Mid-term examinations	1

Table 4 *Resume of occurrences and monthly fraction of students residing in the dorm*

The following assumptions have been done to estimate these coefficients:

- January: because of Christmas holidays (15 days) and Epiphany (2 days), a coefficient of $0{,}75$ has been chosen;
- February: supposing that during examinations period most of the students is still residing in the dorm, while almost every student leaves the Campus during vacation, a coefficient of 0,7 is chosen;
- March, October: one week of vacation out of for weeks in a month, hence 0,75;
- July: a coefficient of 0,5 is chosen, as there are two weeks of examination and one week of graduation, which is not interesting every student;
- Aug, Sept: during these months, neither lectures nor examinations occur, but considering the commodities offered by the campus, a considerable percentage of the students might opt to reside in the dorm. A coefficient of 0,5 is therefore adopted.
- May, June, November, December: the dormitory is nearly full.

The maximum monthly hot water load is 75,7 m^3 of water at 45°C (December); in terms of energy to be collected to obtain such amount of hot water, considering a temperature from cold supply of 17°C, the value of 75,7 m^3 of hot water at 45°C corresponds to 2465 kWh_t (approximatively 8,9 GJ). This value has been multiplied for the monthly coefficient representing the presence of the students in the dorm, thus Figure 17 Estimated monthly thermal load for C1 building was obtained.

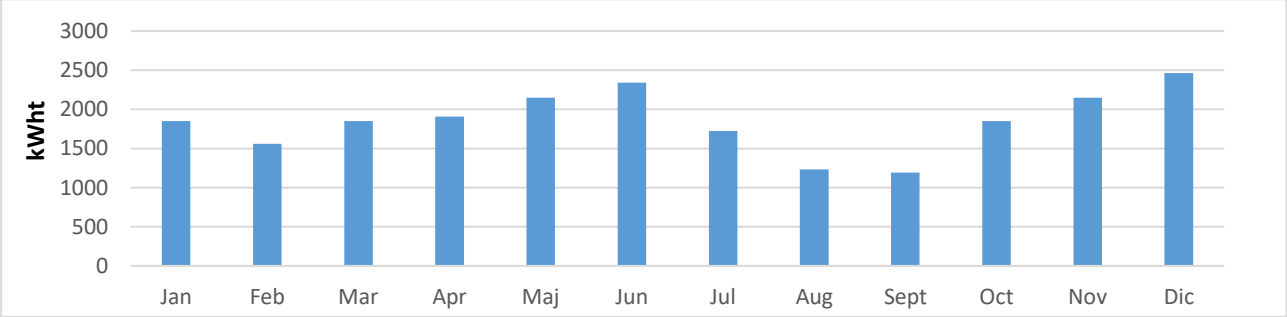

Figure 17 *Estimated monthly thermal load for C1 building*

2.4 EVALUATION OF THE MOST SUITABLE SYSTEM CONFIGURATION

2.4.1 Analysis of water quality in the site

The adoption of a direct circulation system would much simplify the installation and decrease investment costs of the system, regardless if a forced-circulation or thermosyphon type will be chosen. At the same time the efficiency of the system would be higher, as no heat exchanger between primary and secondary circuit would be necessary.

Anyhow, the possibility to adopt a direct circulation system undergoes to the quality of the water circulating in the system. Water must be of high enough quality to avoid scaling issues that would reduce the efficiency of the system and, in the worst case, completely occlude copper risers.

Description	Values from Water Analysis	Maximum Recommended Level
Ph	7,35 mg/l	6,5 – 8,5
Total Dissolved Solids	240 mg/l	600 mg/l
Total Hardness	126,5 mg/l	200 mg/l
Chlorides	11,3 mg/l	300 mg/l
Magnesium	9,2 mg/l	10 mg/l
Calcium	34,04 mg/l	12 mg/l
Sodium	36 mg/l	150 mg/l
Iron	0,06 mg/l	1 mg/l

Table 5 *Water conditions suitable for direct systems. Source for recommended values is* [19]

All the values beside Calcium fits to the prescribed ranges.

Alternatively, the Ryznar Index can be adopted to evaluate if water quality is suitable for the adoption of a direct circulation system[20]. Ryznar index is calculated as

$$RI = 2(pH_s) - pH$$

where

$$pH_s = 9{,}3 + A + B - (C + D)$$

where term

- A is proportional to Dissolved Total Solids content
- B depends on the temperature of the fluid
- C is a factor for calcium hardness
- D factor for alkalinity

For direct use of the water in a solar system, the RI must be between 5 and 7 [20].

Calculation of RI for a temperature of 20°, which may correspond to the operation of the system in the first hours after dawn, values from water analysis and coefficients A, B, C, D (see Appendix) led to the valued of

$RI = 7{,}65$. This value falls outside the suggested range and significant corrosion is to be expected.

Both these methods indicate that the quality of the water in the site in not fitting every requirement, thus it is assumed that the adoption of direct circulation systems would imply scaling or corrosion issues as time goes on.

2.4.2 Influences of climatic features of the area on the design of a solar thermal system

If freezing temperatures occur in the area, then frost protection must be provided to the plant. Various strategies are adopted to protect solar thermal systems from damages occurring by frozen water in the piping of the system: use of water-glycol solution in the primary circuit, to decrease the freezing point of water; drainage of the fluid from collectors; night recirculation of hot water from the storage. To avoid increased complexity of the system it is auspicial not to have a need for frost protection. As it has been outlined in section 2.1.3, the minimum

temperature registered in Addis Ababa since 1990 is 0,6°C in the month of November. Hence, frost protection is considered unnecessary.

On the other side, overheating prevention is considered of primary relevance because of the high radiation characteristic of the latitude. In the case of Addis, high levels of radiation encountered in most part of the year can lead to frequent events of stagnation, that might damage the system even if it has been properly designed. Considerable attention is given to the overheating prevention capabilities of the system in this study.

2.4.3 Choice of system typology

First, it has been evaluated whether it is convenient to adopt a natural circulation or a forced circulation system.

Natural circulation (thermosyphon) solar systems are attractive as they offer the simplest system configuration. The flow in the collectors is driven by natural convection, neither pump nor controller are required. The major drawback of this configuration is that the bottom of the storage tank must be placed above the top of collector's array, in order to allow thermosyphon circulation[7]. When a large storage is required to meet considerable fractions of the load, as it is the case of the dormitory, a dedicated structure to support the tank is needed. It is believed that this requirement poses some bonds on the adoption of this typology for the dormitory: the storage tank should be placed above the roof cover, therefore an unpleasant supporting structure would be required. Commissioning, inspection and maintenance of the system would also be more problematic.

Nonetheless, an alternative solution that adopts natural circulation systems might be possible, as it has been tested in [21]: a combination of small closed-coupled units, properly connected, could lead to the production of enough hot water to supply considerable fractions of the load. This solution is represented in the picture below, where two groups of two serially connected thermosyphon units are connected in parallel.

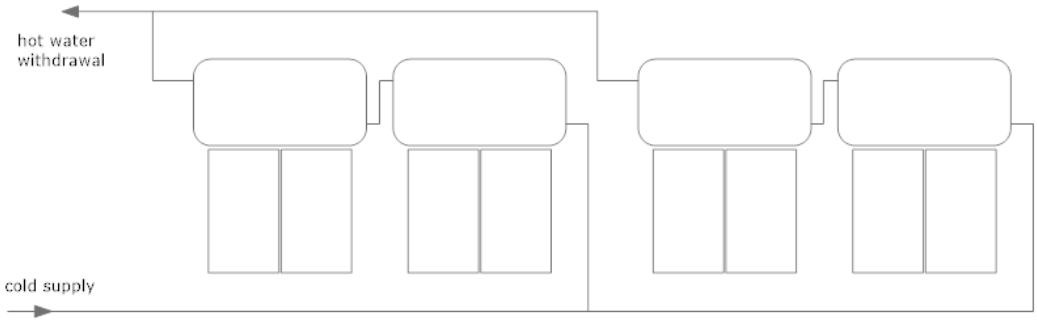

Figure 18 *Possible layout of a combination of small thermosyphon units (plant view)*

This system would be characterized by the connection of several domestic units, each of those presents an integrated storage tank. Therefore, this solution requires to buy many storage tanks, each one approximatively of 300 liters. Regarding this consideration, a forced circulation system might have the advantage of allowing the installation of a single bigger storage tank in the area under the roof, taking advantage of the scale economy. To compare the convenience of adopting a natural circulation with a forced circulation system an economic analysis has been undertaken.

A cost per square meter of collectors' surface has been estimated for both cases. In the case of forced circulation system, the cost of its main components has been estimated by investigation of market prices. It has been assumed to adopt flat plate collectors, whose price per square meters has been assumed to be 150 $€/m^2$, increasing proportionally to collectors' surface. It has been assumed a ratio of 75 liters of storage for square meter of collectors, which is the default value for F-chart calculations.

To estimate the marginal cost of the storage tank for the forced circulation case, prices of commercial insulated heat storage tanks of different capacities, with integrated electrical back-up element, have been adopted; these values are summarized in the chart below.

m3	0,5	1	2	3
€	882	1048	1767	2367

Table 6 *Cost of storage tanks of increasing sizes*

These values have been interpolated with a polynomial of the form

$$y = ax^3 + bx^2 + cx + d$$

, where y represents the price [€] of the tank and x its volume. A similar approach was undertaken to estimate the marginal cost of the pumping group.

Regarding the natural circulation unit, the price of 1400 € was assumed for a system composed by 4 m^2 of flat plate collectors and 300 liters of storage (equivalent to 75liter/m^2), consistently with current market prices. The values obtained are resumed in Table 7.

Collectors [m2]			**8**	**10**	**12**	**14**	**16**	**18**	**20**	**22**	**24**	**26**	**28**	**30**	**32**
forced circulation	collectors	[€]	1200	1500	1800	2100	2400	2700	3000	3300	3600	3900	4200	4500	4800
	tank	[€]	898	939	999	1076	1165	1266	1376	1491	1609	1729	1846	1959	2065
	pumping group	[€]	1261	1392	1524	1655	1786	1917	2049	2180	2311	2442	2574	2705	2836
	total cost	**[€]**	**3359**	**3832**	**4323**	**4830**	**5351**	**5883**	**6424**	**6970**	**7520**	**8071**	**8619**	**9164**	**9701**
natural circulation	units	-	2	3		4		5		6		7		8	
	total cost	**[€]**	**2800**	**4200**		**5600**		**7000**		**8400**		**9800**		**11200**	

Table 7 *Comparison of the investment cost for natural and forced circulation systems*

Plotting the cost of the natural and forced circulation systems against collectors' area, it resulted that: from an economical point of view[2], it is convenient to adopt the solution of connecting several thermosyphon units only if the total collector's area does not exceed 12÷14 m^2; otherwise, a forced circulation solution is preferable.

[2] Only investment costs needed for buying the equipment are considered in the analysis. Operating costs, maintenance, installation and delivery to the site are neglected.

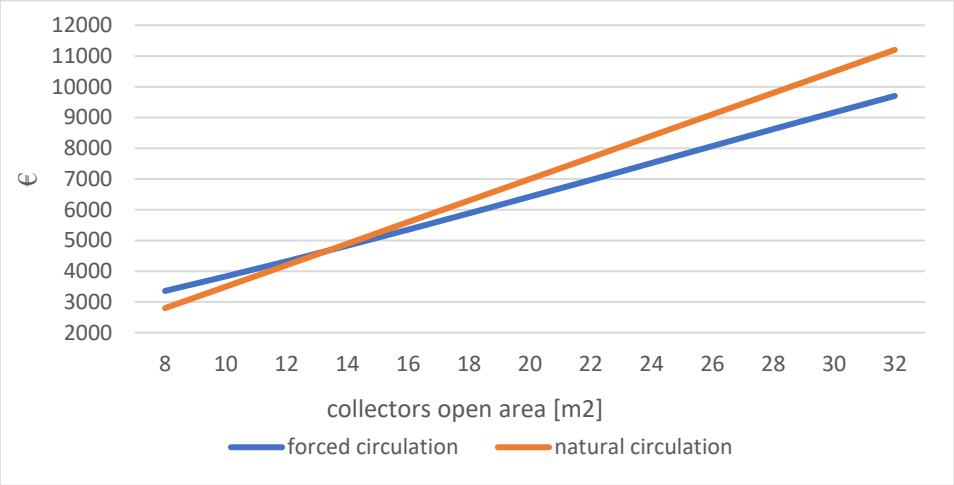

Figure 19 *Comparison of the total cost of the system, for natural and forced circulation typology*

To validate this approach, it should be discussed whether a natural circulation system allows the same solar fraction of a forced circulation system, for the same storage volume and collector's open area. Several references report that the producibility of a passive water heater is comparable to that of a forced circulation units [22][21]; the efficiency of a thermosyphon unit is actually highly depending on the arrangement of the system, whether its arrangement facilitates the establishment of a thermosyphon driving head or not, thus allows an effective thermosyphon flow rate. In this analysis, it has been assumed that thermosyphon units have the same efficiency of forced circulation; this assumption might lead to sensibly overestimate the performance of a thermosyphon unit in case of poor installation.

Several other aspects regarding the choice of the most suitable typology must be analyzed. First, the choice of the configuration depends on the budget of the project. If generous funding could not be obtained, then the installation of thermosyphon units would represent the best solution. It is hereby anticipated that 14 m^2 of collectors and 1 m^3 of storage can allow a solar fraction up to 50% of the total thermal load, thus such system could ensure a base solar-coverage of the load. It should also be considered that, beside economical convenience, a simpler configuration and lower operational costs would be encountered.

Anyway, this solution is not recommended, as a low solar fraction would make hot water provision relying on electrical auxiliary heating. Considering that power outages are frequent, this would mean that hot water is partially produced with power from diesel generators, which is unreasonable in the context of renewable energies promotion and unwillingness to rely on fuel consumption.

Then, installing more than 4 thermosyphon units to cover higher fraction of the loads would result in higher investment costs compared to the forced circulation solution, for the same achievable solar fraction. Thus, even longer payback times would be encountered. Other issues can be expected during transportation and installation phase, as handling a large number of units might be problematic.

Another concern with the adoption of this kind of system, having potable water directly circulating in the collectors, is about the quality of this water[3]; from section 2.4.1, it has been understood that the percentage of calcium dissolved in the water of the site in considerably above the recommended limits. Scale issues can lead to decreased efficiency of the system, decreased flow rates, and shorten the life of the plant. As it is suggested

[3] These economic evaluations are based on the price of *direct* circulation thermosyphon units.

in [6], the operational period of a thermosyphon unit is expected to be 10 years, instead of up to 25 years for a forced circulation system.

For the considerations expressed above, and assuming that generous funding can be obtained, a forced circulation solution is further analyzed.

2.4.3.1 Forced circulation solutions

Two possibilities have been evaluated regarding the installation of a forced-circulation system: a closed-loop pressurized system and a closed loop drain-back solution.

Closed-loop pressurized system is the typical configuration adopted in Southern-Europe, where the primary circuit is usually filled with a water-glycol solution to prevent freezing of the thermal fluid. This expedient is not required for installations in Addis' area, as no freezing temperatures occur. The major issue regarding this typology is the difficulty in providing it with an effective protection against overheating. The usual strategies to handle stagnation in closed-loop pressurized systems consists of an oversized expansion vessel to accommodate the expanded fluid and vapor, and eventually a heat dump. These precautions might not be enough to guarantee a long life of the installation, considering that irradiance levels in the site are higher than those typical of European localities for most part of the year, and events of stagnation can be frequent. Plus, there is uncertainty in the estimation of the load profile, both due to the actual number of students that will reside in the dorm after commissioning of the plant, and to difficulty in the characterization of hot water consumption habits. The system could then result to be oversized. The adoption of more sophisticated overheating prevention strategies such those presented in section 2.2.3 is in contrast with the requirement to avoid complex configurations.

Another system configuration that have been considered is the drain-back typology; the functioning of the system has been outlined in section 2.2.1.4. This typology is characterized by a simple and reliable configuration, and offers inherent protection against overheating [14]. Being an unpressurized system, several elements required in closed-loop pressurized systems are not necessary with this configuration: no expansion vessel is required; less valves are present (no check valves). On the contrary, a drainage tank is necessary.

A concern about the adoption of a drain-back typology for the dormitory is the fact that no companies that deal with drain back configurations has been encountered in Addis. Anyway, it must be noted that the elements found in a drain-back system (beside drainage tank, which is a maintenance-free component) are the same of a pressurized one, thus the availability of spare parts is not considered and issue. For what concerns the availability of skilled technicians, the producer of the drain back equipment could properly instruct the local company that will take care of the system after commissioning about its functioning.

The adoption of a drain-back configuration is suggested basically because of two reasons: it offers inherent protection against overheating and allows a simple and reliable configuration. By the way, when the pumps are switched off and collectors are drained, they are exposed to irradiance and the only way to dissipate heat is by heat losses to the ambient, thus collectors reach their stagnation temperature.

Anyway, a distinction can be made between dry and wet stagnation: wet stagnation occurs when collectors are filled with thermal fluid which, for any reason, do not circulate anymore. Evaporation begins within the collectors and the process encountered are those described in section 2.2.3.1. Dry stagnation occurs in drain-back system: fluid is drained out of collectors when the pump is not operating, collectors are empty and reach their stagnation temperature without transferring further energy to the fluid. Dry stagnation does not pose the system under pressure and thermal stresses (beside collectors). Therefore, a requirement for the long durability of the installation is for the collectors to be capable to stand their stagnation temperature; careful check of the material used for constructing the collectors must be done.

The installation of such system requires the observance of some principles such as the proper sloping of the piping and the filling of the primary circuit with the correct amount of fluid. If these requirements are not

respected the functioning of the system is compromised and damages to it should be expected. It is believed that need for care during installation phase is overtaken by the advantages offered by this typology: simple configuration, reliability and inherent overheating protection.

2.4.4 Choice of collectors' typology

The system configuration was treated as a design variable of higher priority than collector's typology. Now the purpose is to identify the typology of collector which fits to the weather of the site and to drain-back typology the most.

In general, both flat plate and evacuated tube collectors can be adopted in a drain back-typology. The requirement is that the collectors must allow the drainage of the fluid without trapping it inside the risers. Not every absorber's tubes configuration allows this; a requirement for flat plate collectors is that at least one connection must be located at the bottom of the collector[9]: "down and back" configuration is not allowed. The typologies of collectors adopted in drain back systems are flat plate, both meander and harp absorber, and ETC heat pipe.

Regarding the high levels of irradiance found in Addis, there is a concern about the maximum temperature reached by the collector when no running fluid removes heat from it (stagnation temperature). This temperature depends mainly on the available solar radiation and the heat loss coefficients for the collector, which is in turn depending on collector's design. Excessive stagnation temperatures lead to heavy thermal stress to the components of the collector. Among the manufacturing technologies for solar collectors, evacuated tubes have the lowest heat loss coefficients, thus the highest stagnation temperature.

With this regard, the adoption of single-glazed flat plate collectors is recommended: this choice represents a passive measure to prevent overheating as this typology of collectors lead to the lowest values of stagnation temperature.

2.5 SIZING THE SYSTEM

2.5.1 Determination of the optimal tilt

Choosing a tilt of the panels different than the roof's one, hence adopting mounting structures, could lead to a more uniform degree of utilization of the solar thermal plant during the year, absorbing more solar energy when it is needed, meaning when the number of students residing in the dorm is maximum, and less when it is not required.

From PV-GIS database, data about the global incident irradiation for Ecusta's Campus location was obtained. Differently tilted surfaces were considered, while the azimuth was kept constant at 0° degrees, as C1 Building's roof is South-faced.

As it can be seen from the graph below, increasing the inclination of the panels leads to higher levels of irradiance during winter months and to lower levels during summer months. Depending on the inclination of the panels, the daily average global radiation on a year varies from 6013 Wh/m^2day for a 0°-sloped surface, to 5992,5 Wh/m^2day for a 30°-sloped surface, with a maximum of 6169 Wh/m^2day for a surface sloped at 10°.

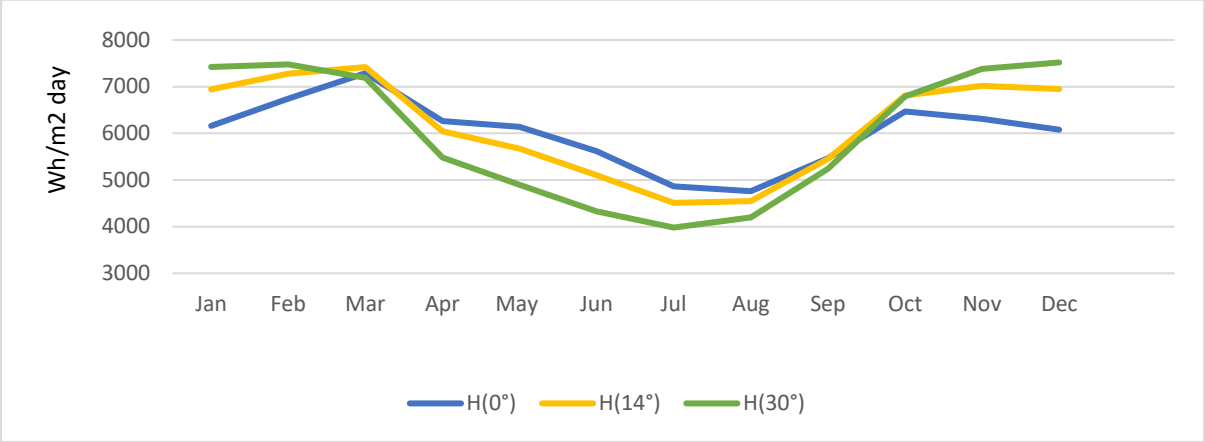

Figure 20 *Daily mean solar radiation for differently tilted surfaces. Data from PV-GIS database.*

Data about the global irradiance for differently tilted surfaces, jointly with the monthly thermal load, has been processed with the f-chart design method to investigate how the inclination of the panels influences the monthly solar coverage factors. The f-chart method allows an estimation of the solar fraction achievable for different system's configurations. Input parameters required by the method are: collector's total area, storage tank volume, average air temperatures, monthly thermal load, monthly radiation investing collectors' tilted plane, other values characteristic of the system. The output is a set of monthly solar fractions.

The optimal tilt of the collectors can be defined in different ways, as instances: the slope that the collectors should have to maintain the degree of utilization of the solar thermal system as constant as possible during a year; the slope that the collectors should have to collect as much energy as possible during the year. Keeping the solar fraction as constant as possible during the year offers an indirect protection against overheating.

To find this optimal tilts, the f-chart method has been applied several times. The values of monthly mean radiation for each inclination and the monthly thermal load were given as inputs to the method. The output from the process is a different set of monthly solar fractions (12 values) for each inclination considered; inclinations of -10°, 0°, 14°, 30° have been evaluated. This analysis was done for a fixed collector's total area of 20 m^2.

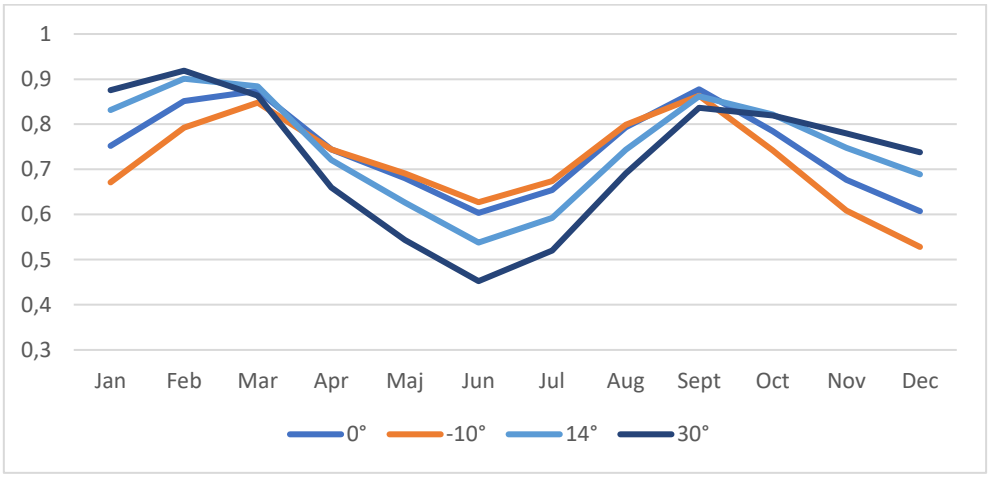

Figure 21 *Monthly solar fractions for different inclinations of the collectors*

To find the optimal tilt from the point of view of keeping the solar fraction as constant as possible, the standard deviation formula has been applied for the different sets of monthly solar fractions obtained; the optimal tilt is the one giving the set of monthly solar fractions whose standard deviation is at minimum, meaning the monthly values of solar fraction are globally the closest to the annual average solar fraction. The values of standard deviation for different tilts have been normalized to the annual solar fraction achieved for the respective tilt to allow the comparison of the results.

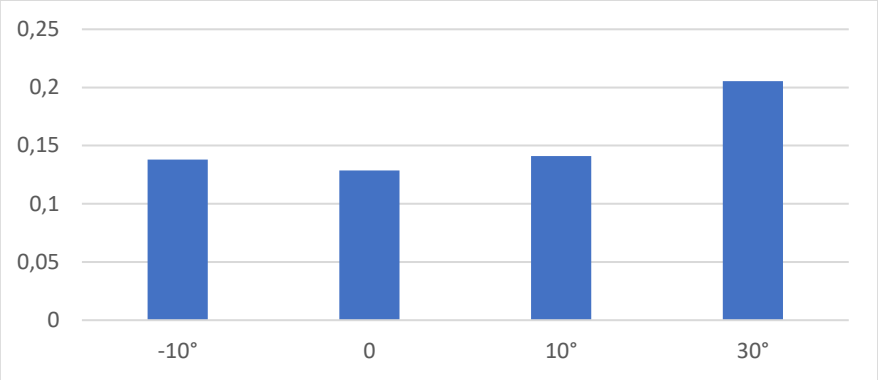

Figure 22 *Normalized standard deviations of the monthly solar fractions, for a fixed collectors' surface of 20 m^2, for different*

The standard deviation is at minimum for a horizontally inclined surface. The lowest solar fraction is found in June, and adopting mounting structures to place the collectors horizontally would decrease the energy required by auxiliary heating system for each day of June from 35 kWh_t to 30 kWh_t (for a total collectors' area of 20 m^2).

Regarding the influence of the tilt of the collectors on the total energy required by auxiliary heating, it is shown by the graph below that the minimum is obtained for a slope of 14°, which is the slope of the roof.

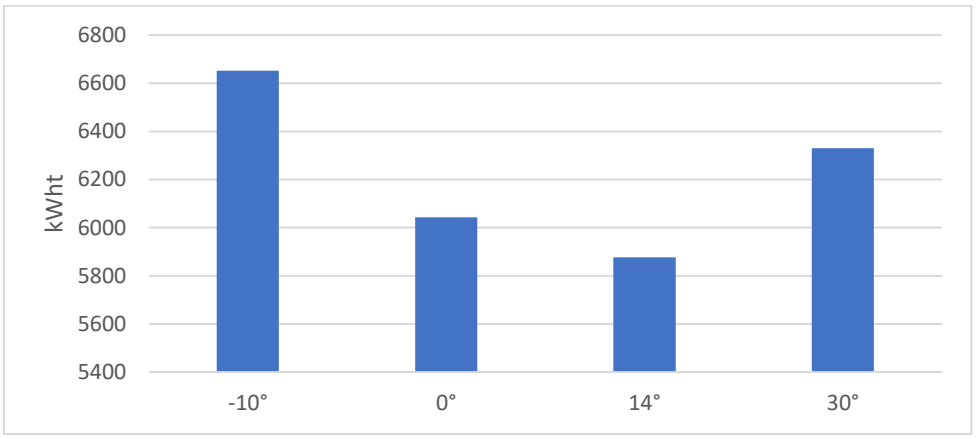

Figure 23 *Influence of the tilt of the collectors on the annual energy to be supplied by auxiliary heating*

The only advantage of adopting mounting structures would be a slightly more constant utilization of the solar thermal plant, while more energy would be required by auxiliary heating. Thus, the increased complexity of the installation phase of the system and the increased investment costs do not justify the adoption of mounting structures. It is assumed that the results of this preliminary analysis are valid for different total collector's area; in fact, a collectors' total area of 20 m^2 has been chosen for this analysis, while it will be investigated in the next section which is the optimal size of the system, by means of economic optimization.

2.5.2 Solar fraction for different systems' sizes

The f-chart method has been exploited to estimate the solar fractions achievable for increasing system's sizes. The f-chart method has been developed by Klein et al. (1976, 1977) and Beckman et al. (1977) for estimating the annual thermal performance of active heating systems for buildings. To develop this method, the results of hundreds of numerical simulations have been correlated by the authors in terms of dimensionless groups. Detailed description of the method is reported in the Appendix.

A total collector area varying from 10 to 40 $m^2$was considered in the analysis. Values of monthly average air temperature, thermal load and average radiation for the optimal slope of 14° are reported in the chart below.

Parameter	Unit	Jan	Feb	Mar	Apr	Maj	Jun	Jul	Aug	Sept	Oct	Nov	Dec
Daily load	[MJ]	214	199	214	228	257	271	199	142	142	214	257	285
Average radiation	[MJ/m2day]	25	26	27	22	20	18	16	16,4	19,6	25	25	25
Air temperature	[°C]	15	16	17	18	18	16	16	15,5	15,5	16	15	14

Table 8 *Input parameters to F-Chart Method*

Other parameters given as input to the method are reported and described in the chart below.

Parameter	Description	Unit	Value
V_{act}	Actual storage volume/collector's area ratio	liters/m^2	**75**
V_{ref}	Reference value for storage volume/collector's area ratio	liters/m^2	**75**
T_m	temperature of water from cold supply	°C	**17**
T_w	temperature of delivery of hot water	°C	**45**
F_R	Collector heat removal factor	-	**0,723**
F'_R/F_R	indication of the penalty in collector performance incurred because the heat exchanger in the tank causes the collector to operate at higher temperatures	-	**0,9**
$F_R U_L$	Collector heat loss coefficient	$W/m^2°C$	**4,548**
$(\tau\alpha)$	property of the combination glass covering-black absorber: product of the transmittance of the covering per the absorptance of the coating	-	**0,95**
$(\tau\alpha)/(\tau\alpha)_n$	transmittance-absorptance product for normal beam radiation	-	**0,97**

Figure 24 *Input parameters to the f-chart method*

The application of the f-chart method for different collector's total area led to the graph below, where the total solar fraction in a year is reported.

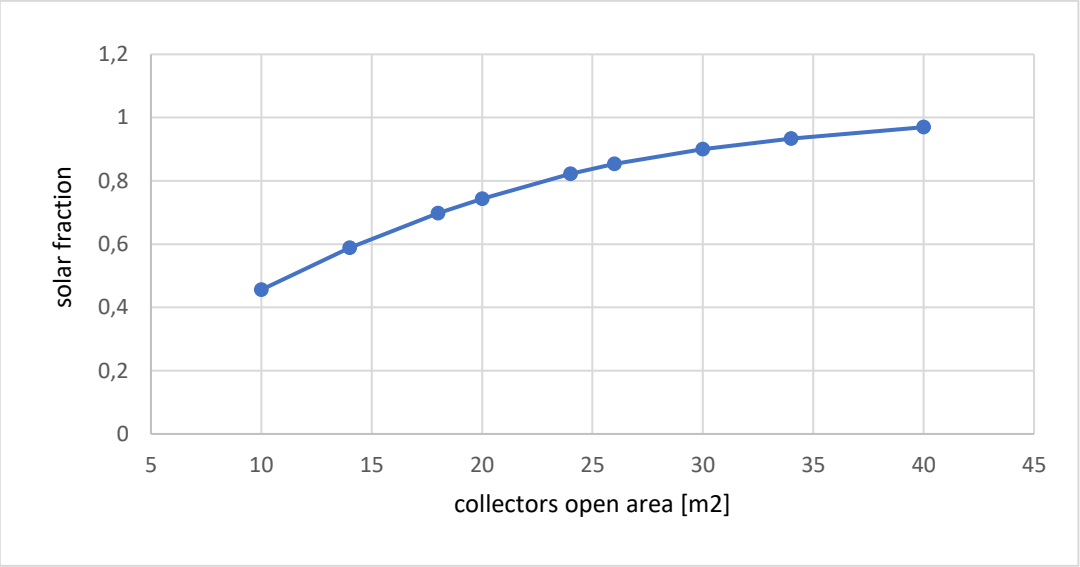

Figure 25 *Results from the application of the f-chart method*

It is interesting to evaluate which is the size that the system should have, in terms of collector's area and storage tank volume, to achieve a unitary solar coverage factor for the whole year, meaning all the energy required for showering comes from a renewable source, and the system is completely untied from fossil fuel consumption.

The application of the f-chart method reveals that an almost unitary solar fraction is reached with a collector's area of 52 m^2 and a thermal storage of 3,9 m^3 (values not shown in the graphs); the solar coverage factor is above unity for great part of the year, while only in June a neglectable amount of energy from auxiliary system should be provided. However, the installation of such a large system is not considered to be a suitable option. The system would result to be oversized for most part of the year, resulting in prolonged periods of exposure of the collectors to their stagnation temperature. Plus, excessive investment costs would be encountered.

2.5.3 Economic optimization of the system

Different economic criteria, or figures of merit, have been proposed to evaluate and optimize solar energy systems. As an instance, *least cost solar energy* is a figure of merit adopted for systems where solar energy is the only energy resource; among different possible solar systems, an optimization carried on as per this criterion would lead to choose the system whose owning and operating costs over its lifetime are at the minimum. When other energy resources are available, the crucial point is to identify which fraction of the load should be met by solar energy, and which one by traditional resources.

A figure of merit which takes into consideration both solar and traditional energy resources is *Life-Cycle Savings;* life-cycle savings are defined as the difference between the life cycle costs of a conventional system (fuel or

electrical), and the life-cycle cost of the solar plus auxiliary system. As per this figure of merit, the most suitable system is the one that allows the highest life-cycle savings.

P_1P_2 method has been used to calculate life-cycle savings. This method was developed by Brandemuehl and Beckman (1979); it allows the calculation of life-cycle solar savings in a simple form, expressing them as per the equation

$$LCS = P_1 C_{F1} LF - P_2(C_A A_C + C_E)$$

, where:

- P_1 is the ratio of the life-cycle fuel cost savings to the first-year fuel cost savings;
- P_2 is the ratio of the life-cycle expenditures to the initial investment;
- C_{F1} is the fuel cost [€/kWh]
- L is the total thermal load for a year [kWh_t]
- F is the solar fraction
- C_A are the total area-dependent costs [€/m^2]
- A_C collector area [m^2]
- C_E is the total cost of equipment which is independent of collector area [€]

A more detailed description of the method is reported in the Appendix.

To optimize the system with P_1P_2 method the above-mentioned information is therefore required. The calculation of terms P_1 and P_2 requires to assume: the life-time of the plant, a discount rate and a fuel inflation rate, to bring back to present future expenditures. The lifetime of the plant has been set to 15 years, as it is suggested in [6]. Values of $d = 5\%$ and i_f = 10% have been chosen, respectively for discount rate and fuel inflation rate. Consistently with the local habit to heat water with electric water heaters, electricity is considered as the complementary resource to solar energy, thus the fuel cost is the customer price of electricity divided by the efficiency of a typical electric water heater, assumed to be 85%; it results that the fuel cost is C_{F1}= 0,033 €/kWh. The total thermal load for a year has been calculated in section 2.3, and is $L = 22265\ kWh$; the solar fraction has been calculated in section 2.5.2.

Regarding area dependent and area independent costs, it has been estimated the amount of C_E =1000€, while for area dependent costs the value of 330 €/m^2, consistently with what has been calculated in section 2.4.3 and with the values reported in [6].

From the application of P_1 P_2 method, it resulted that the maximum life cycle solar savings are obtained for a collector's surface of 24 m^2; the corresponding yearly solar fraction is 0,82. The total amount of 7314 € is saved on electricity bills, during the 15 years of lifetime of the plant. The investment costs of the installation, for what concerns the equipment only is estimated to be 8920 €.

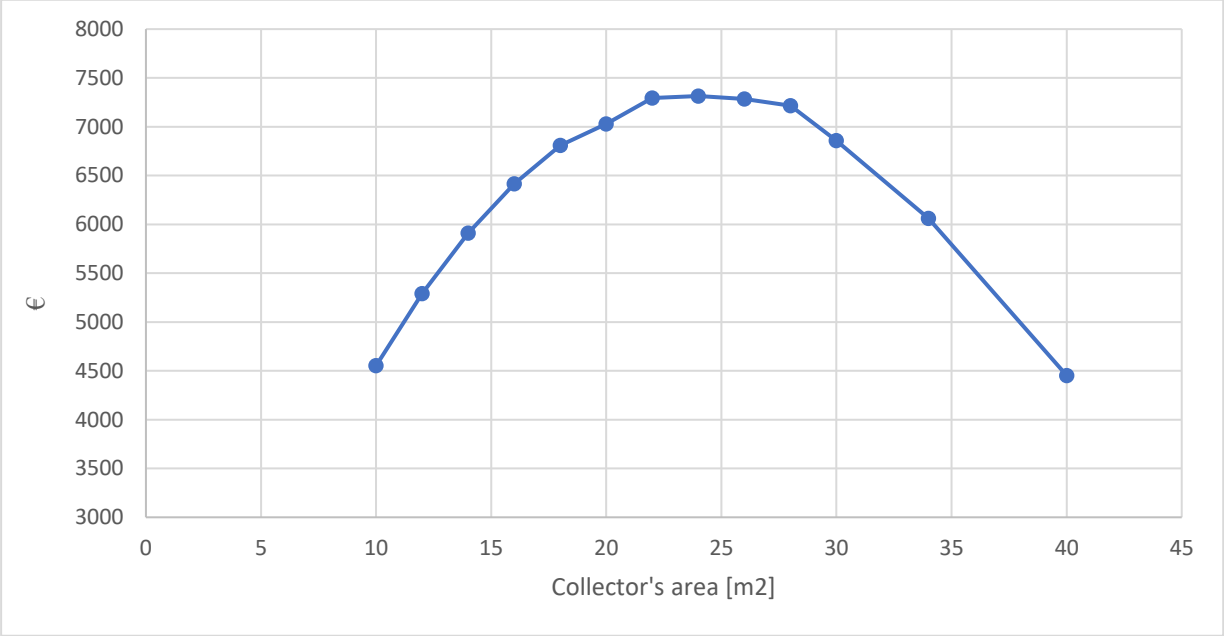

Figure 26 *Life Cycle Solar Savings*

The corresponding monthly solar fractions for a system of 24 m^2 and 1800 liter of storage are reported in the graph below. The lowest solar fraction is in June, value f=0,61; February and March instead take advantage of an almost unitary solar fraction.

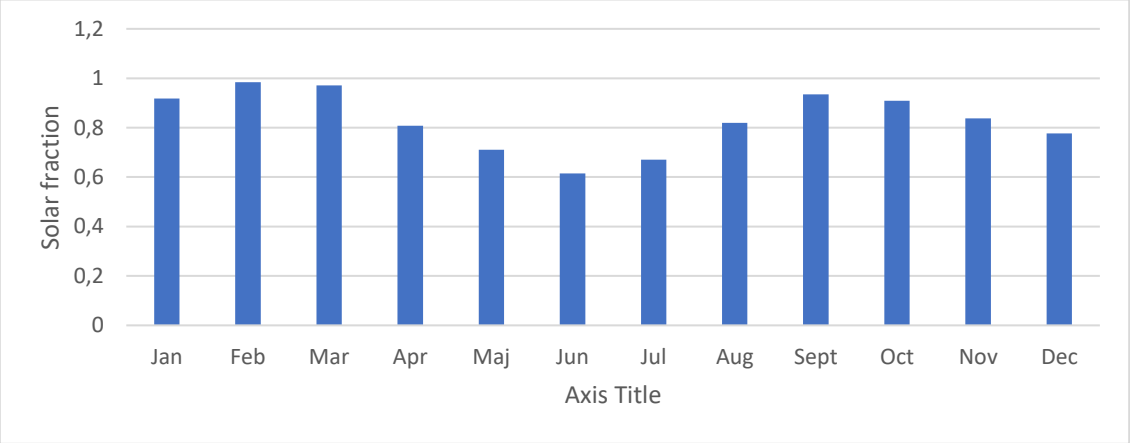

Figure 27 *Monthly solar fraction of the system*

The graph below shows the daily contribute of auxiliary heating; as it is expected, the highest requirements from auxiliary system are encountered in June, when further 29 kWh must be provided to meet the load.

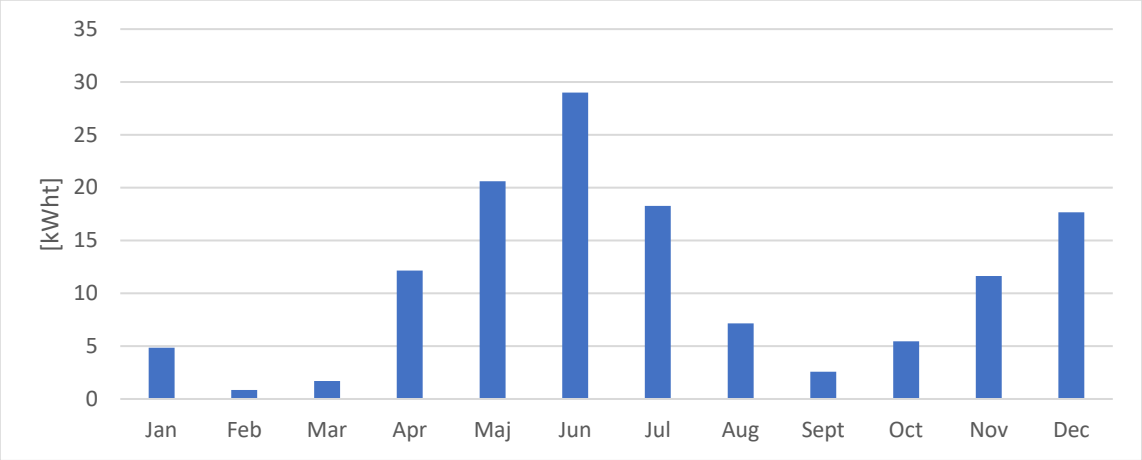

Figure 28 *Daily energy to be supplied by auxiliary heating*

2.5.4 Proposed layout of the system

Figure 29 represents the proposed layout of the collectors. Collectors and piping must be properly sloped to allow air to be pushed by water towards the drain-back reservoir, downstream the flow pipe, during the filling phase; during the draining phase, water must easily draw back through the return pipe. It is reported in several references that a minimum slope of 4% should be guaranteed.

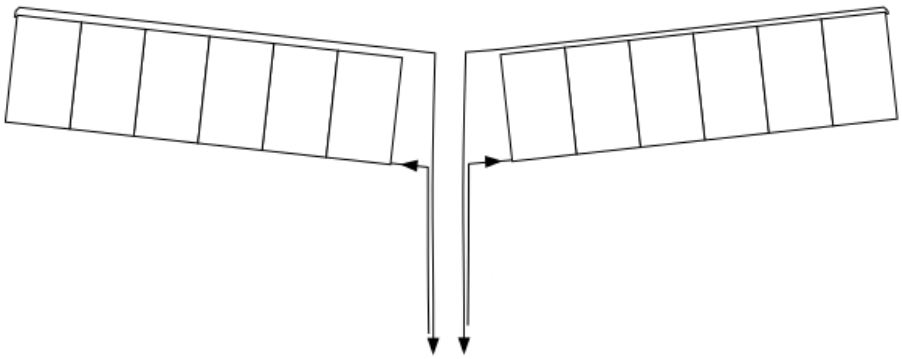

Figure 29 *Proposed layout of the collectors – roof area*

The layout consists in a parallel connection of 12 collectors, divided in two groups to allow a more uniform flow distribution from the closest collector to return pipe to the furthest; parallel connection allows the maximum efficiency of the systems as temperature at the inlet of collectors is at minimum, and minor losses are encountered.

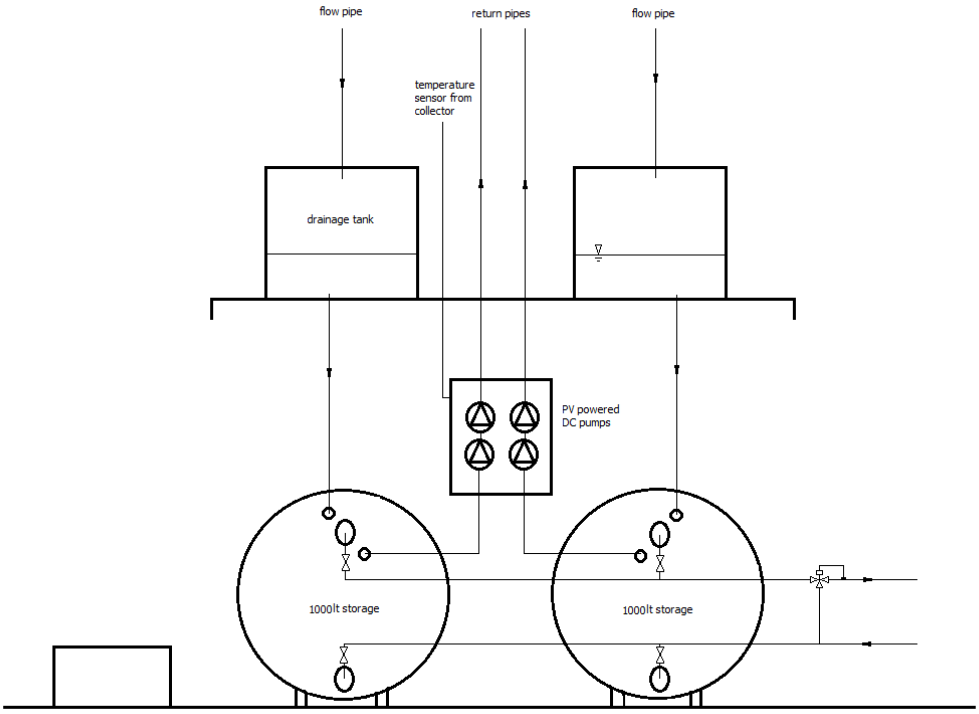

Figure 30 *Proposed layout of the system – under roof area*

As the system will be installed in a crawl space under the covering of the building, there is a constraint for the storage tanks to be placed horizontally; a lower level of temperature stratification in the tanks must be accepted. The system is composed by two independent sub-systems; in that way, the weight of the tanks is divided on a larger surface. A drainage tank must be placed above the storage, as high as possible, to reduce the power required by the pumps during the filling phase.

2.5.5 Verification of the size of the tank

As hot water withdrawal is mainly concentrated in just few hours in the evening, further analysis has been undertaken to verify if is the size of the tank is adequate to supply the load. The concept of *utilizability of solar radiation* has been exploited to estimate the temperature of the water inside the tank at the end of the insolation period, which almost corresponds to the beginning of the peak hot water demand period. A simple Trnsys simulation was done to show the dynamics of hot water withdrawal, using the calculated values of temperature of water inside the tank at the beginning of demand as initial conditions.

The useful output of the collector can be expressed as [17]:

$$Q_U = A_C F_R(\tau\alpha)(I_T - I_{Tc})^+$$

Where I_{Tc} is the critical radiation level, defined as the value of incident radiation level that must be exceeded to produce useful output. In equation terms, it is defined as

$$I_{Tc} = \frac{F_R U_L(T_i - T_a)}{F_R(\tau\alpha)}$$

The total amount of solar energy collected by the system in a day can be calculated as the integral of the first equation for the daily evolution of I_T and I_{Tc}. A time-step of 1 hour was used; during this time, values of I_T, I_{Tc} , T_a , T_i have been considered constant. Water temperature at the end of each hour has been calculated supposing full mixing of water in the tank, and no cold-water replacement due to hot water consumption. Value of water temperature at the end of each hour has been used as initial value of inlet temperature T_i for the successive hour[4].

In the case of June, which is the month when the lowest solar fraction occurs, daily evolution of the temperature inside the tank is represented in the graph below. Value of initial temperature of water in the tank of 20°C has been chosen, and tank volume of 1,8 m^3.

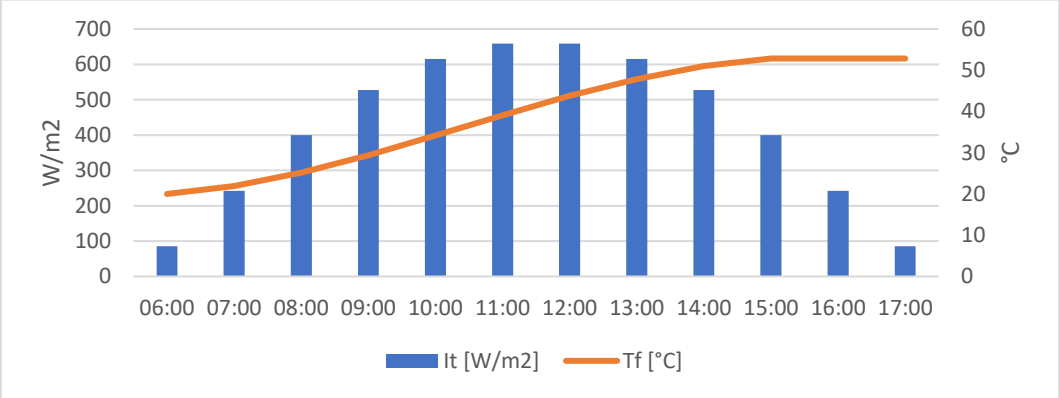

Figure 31 *Daily evolution of irradiation and water temperature in the storage, June*

It is therefore assumed that water in the tank has an average temperature of 53°C at the end of the insolation period. This value is used as initial condition for a Trnsys simulation, whose diagram is reported below.

[4] Considering only $F_R(\tau\alpha)$ coefficient (and not F'_R), the presence of the heat exchanger coil in the tank is neglected. This assumption is not conservative (leads to higher amounts of energy collected during the day than it would happen with an indirect system).

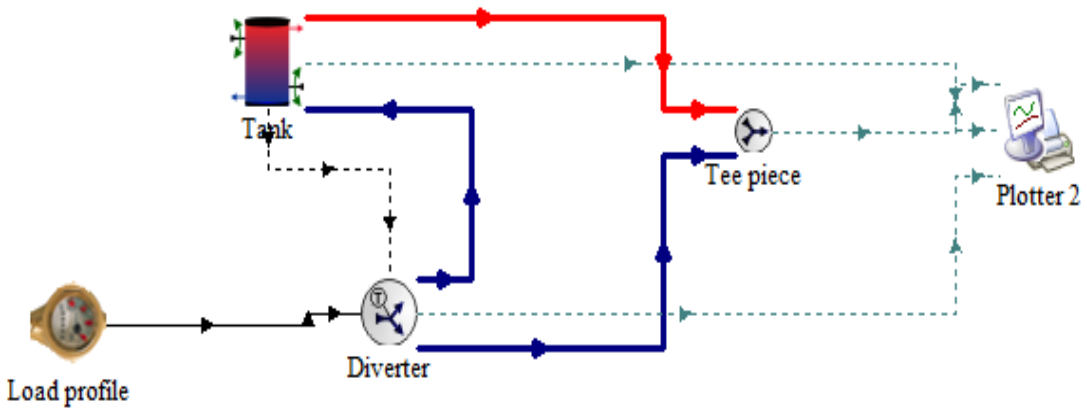

Figure 32 *Capture of the simulation diagram used to analyze temperatures in the tank after water withdrawal*

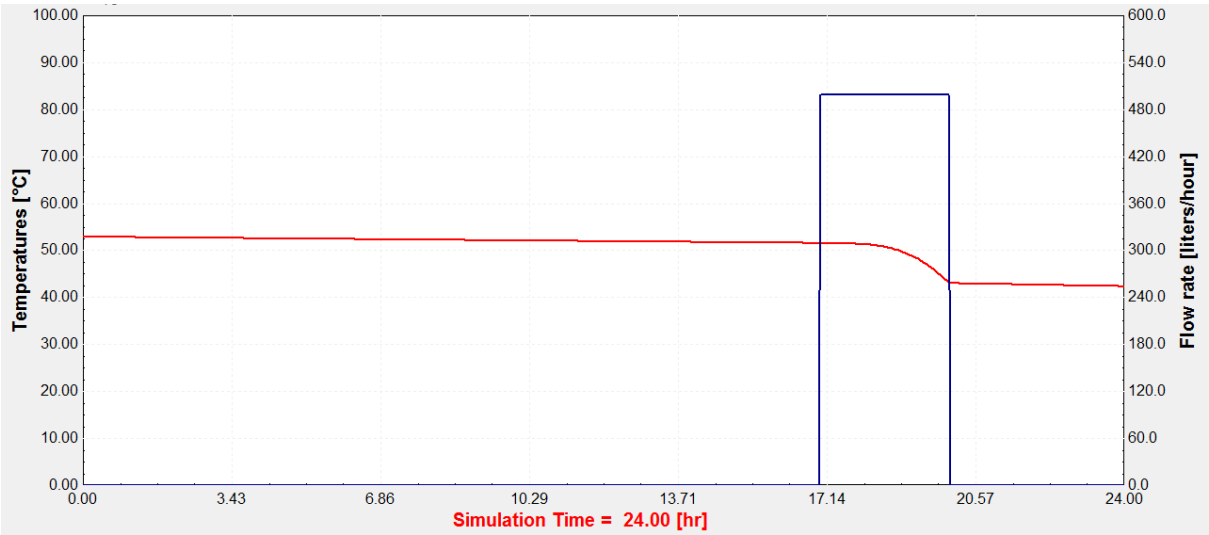

Figure 33 *Scope of the TRNSYS Simulation*

The graph above represents the scope of a Trnsys simulation. It shows that hot water withdrawal (blue line) is concentrated in three hours from 17 to 20 pm. No auxiliary heating is necessary if the tank is charged at 53°C at the beginning of the peak period, in fact: the temperature of the tank does not fall below 42°C, and with a dead-band of the auxiliary heating of ±5°C the heating element is not switched on.

It results from the simulation that 24 m^2 of collectors and tank volume of 1,8 m^3 is sufficient to meet the load, if charged until 53°C. Nonetheless, as increased storage capacity is beneficial to the solar coverage fraction, and 1,8 m^3 is not recognized as a common commercial size for heat storage tank, the adoption of slightly bigger capacity of 2 m^3 is recommended.

As per this simulation, the system is capable to meet the load even in June; this is in contrast with the results from f-chart calculations, where it was determined that June is the month of lower solar fraction. Several considerations regarding the approach of the latter simulation can be identified like leading to overestimate the capabilities of the thermosyphon system:

- Hot water consumption in the morning was neglected, as the purpose of the simulation is to verify the behavior of the system during peak load;
- High level of stratification (6 nodes in the storage tank) is modelized in the simulation, which is hardly achievable with a horizontal tank.

2.6 ECONOMIC ANALYSIS

The estimation of the cost of the system takes into consideration:

- European market prices: to determine a cost per m^2 prices of many flat plates collectors found in the online market have been averaged; the same approach has been undertaken to estimate the cost of the pumping group and the cost of the storage tank;
- Market surveys by the International Energy Agency [6]

The estimation of the costs does not consider:

1. Transportation to the site
2. Labor cost
3. Other material such as piping and valves.

As the final cost of the system could vary sensibly, depending on the will whether to acquire the components from the local market or to import the installation from Europe, and the market price of the installation will change from the time of the study to the moment when the installation will be bought, the results of the economic analysis are presented in form of a sensitivity analysis dependent on the final cost of the installation. From the results of the previous sections, the optimal size of the system is 24 m^2 of collectors and 2 m^3 of storage, if the cost of the installation will result to be 8920 €; such size allows an annual solar fraction of 82%. The size of the system is regarded as a constant. Payback times are calculated with the formula

$$N_p = \frac{\ln\left[\frac{C_s i_F}{FLC_{F1}} + 1\right]}{\ln(1 + i_F)}$$

Assuming an electricity inflation rate $i_F = 0{,}1$ and the undiscounted cost of fuel (electricity) $C_{F1} = 0{,}033\ €/kWh$, it results that the payback time for the cost of the installation of 8920 € is 10,6 years. If the cost of the installation results to be higher, payback times increases, and it results that the payback time is shorter than the lifetime of the plant until the investments cost is minor than 16000€.

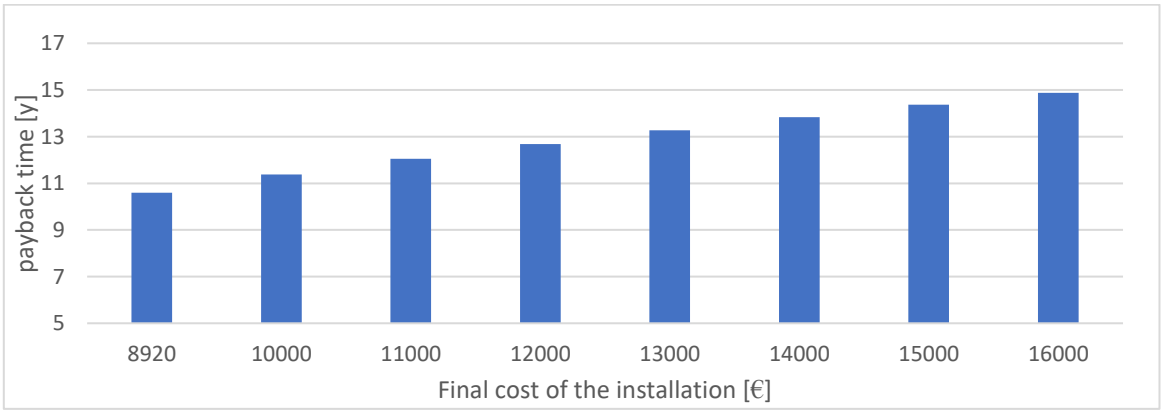

Figure 34 *Payback time for different final cost of the installatio*

2.7 CONCLUSIONS

2.7.1 Summary of the chapter

In this Chapter, the design of solar thermal system to produce hot water for the showers of the dormitory of the Campus is presented. After a brief introduction on the climatic features of the site and a review of the current solar thermal technologies, the estimation of the monthly hot water requirements of the dormitory is undertaken. It is then discussed whether it is convenient to adopt either a natural circulation of a forced circulation system, from the economical point of view; among the forced circulation solutions, it is discussed which is the configuration that allows the highest level of protection against overheating. The design of the system is carried on by means of a design tool, the f-chart method, which has been used to evaluate the influence of the tilt of the collectors on the performance of the system, and to find the relation between the total collector's surface and the fraction of the load met by solar energy. The results from the application of the f-chart method have been used to optimize the system from the economical point of view, by maximization of the life cycle solar savings. A layout for the collectors have been proposed. By means of a TRNSIS simulation, it was verified that the proposed tank size is adequate to serve the load.

2.7.2 Results

It is estimated that the maximum monthly thermal load is of 2465 kWh_t, and occurs in December. The hot water consumption (at 45° C) for a day from Monday to Friday in the month of highest consumption is of 2,1 m^3, which corresponds to $67{,}15\ kWh_t/day$, while for Saturdays and Sundays the estimated consumption is of 3,2 m^3. Considering that the presence of the students in the Dormitory varies during the year, it results the annual thermal load is of 22,265 MWh_t.

From the comparison between the required investment costs for a forced circulation and natural circulation system, it resulted that a forced circulation solution is economically preferable for meeting a solar fraction higher than 50%. A forced circulation solution is therefore recommended. An indirect drain-back configuration is suggested, to inherently protect the system from overheating and ensure a longer operativity life of the plant.

The evaluation of the influence of the tilt of the collectors on the performance of the system showed that the roof's inclination leads to the minimum energy require by auxiliary heating, thus the adoption of mounting structures is not required. By application of the f-chart method and Life Cycle Savings optimization criteria, it was found that the optimal size of the system is of 24 m^2 of collectors. It was then verified that a total amount of 2 m^3 of storage is adequate to supply the peak period of the load. The percentage of the total thermal load, on a year basis, supplied by solar energy is 81%. The estimated investment cost of the system for components only is 8920 €. Considering the cost of the material only the payback time for the installation is 10,6 years.

3 DESIGN OF A PV PLANT FOR ISPEMA CENTER

3.1 INTRODUCTION TO THE CHAPTER

3.1.1 Purpose of the study and design criteria

The purpose behind the design of a PV system for ISPEMA Building is double-sided. From one side, it is intended to increase the reliability of the electrical installation by supplying back-up electrical power when power outages from the grid occur; from the other, it aims to unbound the operativity of the clinic from fossil fuel consumption, meaning from noisy and polluting diesel generators.

The power sources of ISPEMA are represented by the public utility grid and by a diesel back-up generator. Both relying on the diesel generator or on the public grid implies several uncertainties on the availability of power: the public grid in Ethiopia is characterized by frequent power outages, which are estimated to be in the order of 600 hours per year[1]. The frequency of these power outages is variable in the different areas of the Capital, and can be up to 8 hours every two days. For what concerns relying on generator's supply, it must be noted that the diesel generator that will serve ISPEMA building results to be largely oversized. In fact, sudden generator has a nominal power of 165 kVA (132 kW, datasheet reported in the Appendix), while the maximum peak power required by ISPEMA is estimated to be 35 kW. Considering that a typical value of power absorption is estimated to be about 10 kW, the generator would result in frequent operation at very low load percentages during power shortage from the grid, even at less than 10%.

Several issues are related with the operation of a generator at low load fractions: the efficiency is lower, and higher maintenance costs are to be expected due to the problem of wet stacking[23]. Most of the manufactures of diesel backup generators recommend that the engine should not be operated at load fractions less than 30-40%[24]. It must also be considered that the location dedicated to the generator is just few meters beside ISPEMA building, hence the operation the generator would result in disturbance of the patients and reduced comfort in the area.

Due to these considerations, one of the design criteria for the systems is to reduce at minimum the operation time of the diesel generator, still not neglecting its presence, as it has already been bought by Ecusta, but optimizing its operation.

It should then be remembered that ISPEMA building includes a medical section, where electromedical devices are operating, and lack of power supply in this area could endangers patient's life. In this sense, the design of a PV system aims to increase the reliability level of the electrical plant of the building, providing a power reserve to guarantee an autonomous operation of the high-priority medical sections for at least 10 hours of power outage from the main grid. However, as it is specified in the technical documentation of SMA Battery Inverter[25], such a system should not substitute a UPS system dedicated to those electromedical devices which are lacking of an integrated power reserve. Thus, the adoption of small UPS systems is still recommended, to protect sensible devices during those instants when a power failure occurs, and the PV system could not set up an autonomous grid yet.

Contextualizing the design of this PV plant within the frame of a 100% renewable energy Campus, striving to reach the highest solar fraction might sound like an attractive solution. Nonetheless, it must be considered that ISPEMA's PV plant is just a first step in the creation of a microgrid connecting all the power sources and loads within the campus. Considering that there is a concern with the capability of the roof of supporting high extra load due to the PV collectors, ISPEMA's building is not believed to be the most suitable site to install a large (above 20kWp) PV system.

Resuming the considerations expressed above, the desired system should meet the following requirements:

- Guarantee an autonomy of at least 10 hours to the high-priority loads within the building, independently from public grid and generator supply;
- Supply the loads of the Center with a considerable renewable fraction, allowing an optimized operation of the generator.

3.1.2 Description of the building

The entrance of the ground floor is on the southern façade of the building. On the eastern side from the entrance, two classrooms are located, each of $36{,}5\ m^2$; there are also general manager's and administration offices, and the laundry. Between the eastern and western sides of the floor, a central staircase leads to the first floor; in the under-stair space of the ground floor, the main electrical distribution board of the building is located. In the eastern end of the floor the following locations are found: kitchen and dining room; a study room of $31{,}5\ m^2$; pharmacy and its relative store; reception; a birth simulator room, for educational purposes; toilets and janitor room.

The entrance of the first floor is located on the northern façade of ISPEMA Center. The first floor represents the medical section of the building: two operating rooms are found on the south-western end of the floor, close to the anesthesia room and x-ray unit. In the north-eastern side of the floor we find: neonatology and infant care unit; delivery room; post-natal room; a large section of 105 m^2 is dedicated to inpatients, where 10 beds are settled. The northern side of the building, from east to west, houses reception and waiting areas, consulting rooms, emergency room, treatment and injection rooms. In the southern side two laboratories are found, provided with the necessary equipment for chemical and clinical analysis.

Picture 2 *View of the northern facade of the building*

3.2 ANALYSIS OF THE EXISTING ELECTRICAL INSTALLATION

3.2.1 Description of the system

Three distribution board are installed in the building at the time of the study; two of them are located within the ground floor of the building, while the third is on the first floor.

On the ground floor, Low Voltage Main Distribution board (MDB) is fed by the main power source (from the power room of the Campus, which is in turn fed by EEU substation), and from a back-up utility (diesel generator) in case of power outage.
Low Voltage Main board supplies Ground Floor Distribution Board (GF_DB); downstream to the ground floor distribution board, the first-floor distribution board (1F_DB) is serially connected; this board is physically located on the first-floor main corridor, and supplies the medical section of the building.

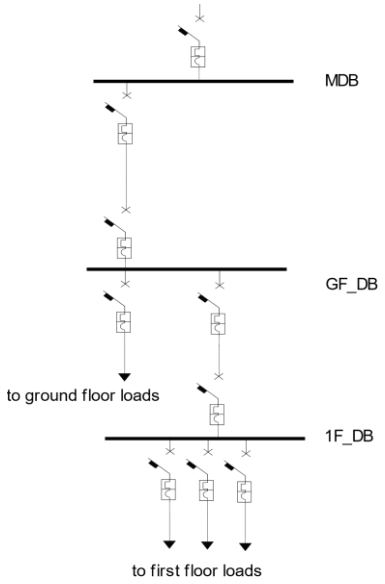

Figure 35 *Schematic configuration of the existing distribution plant*

Ground floor distribution board is protected by an overcurrent protection (thermal-magnetic type) whose intervention threshold is of 160A, while first floor distribution board by a 100A thermal-magnetic overcurrent protection.

The following magneto-thermic devices are found inside MDB and SDB-1F to protect the lines to the loads:

- C10, rated current 10A: supplying the lines of the lighting installation;
- C16, rated current 10A: supplying the electrical boilers;
- C25, rated current 25A: supplying the lines of high power demanding loads, such as electric stove
- C25-3F, rated current 25A per phase: dedicated to x-ray room, sterilization, laundry (washing and iron machines)

At the time of the study, the neutral lines within the distribution boards were connected to the grounding system of the generation sources through PE cables, coming from Main Distribution Board; grounding cables from the

sockets were not connected to any bar; however, a technician working on the electrical installation reported that those lines will be connected to the earthing rod of the building. Thus, the electrical system can be classified as a TT system. The following schematic represents how the electrical installation is supposed to be completed.

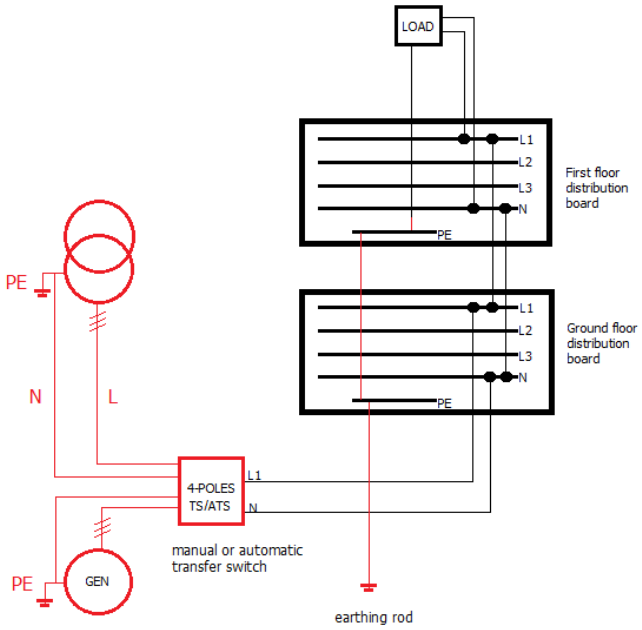

Figure 36 *Schematic representation of the electrical plant of the building. Black lines represent existing installation – red lines represent supposed completion.*

3.2.2 CHARACTERIZATION OF THE MEDICAL LOCATIONS

The medical locations of the building have been classified into three categories according to standard CEI 64-8. The standard identifies three typologies of medical locations, characterized by increasing electrical safety requirements:

- Medical location of **group 0**:
  "medical location where no electromedical equipment with parts applied to the patients is used, and where interruption of power supply does not endanger patients' life";
- Medical location of **group 1**:
  "medical location where the parts applied to the patients are used in the following way:
  - externally,
  - invasively, within every part of the body, excluding the heart region, and where interruption of power supply does not endanger patients' life";
- Medical location of **group 2**:
  "medical location where the applied parts are used in applications such as intracardiac surgery, general surgery, or where patients are subjects of vital treatment and interruption of power supply can endanger patients' life" (translation from [26]).

Every location within the ground floor of the building is a general-purpose location, thus prescriptions from CEI 64-8 are not applied to the ground floor of the building. The first floor of the building instead includes medical locations of every group; group 1 has been assigned to treatment and injection room, emergency room, inpatient

room, laboring/pre-natal room, X-ray room, ultrasonography room; group 2 has been assigned to: isolation rooms, recovery room, delivery room, post-natal room, neonatology and infant care unit, major and minor operational room, anesthesia supply room. Group 0 has been assigned to all the other locations. The assignment of the groups has been done following the flowchart represented below.

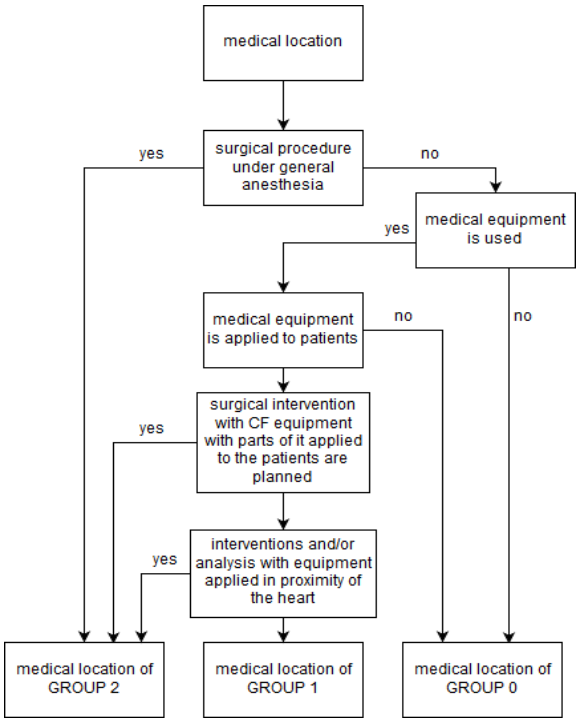

Figure 37 *Flowchart adopted for the classification of the medical locations*

Medical locations require a safe and highly-reliable electrical installation. Both protection from direct and indirect contact must be provided, taking into consideration that the physical conditions of patients in a clinical/medical area might be very poor. Medical patients are highly sensible to any electrical disturbance; for this reason, the maximum admitted touch voltage for medical locations (as per Standard 64-8) is set at 25V instead of 50 as it is for general-purpose locations.
In addition to protection from direct and indirect contact, precautions must be taken to guarantee the reliability of the power supply, in particular for that equipment whose interruption can endanger patient's life.

Figure 38 *Plant of the first floor of the building. Red zones represent area-2 sections; Yellow zones represent area-1 sections.*

3.2.3 Prescriptions from CEI 64-8/7

Normative CEI 64-8/7 prescribes different requirements for the electrical installation of every location, depending on which group has been assigned to it. The electrical installation can potentially represent a source of risk to the patients by means of:

1. Electrocution, both from direct and indirect contact
2. Interruption of power supply for vital equipment

Protection against electrocution from **direct contact** must be provided by equipment with isolation level not below IPXXD (or IP4X) for every easily accessible horizontal surface, and IPXXB (or IP2X) for every other situation.

The normative prescribes different solutions to reduce at minimum the risk of electrocution from **indirect contact**, depending on the group of each location.
Regarding group 0, The maximum touch voltage admitted for every location of this group (e.g. ambulatory room) should be limited to 25V, instead of 50V for every ordinary location (e.g. waiting room). This is achieved by installation of earth-leakage protecting devices whose I_{dn} satisfies the relation

$$R_e \cdot I_{dn} \leq 25\ V$$

where R_e is the resistance of the grounding rod and I_{dn} is the intervention current of the earth-leakage protection device.
Regarding medical locations of group 1 (supplied by a TT system), the normative prescribes the protection with residual current-operated circuit breakers with $I_{dn} \leq 30$ mA for every line up to 32A.
For what concerns electrical installations for Group-2 locations, normative CEI 64-8/7 prescribes the adoption of a medical IT distribution systems (IT-M). Such system is composed by an isolation transformer and a ground insulation monitoring device. The isolation transformer is adopted for two reasons: to guarantee the continuous supply in case of a first ground fault, and to reduce within admitted limits the voltage that could interest the patients (thus limiting the current, protecting the patients from micro shock). Being a second ground fault equivalent to a short circuit, that would implicate the interventions of the protections, it is necessary to adopt a ground fault monitoring device to detect the first ground fault. The lines supplied by an IT-M subsystem should not be protected with earth-leakage breakers as in case of a first-ground fault only capacitive currents would flow to earth. All the lines which are not supplied by the IT-M system must be protected with an earth-leakage detection breaker with $I_{dn} \leq 30$ mA.

In addition to these prescriptions, normative CEI 64-8/4 requires that locations of group 1 and 2 must be equipped with an additional equipotential hub, connecting all the medical devices and conductive equipment of the location. In this way, in case of a ground fault of any equipment, all the conductive surfaces that could be touched by patients get instantaneously to the same potentials. For medical locations of group 2 the equipotential hub should have a resistance not above 0,2Ω.

3.2.4 Recommended interventions to increase the safety level of the electrical system

Two aspects of the electrical distribution plant do not comply with the safety and reliability requirements for the installation:

1. lack of earth leakage circuit breakers within the distribution boards;
2. series-connection of the distribution boards of ground and first floor.

The electrical plant of the Center is configured as a series-connection of three distribution boards. This configuration is in contrast with the requirements of highly reliable power supply for the loads in the medical section of the building (loads located on the first floor).
In fact, a fault to ground in the distribution system of the ground floor could imply the intervention of the main overcurrent protection of the ground floor distribution board: in the event of a fault-to-ground whose current is above the threshold of intervention of all the protective devices upstream the fault, then there would be

uncertainty on which device is the first to react. If GF_DB general protection would react at first, then no power would supply the medical section after this intervention.
This is a remote but possible situation: its occurrence depends on how protective devices are coordinated; the intervention curve of the magneto-thermic device protecting the boards is reported in the Appendix, while the intervention curve for breakers protecting the sockets could not be obtained. Further investigation is needed to verify the reliability of the installation. The proposed modification of the system, as per
Figure 39, overcomes this uncertainty.

Normative CEI 64-8/4 requires an IT-M subsystem to supply Group 2 medical locations. The adoption of such system is recommended. It should be considered that the typical configuration of protective devices for medical locations in Ethiopia consists on overcurrent protection. No earth-leakage protection devices were recognized in any of the clinics that have been visited, and no local knowledge about earth-leakage protecting devices has been recognized; in the case that difficulties would be met on the installation of an isolation transformer to set an IT-M subsystem, the installation of earth-leakage protection devices with $I_{dn} \leq 30$ mA is recommended. The resistance of the grounding rod should be accordingly tested to verify that the maximum touch voltage for the medical section is below 25V.

Another required intervention is the re-configuration of the distribution boards within the building, to connect the first-floor distribution board in parallel with the ground floor distribution board. In this way both GF_DB and 1F_DB would be supplied by MDB, and the intervention of overload protection of GF_DB would not imply the disconnection of 1F_DB.
This intervention has a great positive impact on the reliability of the distribution system of the building and does not require major modifications of the existing installations. It could be done accordingly to the schematic below.

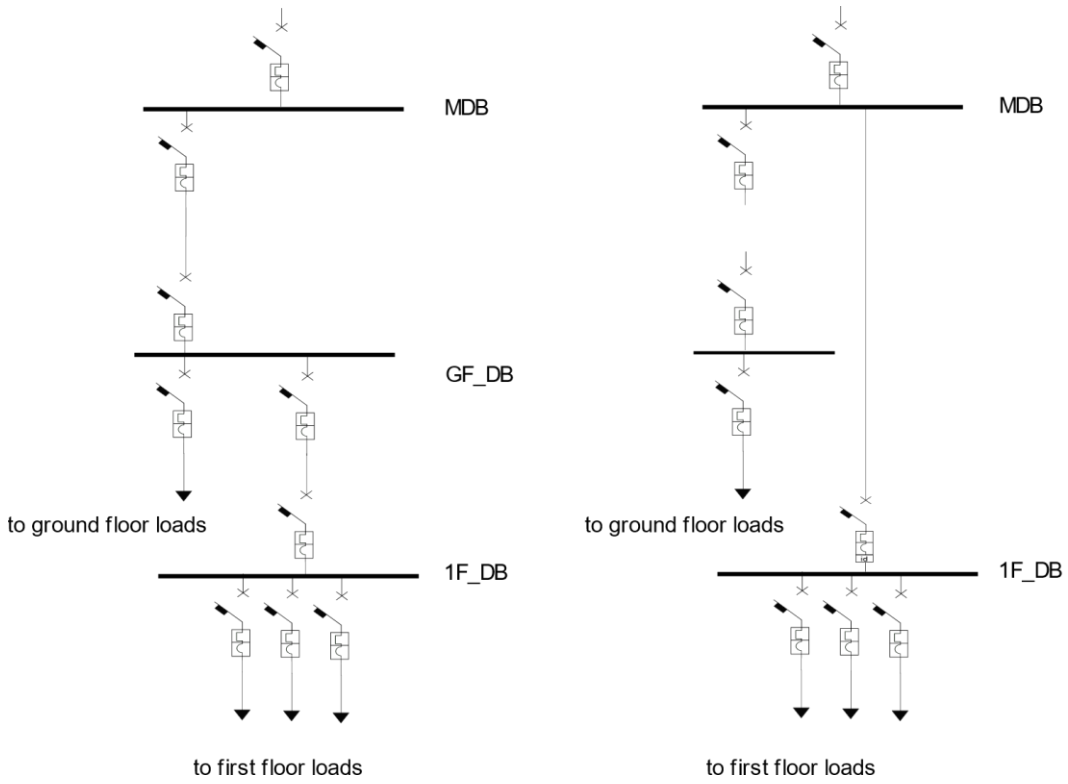

Figure 39 *Proposed modification to parallelize the connection of the boards*

3.3 LOAD PROFILE ESTIMATION

The primary step in the design process of a PV plant for ISPEMA Center has been the estimation of the load profile, for what concerns electric energy consumption. In this section the proceeding adopted for the estimation of the load profile is explained.

First, an inventory of the electrical equipment of the clinic has been done[5]. For each location within the building every socket and lighting bulb have been recorded. A prevision of which kind of devices will be connected to the sockets within each location was carried out, consistently with the power available at each socket. The hourly power absorbed by the lighting installation and the power absorbed by electrical equipment have been calculated separately.

3.3.1 Estimation of energy and power required by the lighting installation

For what concerns the calculation of power and energy absorbed by the lighting installation the proceeding has been as per the following phases:

1. Recording of each bulb and identification of its nominal power
2. Creation of standard light-utilization profiles for different locations within the building
3. Attribution of a standard load profile to each bulb
4. Calculation of the daily load profile

The lighting installation of the Clinic is composed by neon tubes with three different configurations. Depending on the configuration (number of tubes for each lighting point, and length of the tubes) each light point requires 72, 40 or 18 W.

Depending on the location where each light is installed, a different profile was attributed to it. Six different profiles were identified: *office, corridor, toilet, external, patient area, emergency*. The assumptions that were done to create the profiles are reported below.

- During night-time (from 6 pm to 6 am), all the 20 luminaires installed on the *external* perimeter will be simultaneously switched on, hence a unitary hourly utilization factor has been attributed to this typology;
- A factor of 0,8 has been attributed to lights of *Emergency* typology, meaning that it is supposed that the 80% of these lights are continuously switched on during night time. Most of the *Emergency* lights will be switched on even during day time to help to manage emergency situations;
- *Toilet lights* are supposed to be used quite often (coefficient of 0,6) from 7 pm to 22 pm as no light from the sun is present anymore while most the patients are still awake. From 11 pm to 6 am these lights are supposed to be used just occasionally (coefficient of 0,2);
- *Corridor lighting* is supposed to be used prevalently during evening hours (coefficient of 0,8 from 6 to 10 pm), then most of these lights are switched off (coefficient of 0,3 from 10 pm to 6 am).
- *Patient area* lights are supposed to be switched on from 6 pm to 22 pm, then prevalently switched off to facilitate night resting;

[5] At the time of the study (October 2016), no electrical devices beside lighting bulbs were already installed in the clinic. A list of the equipment to be installed was provided by Ecusta (see appendix ---); such list was not representative of all the equipment needed by the clinic as for a considerable number of devices no specific items to be acquired had been identified. In this terms, what is considered in the following section to be the inventory of the electrical equipment of the clinic is actually a prevision of the equipment needed by the clinic to be fully operative, both for its didactical and medical section. This prevision was carried out jointly with Ecusta's members.

- the 40% of the *office lights* are supposed to be switched on from 9 am (beginning of the working day) to 5 pm.

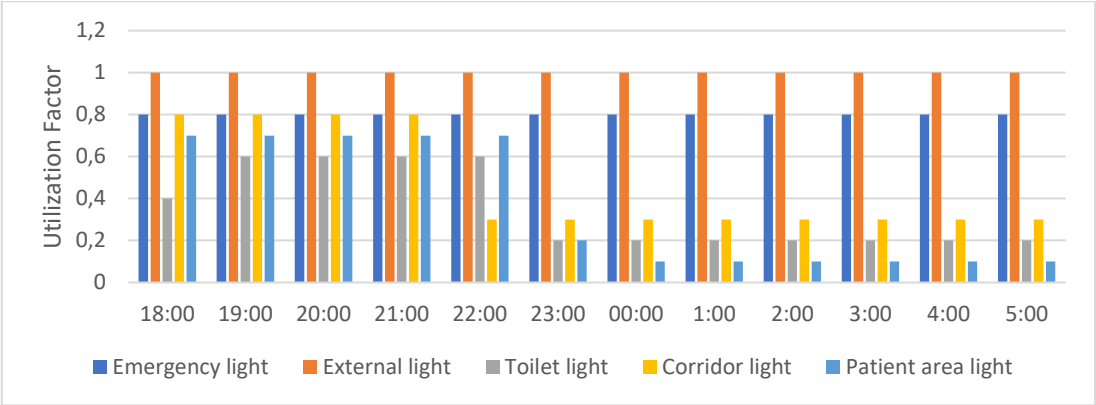

Figure 40 *Hourly utilization factors for night-time (18pm-6am)*

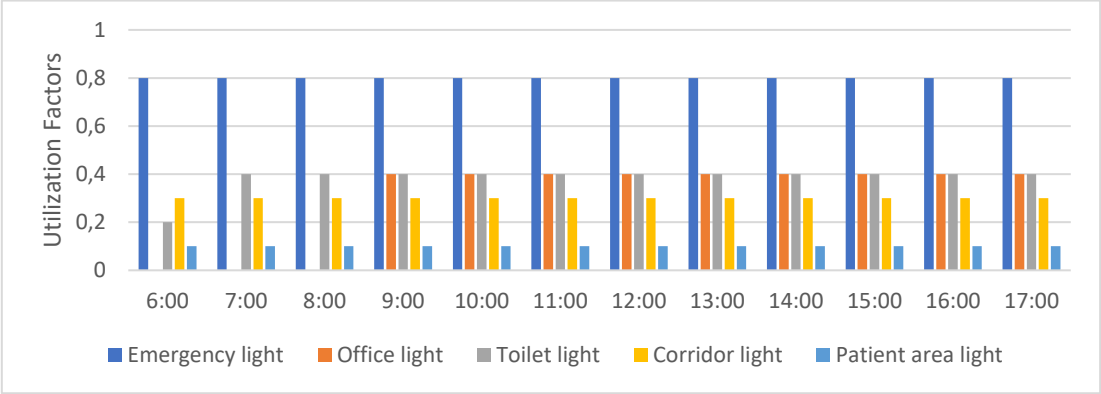

Figure 41 *Hourly utilization factors for day-time (6am-18pm)*

Different kinds of bulbs are sometimes installed within the same location; thus, the same profile has been attributed to lights absorbing different nominal power. A resume of the lighting installation of the building is presented in Table 9 Resume of lighting installation.

Profile	W	First Floor	Ground Floor
Office light	72	46	26
	18	6	0
corridor light	72	0	5
	40	0	10
	18	27	8
toilet light	40	0	3
	72	3	0
external light	40	20	0
	18	0	1
patient area light	72	23	7
	40	1	0

Table 9 *Resume of lighting installation*

The total power absorbed during each hour of the day by the lighting installation has been calculated as per the formula below:

$$P_h = \sum_i F_{ih} * (\sum_k N_{ki}\, P_{N_{ki}})$$

where,
P_h = total power absorbed by lighting installation in hour h
F_{ih} = hourly utilization factor for hour h and profile i
N_{ki} = number of lights of kind k associated to profile i
$P_{N_{ki}}$ = nominal power absorbed by light of kind k associated to profile i
h = hour in the day
i = hourly utilization profile
k = kind of light (wattage)

The result is graphically represented below.

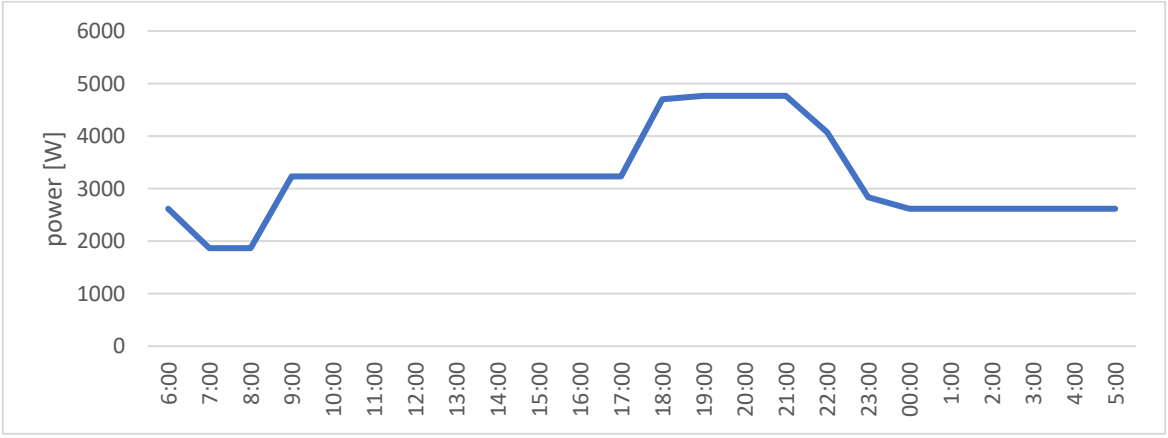

Figure 42 *Daily load profile for the total power absorbed by the lighting installation*

It is worth to note how the will to keep external lights switched on during night-time implies a considerable power and energy absorption. The reason behind this desire is to give a reference point to the neighboring community in case of emergency. It results that the external light installation is composed by two groups of 10 and 9 lights connected in cascade; therefore, to decrease night consumption by switching on only several lights, the actual plant should be modified.

The peak power absorption is found in the evening, from 18 to 22, when up to 4766 W are absorbed. This is due to the simultaneous operation of external light and most internal lights. The minimum is found between 7 and 8 in the morning, as no external lights are switched on, and most of internal lights are switched off as daily activities have not started yet.

In terms of energy consumption, the integration of the curve in the graph above leads to the value of daily energy consumption by the lighting installation of 77 kWh.

3.3.2 Estimation of energy and power required by the electrical equipment

The load profile for the electrical equipment has been calculated through the following steps:

1. **Cataloguing of every device installed in the clinic and identification of the nominal power [W] for each device**
   When available, this information has been taken from the datasheet of the equipment; if the datasheet of a specific item could not be found, information about an equivalent device whose datasheet was available in the internet had been used; datasheets of available equipment are reported in the Appendix.
2. **Determination of the periods during the day when it makes sense to consider each specific device to be operative**
   As an instance, for a chemistry analyzer the night operation was excluded, as such equipment is used during day-time in the laboratories; instead, for a suction pump the night operation could not be excluded, as an emergency surgical operation during night time could not be excluded;
3. **Calculation of the mean absorbed power during the periods of operativity for each device**
   In case of a device whose power absorption is nearly constant if the device is switched on (e.g. television), the mean absorbed power equals the nominal power. Standby power absorption has not been considered.
   In case of a device whose power absorption is highly variable during operation (e.g. electrical oven, incubator) a certain number of hours of functioning at nominal power has been estimated; the total daily electrical energy absorbed by each device (product of the nominal power per the estimated number of hours) has been spread over the numbers of hours of operativity of the equipment[6];
4. **Assignment of an hourly contemporary utilization factor to each typology of device**
   As an instance, a coefficient of 0,5 was assigned to laptops at hour 10 am, meaning that it is supposed that the half of the maximum number of computers are simultaneously operating at 10 am. Details about every hourly coefficient which has been assigned are reported in Appendix.
5. **Calculation of the daily load profile**
   The total power absorbed during each hour of the day by the electric equipment has been calculated as per the formula:

[6] Example. For an incubator, from the datasheet: $P_n = 450\ W$; 24 hours of operativity have been considered; assuming 5 hours of operation at nominal power, the mean absorbed power during operation is $P_{mean} = \frac{450*5}{24} = 94\ W$, meaning an incubator is assumed to absorb continuously $94\ W$ during a day.

$$P_h = \sum_{i=1}^{m} P_{m_i} N_i F_{hi}$$

Where,
h = hour in the day
P_h = total power absorbed by electric equipment in hour h
i = device under analysis
m = total number of different devices
P_{m_i} = mean absorbed power during operation by device i, as per the calculations of point 3
F_{hi} = hourly utilization factor for hour h and device i
N_i = number of items for the typology of device i

This procedure has been followed to obtain an estimation load profile for the electrical power absorption, for what concerns the electrical equipment; the integration of this curve by the time of a day gives an estimation of the total amount of electric energy needed by the building in a normal day of operation.

The chart below represents the inventory of the electrical equipment that will be provided to ISPEMA Center.

First floor		
Device	**Pn [W]**	**Qty**
autoclave	630	5
computer	150	11
table light	40	8
incubator	450	4
radiant warmer	750	1
medical refrig.	200	3
resuscitator	450	1
anaesthesia mach.	150	1
electrical scalpel	150	3
X-ray machine	3000	1
ECG	150	2
centrifuge	400	1
Operational Theather	150	2
Operational Table	100	2
Suction equipment	50	2
Vacuum extractor	50	1
ultrasound	130	1
boiler	1200	5
chemistry analizer	800	1

First floor		
Device	**Pn [W]**	**Qty**
microscope	20	2
hematology analizer	200	1

Ground floor		
Device	**Pn [W]**	**Qty**
computer	150	11
television	100	1
projector	500	2
medical refrig.	200	1
laundry machine	3000	1
electric iron	3000	1
boiler	1200	1
drying machine	3000	1
electric stove	3000	1
microwawe	1000	1
refrigerator	200	1
dishwasher	2000	1
kitchen boiler	1500	1
smoke extractor	500	1

Table 10 *Estimated inventory of the electric equipment of ISPEMA Center*

The graph below represents the daily load profile for the total power absorption due to electrical equipment and lighting.

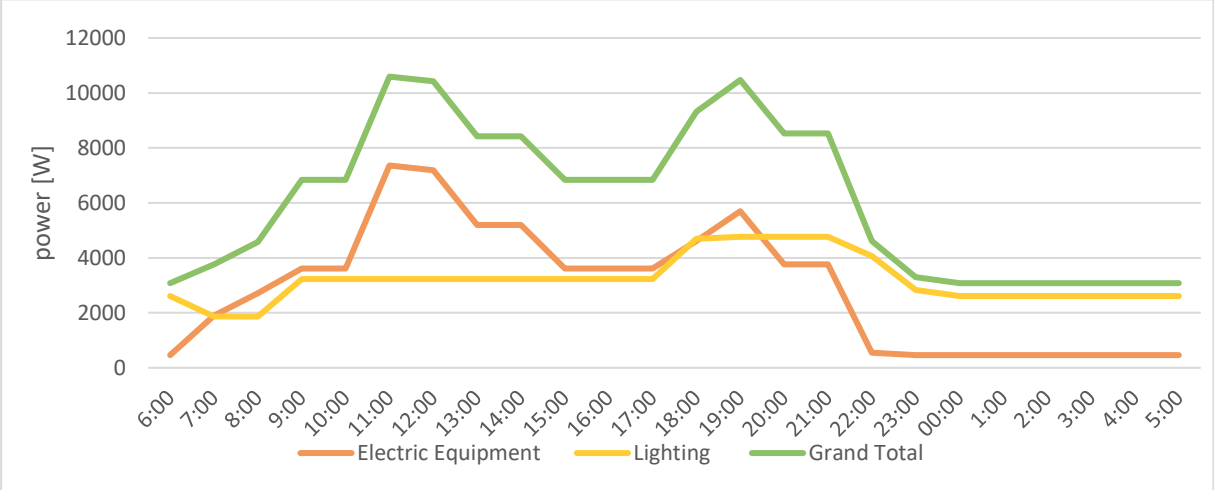

Figure 43 *Estimated total power consumption load profile for ISPEMA*

No information about the peak power requirements can be obtained from this graph; in fact, if a number of devices greater than those estimated by the utilization factors is operating simultaneously, or in the moments when some load whose power consumption has been considered constant (e.g. oven, incubators) is actually absorbing its nominal power, then the peak power requirements might be much higher than those estimated with this procedure.

Instead, the utility of the graph above resides in the fact that it is possible to estimate the total amount of energy required for the operation of the structure in a standard day by integration of the curves of the power.

3.3.3 Results of the load profile estimation

The total energy daily required by the Center is 170 kWh, in the hypothesis to produce hot water with the electrical water heaters. Values of the daily electrical energy consumption per area of the building are represented in Figure 44 Estimated daily energy consumption of ISPEMA Center – hot water produced with electrical water heaters.

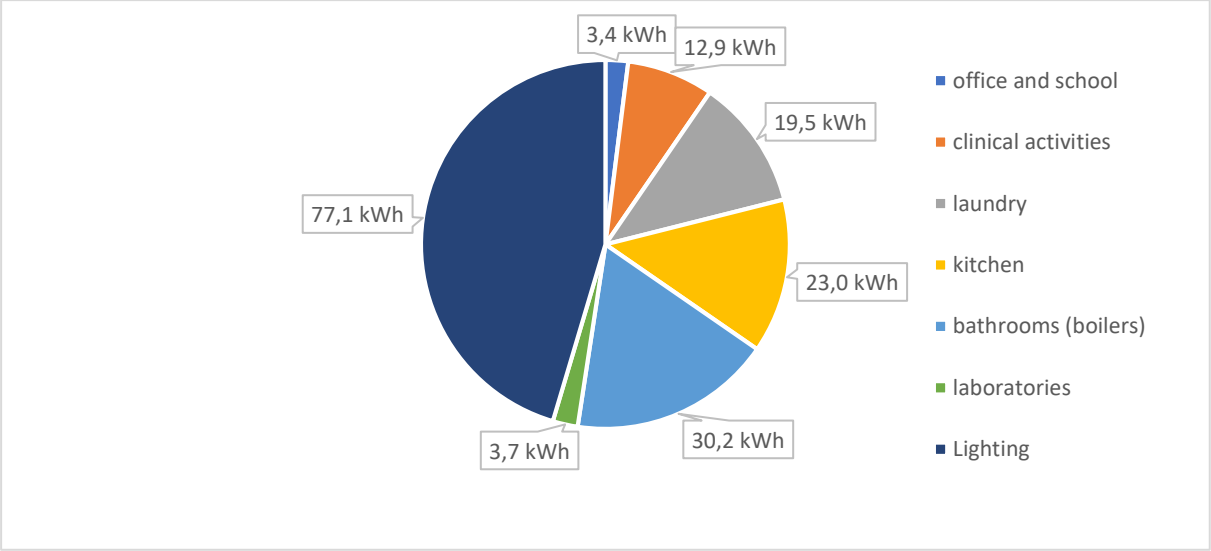

Figure 44 *Estimated daily energy consumption of ISPEMA Center – hot water produced with electrical water heaters*

In a further section of the chapter, the feasibility of designing a PV system to supply the entire building, rather than selected areas of the building, will be analyzed. The results of load profile estimation are therefore presented by conceptually dividing the Center into three sections:

1. a selected area of the first floor, including only (and all) the locations classified as Group 2;
2. the entire medical section (entire first floor);
3. the whole building.

The selected area of the first floor includes those locations where the following equipment is found: incubators and radiant warmers, medical refrigerators, anesthesia machine, electrical scalpel, x-ray machine, ECG, operational theaters and tables, suction equipment, vacuum extractors.

The calculation of the daily energy requirements does not consider the functioning of electrical water heaters, as it is assumed that hot water requirements are almost completely satisfied by a solar thermal plant, and electric water heaters provide a neglectable amount of further energy.

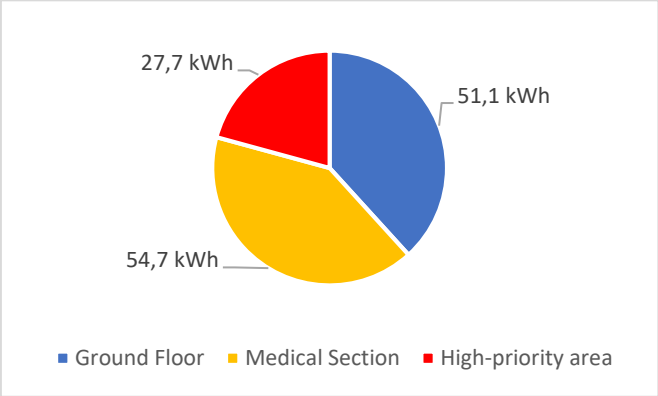

Figure 45 *Estimated daily electric energy consumption of the different sections of the Center*

The energy consumption of the Center is mostly due to the Medical section (first floor of the building), daily requiring 82 kWh, while the ground floor of the building needs 54,7 kWh daily.

The presence of the boilers is not neglected in the calculation of peak power requirements, as, in the hypothesis that the boilers would not be discarded, the power absorbed by the boilers when simultaneously operating represents a considerable percentage of the total power absorbed by the building (8,7 Kw).

For what concerns the estimation of the peak power requirements, it has been assumed that all the loads within a section of the building are simultaneously absorbing their nominal power, and the value obtained has been multiplied by a contemporary utilization factor of 0,7. The values of peak power requirements and daily energy consumption of each area of the building are resumed in the chart below.

Area	kWh/day	max kW
Entire building	133,6	36,1
Medical section	82,5	20,2
Selected high-priority zones	27,7	6,4

Table 11 *Resume of the peak power absorption and energy requirements of ISPEMA Center*

3.3.4 Discussion of the results of load profile estimation

To determine if these results could be realistic or not, the values found in the previous section are compared with values found in the literature, and with field investigation on electric energy consumption for health facilities in Addis' area.

Previous studies from the International Energy Agency [27] on rural health facilities revealed that typical values of electric energy consumption for *medium*[7] size rural health centers are up to 20 kWh; the results from the load profile estimations in this study are one order of magnitude greater. Anyway, it must be noted that ISPEMA Center is not a rural facility, and the Center will be provided with generous equipment, not having constraints on the availability of electrical power. In particular, the lighting installation is responsible of a considerable part of the daily energy consumption (48%).

Field investigation about energy consumption of health facilities revealed that the estimations carried on in the previous sections can be realistic. Analysis of the electrical energy bills from December 2014 to December 2015 of Migbare Senay General Hospital revealed that the average daily energy consumption for the structure is 156,2 kWh; in this calculation, the energy provided by the back-up generator is not considered, thus the daily average consumption can be estimated to be approximatively 180 kWh (approximatively 15% higher, considering 10 hours of power outage every 72 hours). The dimension of the structure is bigger but comparable to that of ISPEMA Center. From these considerations, it results that the estimated energy consumption of the Center might have been over-estimated; anyway these results are considered valid as a conservative choice, being reported in the literature[27] that under estimation of load requirements and inverter's size is one of the causes of PV systems failures in developing countries.

3.4 ANALYSIS OF A COMMERCIAL SOLUTION FOR OFF-GRID SYSTEMS

As power outages of the public grid might happen frequently, at least a portion of the electrical plant of ISPEMA Center must be capable to operate in off-grid modality. When a power outage occurs, reference values of voltage and frequency in the grid must be provided by a grid-forming device, which establishes new references and supply the loads. A grid forming device can either be represented by the diesel back-up generator, that gives the references of frequency and voltage through its electrical generator, or from a static converter, that converts electrical energy from a DC source to the AC side of the islanded grid. A commercial solution capable to fulfill these requirements has been identified. Among the products produced by SMA Company, the Sunny Island family inverters is a family of battery inverters that are capable to operate both in islanded condition and in grid or generator-tied condition.

3.4.1 Description of the components

3.4.1.1 Sunny Island Battery Inverter

This typology of inverters, also referred to as voltage-frequency inverters, are bidirectional converters that exploit their internal circuitry and the energy stored in the batteries to generate reference values of frequency and voltage, creating in such way an islanded grid. These inverters can be connected to an external energy source, such as the public grid or a diesel back-up generator. A primary function of these devices is to manage the battery bank, gently charging it when surplus energy is present in the grid, and discharging it when PV production is not enough to meet the load; depending on the state of charge of the battery bank, the inverter

[7] Capacity ranges from 60 to 120 beds; equipped with diagnostic and surgical equipment; maintain a cold chain for vaccines and blood supply.

can disconnect in successive moments up to two groups of loads characterized by different levels of priority. This is done through load disconnecting devices controlled by two relays integrated in the inverter.

3.4.1.2 Sunny Tripower

The function of these inverters is to convert DC current generated by the PV plant into AC form and supply it to the AC link of the system. The output power of the inverter is maximized by a maximum power point tracking strategy, which basically consists of varying the impedance seen by the panels, to shift the operating point in the I-V characteristic curve of the PV generator to the point where the product $P = I \cdot V$ is maximum.

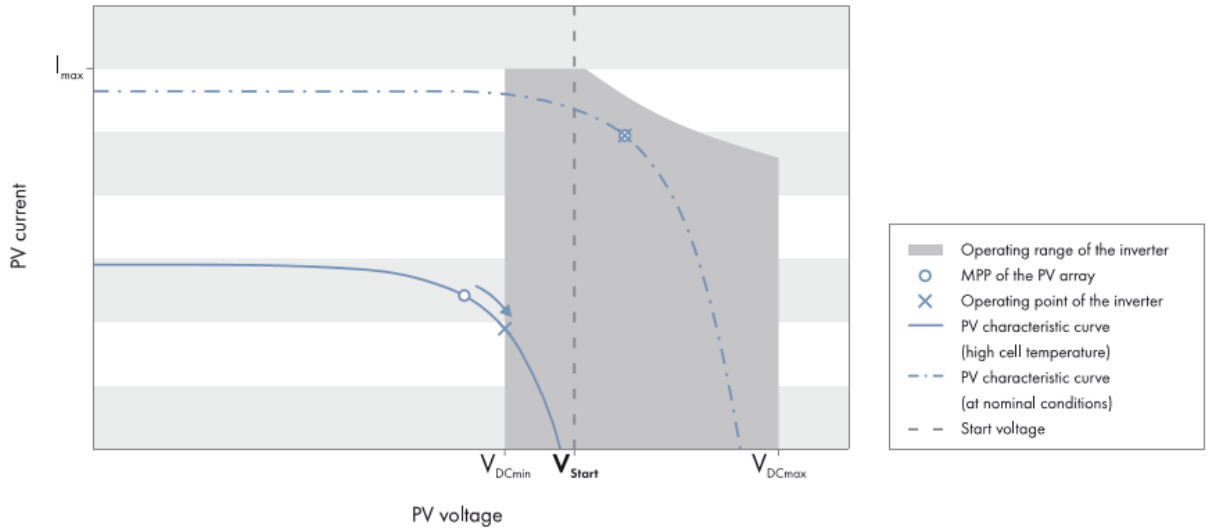

Figure 46 *MPPT strategy and operation below the minimum DC voltage. From* [28]

When the AC link cannot absorb further power, it results that the frequency of the AC link increases. The PV inverter senses this variation and limits its power output accordingly to Figure 46.

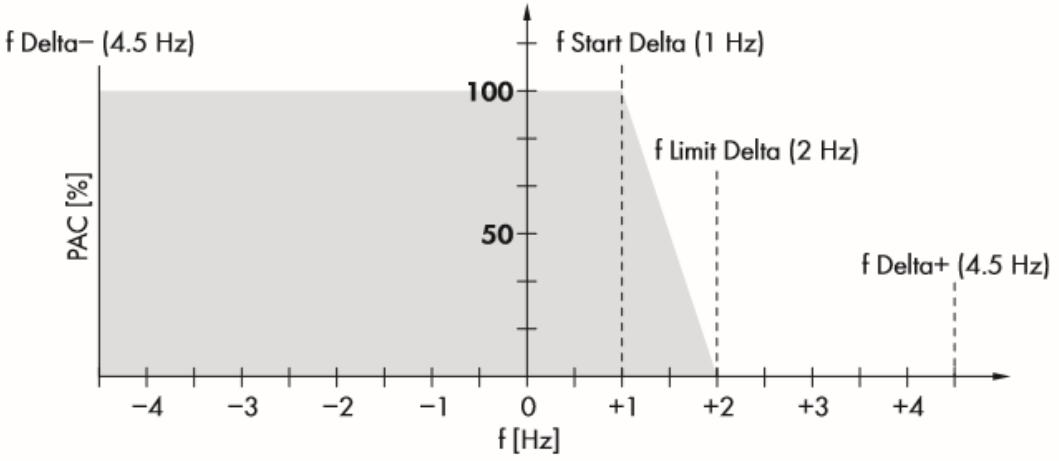

Figure 47 *Frequency-shift power control of the PV inverter. From* [29]

3.4.2 Operation modalities of the system

Figure 48 represents the logical schematic of the connections between the components of the system. The utility grid and the backup generator represent external energy sources; these sources cannot be simultaneously connected to the system, therefore a transfer switch is required. The operativity of the generator is needed when the grid is out of service, and it has to be manually started, not being the generator of ECUSTA provided with auto starting capabilities. Downstream the transfer switch there is the unprotected section of the grid; in the event of a power outage, loads connected to this portion of the link remain unmet until the generator is manually started. In fact, the battery inverter (yellow) disconnects from the grid whenever it senses the absence of power. Downstream the battery inverter, there is the protected section of the system. A PV inverter supplies the grid with power from the AC generator. The battery inverter provides to disconnect the low-priority loads when the energy stored in the battery bank falls below a certain threshold.

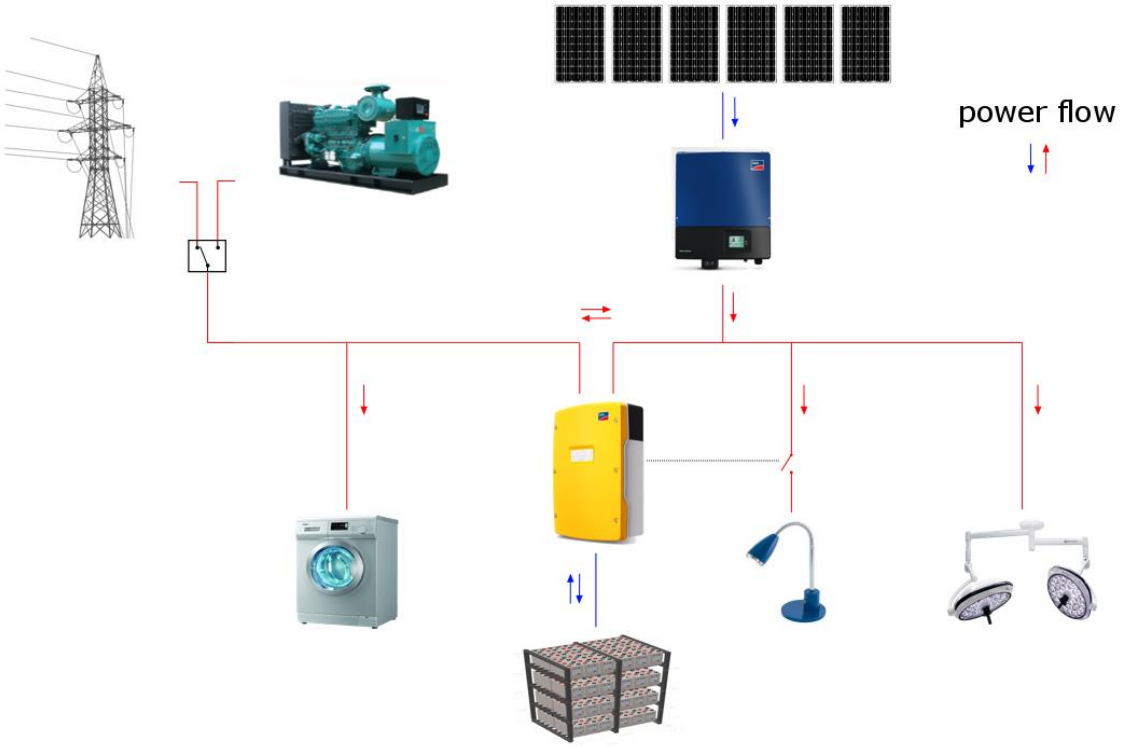

Figure 48 *Logical configuration of the system*

3.4.2.1 Grid or generator connected operation

When there is power available at the *external source* connection of the battery inverter, and the interface device, physically represented by a switch inside the battery inverter, is closed, the Sunny Island inverter is synchronized with the grid or the generator; reference values of frequency and voltage for the grid downstream the battery inverter are those of the external energy source.

The external energy source can be regarded either as a power reserve, or as the primary energy source. If the external source is considered to be the primary energy source, then the battery system represents a back-up energy reserve, and the battery inverter takes advantage of it when a power outage occurs. Alternatively, if the external energy source is regarded a power reserve, the battery inverter synchronizes to it when certain constrains are met. In [29] it is reported that the external energy source can be accessed in the following cases, depending on the settings of the inverter:

1. The battery state of charge falls below a certain threshold, which has been previously set
2. If the power required by the loads exceeds a specified limit
3. When time-controlled operation occurs
4. Because of battery bank charging procedure requests.

When the Sunny Island senses a disturbance in the voltage level of the grid, e.g. in case of a power shortage, the interface device is opened and the grid downstream the interface device starts operating in autonomous, islanded mode.

3.4.2.2 Off-grid operation

When no power from the grid is available, the battery inverter disconnects from it and set up an islanded operation modality. This modality lasts until the generator is manually started, or the utility grid has come back to power. During this phase, the battery inverter sets up an autonomous grid, and provide to serve the loads managing the power fluxes in the islanded grid: if excessive power is produced by the PV generator, then the battery inverter directs it to the battery bank; if not enough power is produced by the PV plant to meet the load, then energy is withdrawn by the battery bank. If the battery bank is at full capacity and excessive power is produced by the PV plant, then the battery inverter regulates the power output from the PV inverters by increasing the frequency of the islanded grid (reference to Figure 47).

3.5 DESIGN PROCESS

3.5.1 Identification of the area to be supplied in off-grid modality

Within the building, different areas with different functions are located, and high-quality and reliable power supply is required with a different degree of priority by the different locations. Power outages could have a modest impact on locations such as kitchen and laundry; on the contrary, a lack of power supply in the medical sections of the building could endangers patient's life.

It is therefore required to understand whether it is feasible and convenient, from an economical and technical point of view, to design a system to guarantee reliable power supply in off-grid mode either to all the locations within the building, or to selected, high-priority locations.

The maximum power required by ISPEMA building is estimated to be approximatively 36 kW. The commercial battery inverters adopted as a reference for this study allow a maximum power output of 8 kW for a single unit, for a maximum of 30 minutes; parallel connection of three units to form a three-phase system makes possible to obtain a maximum power output of 24 kW for 30 minutes, then the power required by the load must decrease to the nominal value of 18 kW. The supply of the loads requiring more power is possible by parallel connection of multiple groups of three-phase systems[8]; each of this group is referred to as a cluster.

In the case of ISPEMA building, a system which adopts components of the kind considered in this study, capable to supply all the building in autonomous mode, would be characterized by a multi-cluster topology. Because of

[8] This analysis does not take into consideration the power available from the PV system, as in cloudy days it would not contribute to supply the loads.

the will to avoid complex configurations, and constraints related to availability of space within the clinic, supplying all the building in a islanded mode not considered as an available option; this would require to adopt a multi-cluster typology, which in turn would require the construction of a dedicated location to house the batteries and the battery inverters.

Advantages of the operation of the entire building in autonomous mode would be the possibility to supply every zone of the building with PV power and with power from the storage in the case of a shortage from the main grid, resulting in increased comfort for occupants of the ground floor. Nevertheless, this requirement is not considered to be of great importance, as many areas of the building (especially within the ground floor) do not include high priority loads, and a lack of power supply for several hours (in the worst case) can be accepted. In any case, it will be explained in a further section that it will still be possible to supply some areas of the ground floor with electricity from the off-grid system, by proper connection of the lines in the distribution boards.

It should be remembered that the two floors of the building are devoted to different functions: the ground floor is (mainly) dedicated to didactical purposes, while the first floor represents the medical section. Plus, most of the high energy-demanding loads is located on the ground floor: iron and laundry machine, kitchen boiler, electrical stove and oven.

These considerations lead to the hypothesis to design a system capable to supply in an autonomous mode all the first floor of the building.

A first verification to validate the feasibility of this hypothesis is that, considering a contemporary coefficient of 0,8 for the load of the first floor of the building, the maximum power required is 23 kW; the entire first floor of the building can therefore be supplied by a single-cluster architecture.

3.5.2 Homer simulations

A microgrid analyzer tool, the Hybrid Optimization Model for Electric Renewables (HOMER), has been used to support the design of the system.

Homer is an economic optimization tool that identifies the architecture characterized by the least Net Present Value, among those capable to meet an arbitrary load. Different possibilities about the components of the architecture are given as input by the user. The software helps in the identification of the most convenient energy sources mix, from an economical point of view, among the possible configurations given as input; for each component of the system, it is possible to consider different sizes for it, by setting different values in the *search space*.

At the same time, this tool allows to identify which architecture, among those given as input to the software, represents a system capable to meet several arbitrary constraints. As an instance, a constraint can be a minimum renewable fraction, or a maximum number of hours of operation for the diesel generator. Homer allows to make sensitivity analysis over the range of values specified for such constraints, and presents the solutions which fulfill the constraints, if found.

3.5.2.1 Preliminary analysis

A preliminary analysis has been done to determine the minimum configuration that guarantees power continuous power supply to the high-priority area.

First, it has been evaluated which is the minimum system size (kWp of PV plant and kWh of electrochemical storage) that allows the operation of the high-priority devices of the medical section in an autonomous mode, for 10 hours, without necessarily recurring to the operation of the generator, under the circumstances of a power shortage of the utility grid. This corresponds to high reliability on the availability of power supply for the medical

section: in fact, the autonomous mode would then be guaranteed even in the event of a failure of the generator. This analysis aims to determine which is the minimum electrochemical storage capacity that must be reserved to the high-priority area, being always charged and ready to supply the loads.

To allow a realistic interpretation of the results, some preliminary calculations have been done. It must be evaluated how much energy is required by the red-zone area for an autonomous operation of 10 hours in the worst possible conditions. The worst case is represented by a power failure during day time, when power requirements are higher, in the event of a very cloudy and rainy day (thus having almost no energy being collected from PV arrays). From load profile estimation, it has been obtained that the red-zone area requires 16 kWh to operate from 8 am to 6 pm. The expected result should not be less than sudden value.

To perform this evaluation, the capability of the software of fixing several constraints has been exploited. A *maximum annual capacity shortage* of 0% has been set, meaning that the system is required to be self-sufficient under the event of a grid power failure lasting several hours (at least 6 hours, as per the parameters set to model the grid; considering the variability of the repair time of 20%, and the randomly-generated periods of black-out which results sometimes overlapped, this corresponds to the request of autonomy for at least 10 hours).

The utility grid has been modeled consistently with the characteristics of the public utility grid in Addis' area. Parameters regarding grid reliability have been modified setting a *mean outage frequency* of 120 times/year, a *mean repair time* of 6 hours, and a *repair time variability* of 20%. A *price* per kWh of 0,028 €/kWh has been set. The load profile of the high-priority area has been given as input; the results of the optimization process are reported below.

Architecture			**Costs**				**Storage**	**Grid**	
PV (kW)	Conv (Kw)	LA (kWh)	COE ($)	NPC ($)	OpC ($)	InCap ($)	Autonomy (hr)	Purchased (kWh)	Sold (kWh)
2	24	21	0,32	42101	1191	26700	11	7341	2058

Table 12 *Selected results of a preliminary Homer analysis*

This simulation shows that the (economically optimized) minimum configuration required to guarantee continuous power supply to the high priority loads of the clinic is of 2 kWp of PV collectors and an electrochemical storage of 21 kWh.

From this analysis, it is assumed that an amount of 21kWh should be reserved to operate the high-priority section of the medical area. This result can be used to set the threshold of intervention for the load disconnecting device, operated by the battery inverter.

3.5.2.2 Optimization of the power generation sources

Homer was then used to find the least Net Present Cost's architecture capable to meet the load requirements of ISPEMA Center. The system has been modeled adopting the following components:

- Generator
- Grid
- PV generator
- Converter
- Lead Acid storage

Being the purpose of the simulation to find the most convenient energy mix to ensure reliable power supply to the Center, the modeling process was intended to represent the actual situation with the highest possible level of fidelity, for what concerns energy generation and supply.

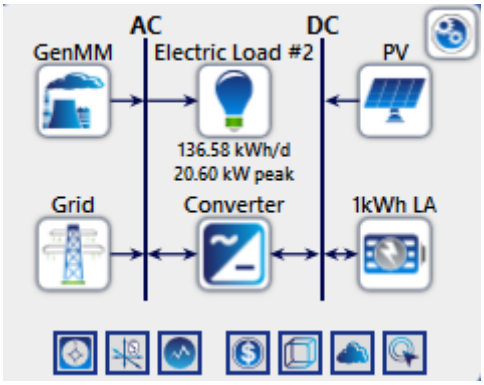

Figure 49 *Homer modeling of the system*

Parameters of the generator were set adopting the values found in its datasheet for fuel curve and nominal power. Schedule constraints have been adopted: forced off from 9pm to 7am, considering that the generator will be located close to the building, to avoid disturbance of night resting. The default parameter of minimum runtime of 60 minutes was kept constant, while the minimum load ratio was set to 30 %. Possibilities offered to the software in the search space were either no generator or the 132kW dedicated to the building. The grid was modeled the same way that was adopted in the preliminary evaluation.

PV generator peak power values entered in the search space have initially been 0, 5, 10, 15 and 20 kWp. Due to the characteristics of the building (roof structure), it is considered as unsuitable the installation of more than 20kWp of PV generators (approximatively equivalent to 80 standard size collectors). The default price suggested by Homer for the *generic flat plate* collector component has been adopted (3000 €/kWp). This value is consistent with the average cost of PV collectors in the African market[30].

The only possibility considered for what concerns the converter has been a 18kW converter; this values represents the nominal power of the inverter, meaning the power that could be provided in continuous operation. As it was explained in a previous section, a bigger size would require to adopt a system's topology which is assumed in this study to be unsuitable. The price for this component has been set to 600 €/kW, consistently with the current market price of SMA inverters.

Values for Lead Acid electrochemical storage initially given as input for the simulation have been: 30, 40, 50, 60, 70, 80, 90 kWh. It is considered that the installation of more than 90 kWh of storage in unsuitable due to the space requirements of such components. The default price of 300 €/kWh has been adopted.

A constraint of 0% of capacity shortage have been set. The renewable fraction has been treated as a sensitivity variable, with values ranging from 0% to 40% scaled by 10%.

Homer offers two predefined controllers that simulate different dispatch strategies. With the *load following strategy* whenever a generator operates it produces only enough power to meet the primary load. With the *cycle charging* strategy generators are operated at their full power, and surplus power is used to serve deferrable load or charging the storage bank. This second option has been chosen, responding to the requirement for ISPEMA's generator to avoid operation at too low load fractions.

The behavior of this architecture has been analyzed with the full load profile of the building. The electric energy required to heat water to meet hot water demand is neglected, as it is supposed that sudden water is mainly produced by the solar thermal plant. A conservative percentage of day to day variability of 30% has been set; in this way, the software considers a peak power requirement of 20,6 kW.

The results of the optimization process are presented in the chart below, where the first column represents the renewable fraction achieved by each configuration, that has been treated as a sensitivity variable.

Sens.	**Architecture**			**Costs [$]**				**Gen**		**Grid [kWh]**	
Ren (%)	PV (kW)	Gen (kW)	LA (kWh)	COE	NPC	OpC	InCap	Hours	kWh	Purchased	Sold
0	0	132	85	0,14	91719	4287	36300	116	4594	48626	460
11	5	132	85	0,15	98630	3661	51300	79	3128	41630	278
24	9	132	80	0,15	100165	2968	61800	45	1782	36132	305
31	**11**	**132**	**77**	**0,16**	**101344**	**2664**	**66900**	**32**	**1267**	**33578**	**577**
42	15	132	75	0,16	109014	2376	78300	20	792	29381	2305

Table 13 *Selected results of the Homer simulation*

3.5.2.3 Discussion of the results

The values given as input to the software allowed it to present alternatives with no renewable sources; in fact, in the search space the possibility of 0 kWp of PV collectors has been considered. It is worth to note that battery bank and inverters are in any case required to avoid any capacity shortage. This is partially due to the constraint of avoiding nigh operation for the generator; in any case a battery back-up system is required to ensure continuous power supply, as the generator could be out of service. Even though the net present cost of the system in correspondence of the 0% renewable fraction system is the lowest, the adoption of this system is discarded as it makes no sense within a context of renewable energy valorization. On the other end, the system with the highest solar fraction which has been considered (40%), leads to the highest amount of energy sold to the grid; considering that during power outages the battery inverter would disconnect from the grid, surplus energy could not be shared and, in the case of fully charged storage, would have to be wasted. Investment costs for this system are the highest.

The chosen configuration is therefore the system composed by 11 kWp of solar generator and 77 kWh of electrochemical storage. This configuration leads to the considerable solar fraction of 31%, while the operation of the generator is limited to 32 hours per year and to the production of 1267 kWh.

It should be considered that the actual behavior of the system during a power shortage from the grid could not have been modeled in the simulation. The actual behavior of the system during a power shortage is the following: the battery inverter would almost instantaneously disconnect from the grid to set an off-grid system supplying all the protected devices. Then, the islanded section of the building would be supplied by solar energy and by energy from the batteries, while the unprotected first floor's load would remain unmet until the generator is manually started, if necessary. After the energy stored in the batteries would have fallen below a certain threshold, the PV inverter would disconnect other loads, accordingly with the configuration of the load-disconnecting devices.

Homer's model of the system differs for two aspects: in the simulation, energy from batteries and PV generator can feed also ground floor's load during a power shortage; the generator is treated as an automatic-starting device, while it is believed that the generator does not have auto starting capabilities (a complete installation

manual could not be obtained). The power that cannot be provided neither by the battery inverter nor by PV inverters in the islanded-modality would therefore be provided by the diesel generator in the simulation.

This different behavior could imply an increased time of operation of the generator with respect to what has been calculated with Homer. This actual amount depends on:

- which loads will be connected to the islanded distribution board; as the majority of the devices were not already bought at the time of the study, the actual load profile and peak power requirements of the building could differ significantly, depending on the difference among the supposed and real power an energy requirements of the loads. It could result that just a small number of high-power demanding loads must be connected upstream the battery inverter;
- the possibility to delay the operation of such unprotected loads until the grid has come back to power.

It is assumed that these differences do not have a significant impact on the results of the simulation and this impact is not considered.

3.5.3 Design of the system with SMA Sunny Design

The PV system is designed with the support of SMA Sunny Design, a commercial tool developed by SMA Company. The first step required by SMA Sunny Design is the choice of the typology of the project; the system for ISPEMA is modelized as an off-grid system, as this modality of operation is required when the grid is unavailable. Values required by the program to characterize the project are: locality, electric link of the system, air temperature, percentage of reduction of the available irradiance out of the maximum due to shadowing of the collectors. The locality of Addis Ababa has been set; the corresponding total global radiation on a yearly basis obtained from the software's database is 1.871,42 kWh/m²a. The electric link of the system has been set to 220/380V, three-phase connection, with a tolerance of ±20%. A maximum asymmetric load of 2 kVA has been considered. The tool then requires to define the load profile. Consistently with the estimation of the total load profile of ISPEMA Center, a value of 48749 kWh of annual electric consumption has been set.

The next step is the setting of the PV generator. From the analysis with Homer, 11kWp is the selected peak power. It is calculated by the software that the required peak power corresponds to 46 modules. The features of the modules adopted by the tool are reported in Table 14 Characteristic values of the PV modules used in the design.

Electrical Features		
Nominal power	240	Wp
MPP Voltage	29,6	V
MPP Current	8,11	A
Open-circuit voltage	36,9	V
Efficiency (STC)	14,75	%
Temperature coefficients		
Open-circuit voltage	-0,31	%/°C
	-114,4	mV/°C
Short-circuit current	0,051	%/°C
	4,31	mA/°C

Table 14 *Characteristic values of the PV modules used in the design*

Successively, the tool requires to size the inverter. The tool offers the possibility to choose the desired inverter manually, alternatively an automatic sizing tool is offered, which calculated the best alternatives in terms either of energy performance or economic profitability. It is suggested in the guide of the tool[28] to sort design suggestions by economic viability, as economic viability takes into account the specific cost of the inverter as well as the energy yield. Anyway, the proposals optimized in terms of economic viability are represented by combination of inverters of the family Sunny Boy, which is not suitable for the installation at the altitudes of the site, as it is warned by the tool. Instead, the optimization in terms of energy yield leads to inverter of the family Sunny Tripower, which are suitable for the installation at the altitudes of the site.

Two solutions are compared; the optimal solution from the point of view of the energy yield is represented by two inverters STP 6000TL-20, each rated 6 kW of nominal power; another solution is represented by the combination of two inverters of the family Sunny Tripower, one rated 5 kW and one of 6 kW.

	Alternative 1	Alternative 2
Inverter	2 x STP 6000TL-20	1 x STP 5000TL-20 1 x STP 6000TL-20
Status	✓	✓
PV modules	46 x .SMA SMA Demo Poly 240	46 x .SMA SMA Demo Poly 240
Total number of PV modules	46	46
Peak power	11.04 kWp	11.04 kWp
Number of PV inverters	2	2
Nominal AC power of the PV inverters	12.00 kW	11.00 kW
AC active power	12.00 kW	11.00 kW
Active power ratio	108.7 %	99.6 %
Max. available PV energy	18,144.70 kWh	18,105.00 kWh
Energy usability factor	100 %	99.8 %
Spec. energy yield	1644 kWh/kWp	1640 kWh/kWp
Line losses (in % of PV energy)	0.22 %	0.44 %
Unbalanced load	0.00 VA	0.00 VA

Figure 50 *Comparison between two suitable solutions*

Alternative 2 is characterized by a slightly minor maximum producibility, and slightly increased line losses. Anyway, alternative 1 is oversized considering the peak power of the plant; this solution is more expensive compared to alternative 2 and the modest increment in system's efficiency does not justify the increased system's cost. Alternative 2 is therefore selected.

The configuration of the inverters is carried on consistently with the possibilities offered by the roof regarding the positioning the collectors. STP-5000 is connected to totally 21 modules, divided in two strings of 10 and 11 modules. STP-6000 is connected to two strings of 10 and 15 modules. This configuration allows an energy utilization factor of 99,9%.

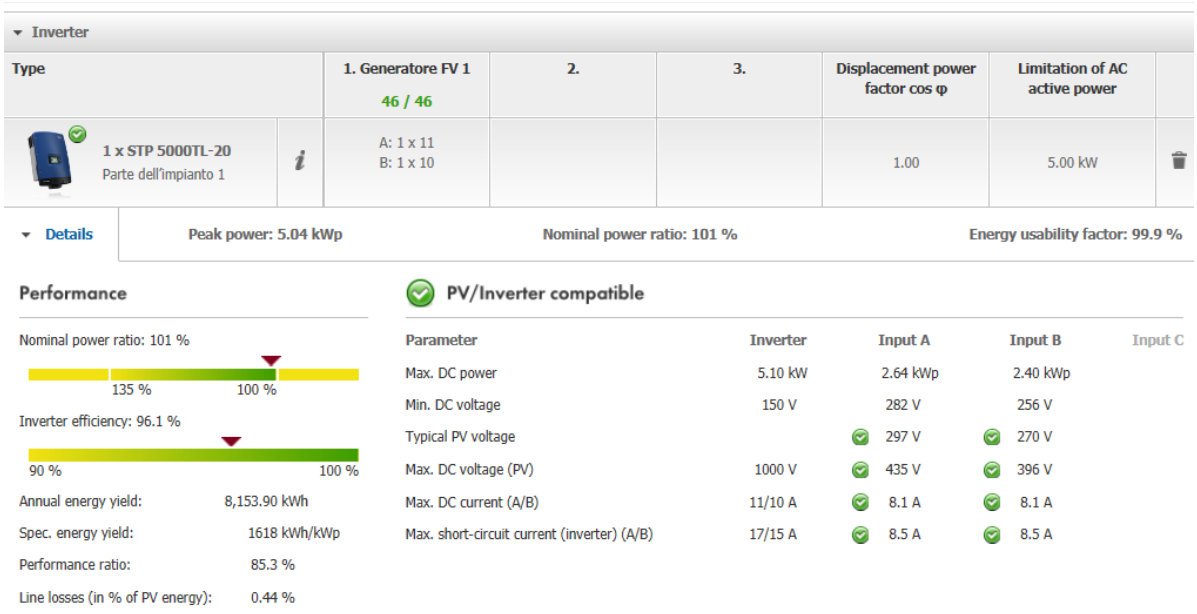

Figure 51 *Configuration of the Sunny Tripower 5000TL-20*

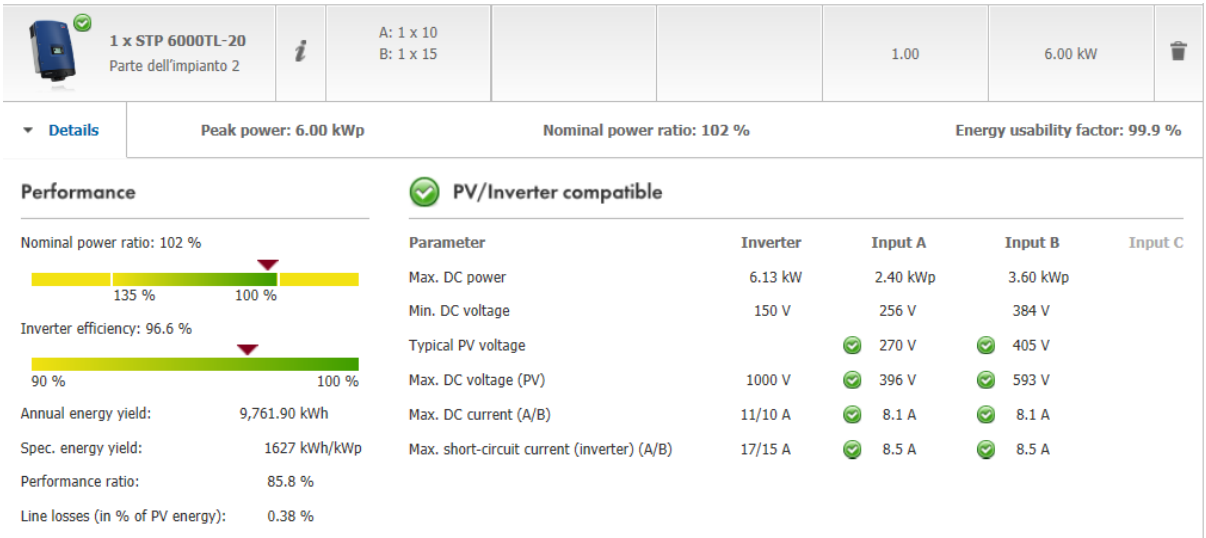

Figure 52 *Configuration of the Sunny Tripower 6000TL-20*

It results from the design process that the performance ratio of the system is 85%; the total annual energy yield is 17914 kWh. The average fraction of the monthly load met by solar energy is is 31 %.

3.5.4 Layout of the electrochemical storage

Different battery typologies are available in the market. It is suggested to adopt lead-acid batteries; the major advantage of this technology is that it is the cheapest battery type in comparison to other available electrochemical storage, while the major drawback is its low specific energy content due to the high molecular weight of lead. Anyway, this is not a problem (beside transportation to the site) considering that their application is stationery. Different manufacturing technologies are available for lead-acid batteries.

Flooded Lead Acid Batteries, also referred as lead-acid vented cells, are characterized by an electrolyte in the liquid phase. These batteries require maintenance usually twice a year to refill the electrolyte with deionized water due to the losses encounter during operation of the battery; this loss is due to water electrolysis, the main side reaction within the cells. Water electrolysis produces hydrogen, which is vented to the atmosphere.

Another typology of lead acid batteries is the Valve Regulated Lead Acid (VRLA), including Gel and AGM (Absorbed Glass Mat) battery design. These batteries are maintenance-free: they do not require water tapping as they are sealed. Small percentages of hydrogen are still released to the atmosphere. Compared to flooded LA, this typology is penalized by a reduced number of cycles; advantages are low maintenance requirements and very low releases of hydrogen.

The proposed location for the installation of the batteries is the under-stair of the ground floor. This location occupies the very central location of the building, and it is only several meters far from ground floor distribution board. Battery inverters should be installed right above the batteries, to allow the shortest DC cables connection. The central disposition of the system limits transmission losses, thus optimizes the efficiency of the system. Other advantages of such location are that the system is readily accessible and could be easily checked in case of trouble-shooting needs.

Being the under-stair location within the same area where occupants of the building often transit, the adoption of a casing for the batteries is recommended for safety purposes. The casing must be necessarily equipped with a forced ventilation system.

As per the optimization process carried on with Homer, the optimum storage capacity is the one that can supply an energy amount of 77 kWh, considering the maximum depth of discharge of LA batteries to be 40% (default value for Homer simulation). Setting the maximum depth of discharge to 50% is beneficial for the storage, and is also the valued adopted in Sunny Design; in this case the nominal capacity of the storage must be increased, in order to allow the storage of 92,4 kWh. In terms of ampere-hour, this value corresponds to 1925 Ah. The capacity of a battery bank depends on the discharge rate, and it decreases as the discharge rate increases. To size the battery bank, a discharge rate of C10 is assumed. From Trojan Batteries datasheet (reported in the Appendix), L16P model has a capacity of 386 Ah at ten-hours rate of discharge.

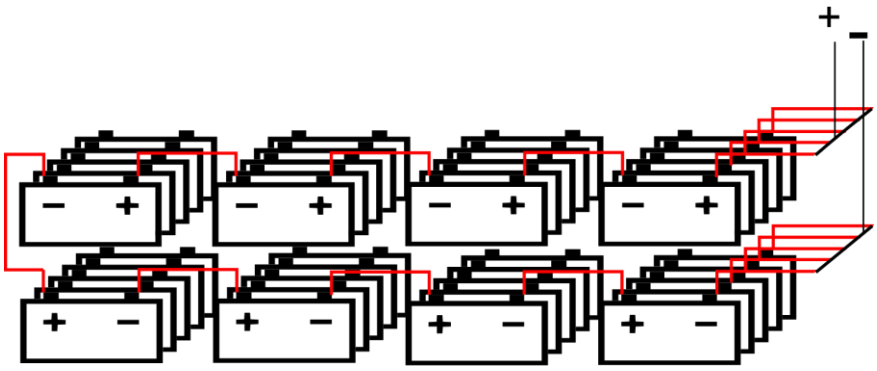

Figure 53 *Representation of the suggested layout for the battery bank*

Connecting 40 units in 5 parallelized rows, each made up of 8 batteries, a total capacity of 1930 Ah would be obtained, and the battery bank would have a nominal voltage of 48 V. Considering that each unit is 29,6 cm long per 17,6 cm wide per 44,6 height, the casing would be characterized by dimensions of 150x120x100 considering to lay out the battery bank as represented in the picture above.

Battery locations and enclosures are to be considered safe from explosions, when by natural or forced ventilation the concentration of hydrogen is kept below the lower explosion limit threshold, which is the $4\%_{vol}[31]$. Standard EN 50272-2, created taking into consideration several European country's national standards, prescribes the minimum air flow rate for ventilation of a battery location or compartment. The required ventilation air flow is calculated with the formula $Q = 0{,}05 \cdot n \cdot I_{gas} \cdot C_{rt} \cdot 10^{-3}$, where I_{gas} depends on the state of the cell, whether it is under float or boost charge condition, and C_{rt} represents the capacity (C10) for cells at 20°C, with voltage of 1,8 mV in correspondence of the maximum depth of discharge. The worst-case condition is represented by the boost charge condition. The calculated ventilation air flow required is $Q = 6{,}22\ m^3/h$.

3.5.5 Integration of the system in the existing electrical installation

The solar project requires the installation of new boards and components. The new components to be installed within the building are:

1. Three battery inverters
2. a battery bank with its relative casing
3. two new distribution boards

With reference to Figure 55, *Protected Loads – High Priority* and *Islanded Area Distribution Board* are the new two boards that have to be installed within the clinic. The devices to be installed on the roof of the building are:

1. 46 PV collectors
2. two three-phase PV inverters
3. relative cabling and structures.

Furthermore, it is necessary to modify the existing board Protected Loads Distribution Board by disconnecting the lines supplying high priority loads to connect them to the new High Priority Distribution Board.

Figure 54 *Rendering of the PV installation for ISPEMA*

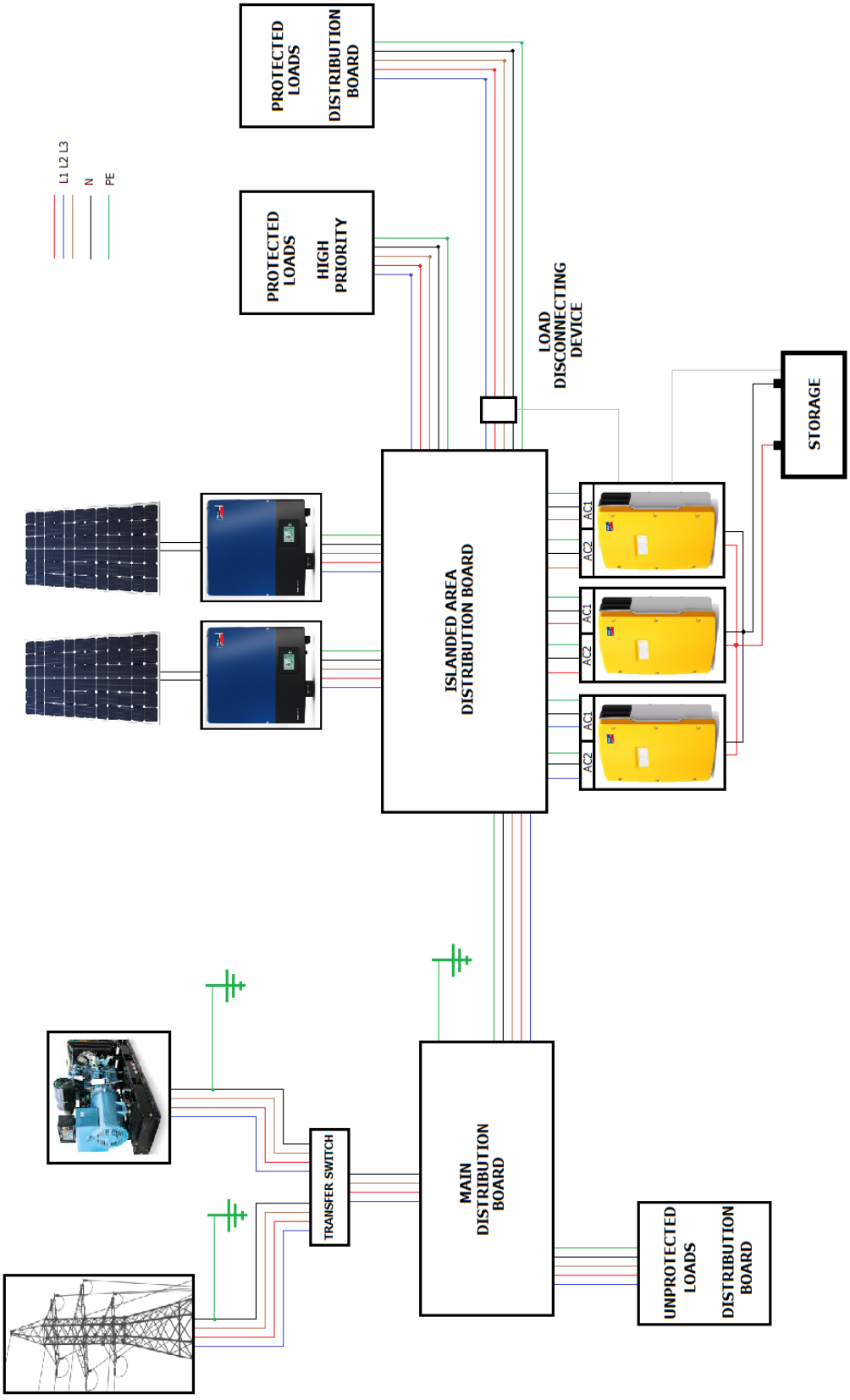

Figure 55 *Outline of PV system's configuration: new boards required*

3.6 ECONOMIC ANALYSIS

The economic analysis of the system is now undertaken taking into consideration current market prices of the components, suggesting several sources where it could be possible to acquire such components. The validity of the Homers simulation resides in the fact that it showed that 11 kWp and 77 kWh of electrochemical storage represent a configuration capable to meet the load of the Center with a renewable fraction higher than 30%. Table 15 Summary of the investment costsresumes the cost of the components suggested for the system.

Component	Unit	Price	Qty	Source
PV modules	kWp	€ 1.440,00	11	Davis&Shirtliff
Battery Inverter SI 8.0H	piece	€ 3.090,00	3	Alma-solarshop.it
PV inverter STP-5000	piece	€ 1.449,00	1	Solar-pur.com
PV inverter STP-6000	piece	€ 1.619,00	1	Solar-pur.com
LA storage Trojan L16	kWh	€ 160,00	77	Wholesalesolar.com
Total	**€**	**€ 40.498,00**		

Table 15 *Summary of the investment costs*

The nominal cash flow has been calculated assuming that an electricity inflation rate of 10% occurs for the next 25 years. Within the operating costs, grid purchases, fuel expenditures and generator maintenance are considered. It is supposed that three battery replacements are necessary, and two converter replacements. The fuel cost is set consistently with current fuel cost in Ethiopia at 0,66 €/l; generator fixed costs are set to 8,8 €/hour while marginal costs at 0,17 €/kWh. With these assumptions, it results that the Net Present Cost of the installation is 9884 €.

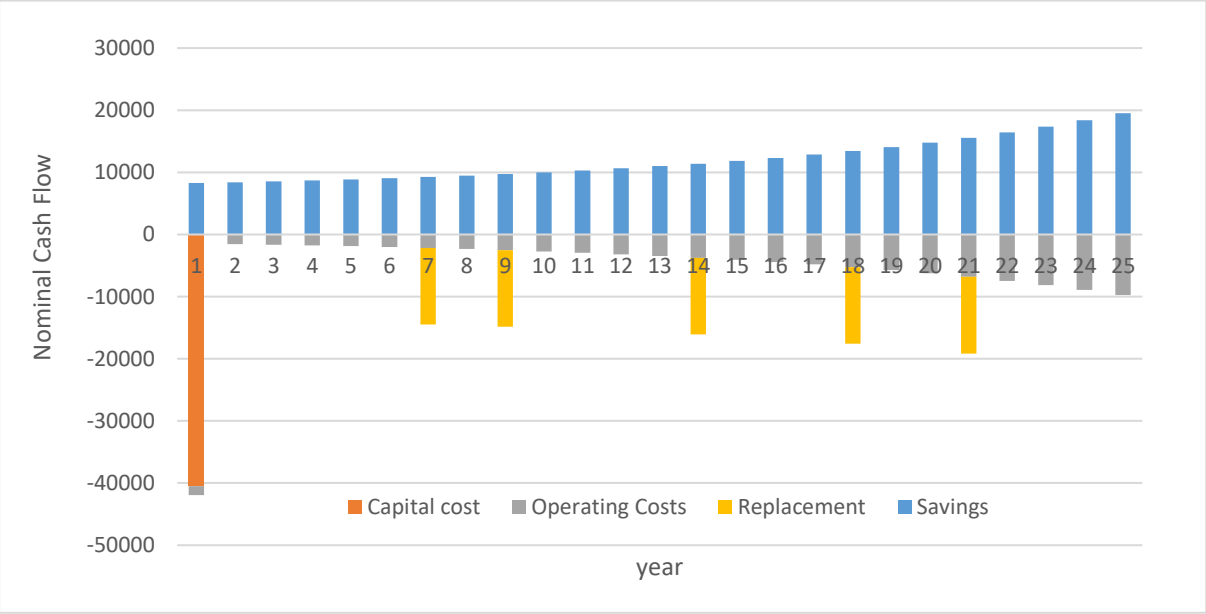

Figure 56 *Nominal cash flow*

3.7 FURTHER PRACTICAL CONSIDERATIONS

3.7.1 Possible extension of the system

The design of the system is based on the load of the Medical Section, meaning the first floor of the building. Design based on the power requirements of the entire building would have required the adoption of a multi-cluster system, which in turn would require the construction of a dedicated location to house the batteries and the battery inverters. As it has been explained in the previous section, supplying the loads of the ground floor with solar energy is still possible by appropriate setting of the battery inverter for what concerns *reverse power settings*. But, in case of power outage from the grid, the battery inverter sets its internal transfer switch to islanded mode and supply of the ground floor loads is not possible anymore. To power up such loads the generator must be manually started. This aspect of the functioning of the system might lead to unpleasant situations, as an instance, the interruption of power supply while the projector is operating to support a presentation, or the unavailability of the lighting system during evening lessons. It is possible to overcome these situations by disconnection of selected lines from the ground floor distribution board, to connect them to the ground floor board, supplied by the battery inverter during power outages.

Considering that at the time of the study no equipment was already installed in the clinic, the actual power requirements of the building could sensibly differ from those that have been estimated, depending on how many devices will be installed, and on their nominal power. If the power requirements of the Medical section of the Building will result to be less than expected, then more loads of the first floor could be supplied by the PV modules in case of power outage. With reference to Figure 55, lines supplied by Unprotected Loads Ground Floor Board could instead be supplied by Islanded Area Distribution Board.

3.7.2 On the operation of the generator

During a power shortage from the grid, the PV system is responsible to supply the high-priority loads, the ordinary loads within the first floor and several dedicated lines of the first floor, while the generator is responsible to supply those high energy-demanding loads such as electrical oven, electrical stove, laundry machine, and to serve the auxiliary heater within the hot water storage tank. Being the loads supplied by the generator not primary loads, and their usage related to fixed hours in the day (e.g. cooking apparatus), the event of a power failure of the grid does not necessarily imply the need to operate the generator. If it results that operating the generator is necessary, then its operation would be optimized if power from the generator would be used for supplying more loads: in fact, the generator is oversized, and a higher load percentage are beneficial for its functioning. Several loads that can be considered as deferrable are: water pumping, complete charging of the battery banks, further heating of the water in the storage tank.

3.7.3 Impact on the system of producing hot water with electrical water heaters

Among the most energy-consuming devices within the clinic there the electrical water heaters used to produce hot water, both for the medical section of the building and for the didactical part. In the first floor, there are 5 water heaters each absorbing 1200W as nominal power; in the ground floor, there is 1 water heater absorbing 1200W and a bigger one of 1500W for the kitchen. The simultaneous operation of such equipment, being of the on/off type, could lead to an increased power absorption of 8,7 kW. In terms of daily energy, it is estimated that the production of hot water with electrical water heaters is responsible of the consumption of 36 kWh out of the total 170 kWh. The functioning of these devices would have a negative impact on the PV and electrochemical storage systems when operating in the islanded mode in moments of low irradiance, as the battery inverter would be required to operate at its maximum power output, and large amounts of energy would be withdrawn from the storage in a short time. It is therefore suggested to discard the usage of electrical water heaters. The necessary hot water can be provided by a solar thermal plant, and delivered to the users through dedicated hot water piping. When not enough hot water is produced by the solar plant, an electric resistor inside the storage tank can further heat-up the water. Alternatively, the boilers could be regarded as back-up water heaters, providing further heating when it is needed, by connection of the hot outlet from the solar thermal system to the cold inlet of the electrical water heaters.

3.8 CONCLUSIONS

3.8.1 Summary of the Chapter

In this Chapter, a photovoltaic with electrochemical storage system is proposed. The actual disposition of the electrical plant of the building is initially analyzed; several proposals to increase the safety and reliability level of the electrical system are outlined. After a discussion about the objective to be met by the system, the load profile estimation is undertaken. A commercial solution for off-grid systems is then described; it has been evaluated which area of the building it is feasible to protect from power outages with off-grid operation. The design of the system is carried on by taking advantage of two software tools. A layout for the battery bank is then proposed, and how it is possible to integrate the system into the existing installation is described.

3.8.2 Results

It resulted from the load profile estimation that the estimated daily electric energy consumption of the Center is 170 kWh, considering hot water to be produced with electrical water heaters; electrical water heaters are responsible of the consumption of 36,4 kWh each day. The most energivorous section of the building is the medical part (first floor) with 82 kWh out of 133kWh (if hot water is produced by the solar thermal plant). An identified commercial solution adopting battery inverters and PV inverters allows the operativity of the plant with three generation sources: PV generator, grid and diesel generator. A three-phase system has been designed, which is composed by: three battery inverters each rated 6 kW, two PV inverters one of 6 kW and one of 5 kW, 40 electrochemical storage units for a total capacity of 1925 Ah (C10). Through proper setting of the battery inverters and proper connection of the load disconnecting device it is possible to guarantee continuous power supply to the high-priority section of the building; a storage capacity of 21 kWh must be reserved to guarantee continuous supply to the high priority area. The annual energy yield of the PV plant is 17914 kWh; this energy supplies the 31% of the annual load. A layout for the battery bank has been proposed; the required ventilation air flow is 6,22 m^3/h. The investment cost of the system is 40500 €; the net present cost of the installation is 9884 €.

4 DESIGN OF A SOLAR THERMAL SYSTEM FOR ISPEMA CENTER

4.1 INTRODUCTION

Several considerations regarding which could be the most suitable system to meet the thermal load of the clinic are hereby presented. First, the location of the clinic does not pose limitations to the installation of a solar thermal system on the ground. A suitable location to place collectors and storage has been recognized in the area surrounding the building, few meters far from its southern façade. This fact represents an advantage considering that the size (hence the weight) of the storage is not limited by the structural characteristics of the building. Secondly, the load profile of the structure for what concerns hot water withdrawal is characterized by a quite constant pattern; it is reported in [21] that a constant load profile has a positive influence on the thermal performance of a passive water heater.

The adoption of a passive water heating system would imply several advantages: the installation phase would be simple and would not require particularly skilled professionals; maintenance needs of the installation would be intrinsically lower than those of pressurized systems due to the lower complexity and presence of less components.

Passive water heaters can be either direct and indirect systems. Indirect systems are adopted where freezing temperatures occurs and a water-glycol solution is required as thermal fluid, or where water conditions are poor and circulation of sudden water in the collectors would result in clogging of the pipes and decreased thermal performances. Indirect systems require a heat exchanger to separate the primary loop from the utilization circuit, thus are more expensive and less performing. The adoption of an indirect system is discarded being the simplicity and economically viability of the installation requirements of primary importance; it is assumed that basic water treating measures (adoption of filters) are effective in increasing the quality of water.

4.2 LOAD PROFILE AND FLOW RATES

The demand of hot water for the building is basically due to:

1. Sterilization and disinfection (laundry)
2. Hot water for hygienic purposes (taps and showers)
3. Production of hot water for canteen service

Normative UNI 11300-2 prescribes the following volumes of hot water at 40°C:

- 80 liters/day·bed for hospital overnight activities with laundry
- 25 liters/day·meal for canteen service
- 15 liters/day·bed for daily hospital activities

Additional hot water withdrawal is considered for preparation of lunch for a daily average of 10 guests and visitors. Considering 10 patients per night, 20 meals per day for patients and additional 10 meals for visitors we obtain:

$$V = 80 \cdot 10 + 15 \cdot 10 + 25 \cdot 20 + 25 \cdot 10 = 1700\ [l]$$

Considering hot water to be delivered at 40°C and average temperature for cold water inlet of 17,5°C, the above calculated number of liters corresponds to an energy amount of

$$Q = \frac{4182 \ * \ (40 - 17{,}5) * 1{,}7}{3600} = 44{,}4 \ [kWh_t/day]$$

Further investigation is needed to estimate the distribution during the day of the withdrawal of hot water. Information from a study[31] conducted in California in recent years provides accurate hourly cold water use data for different typologies of public and private facilities; water consumption in hospitals has been analyzed. It is assumed that hot water consumption is proportional to cold water consumption, thus the shape of the load profile found in sudden study is suitable for the clinic as well.

The study revealed that hospital water use shows two peaks at 10:00 AM and 2:00 pm; 51% of the total daily use occurs between 8:00 am and 4:00 pm; approximately 18% of the daily water use occurs between 2 pm and 5 pm. This information is contextualized for the clinic under analysis supposing that hot water for laundry is withdrawn in correspondence of the peaks. No canteen service is considered in this profile and hot water needed for canteen purposes has not been considered yet. It is assumed that hot water in the kitchen is used from 11 am to 2 pm, and from 6 to 9 pm; it is needed both for meals preparation and for cleaning. A total amount of 0,75 m^3 is withdrawn with a constant rate of 125 l/h during sudden hours. The graph below represents the estimated load profile of hot water consumption for ISPEMA. It is assumed that no hot water consumption occurs during the night.

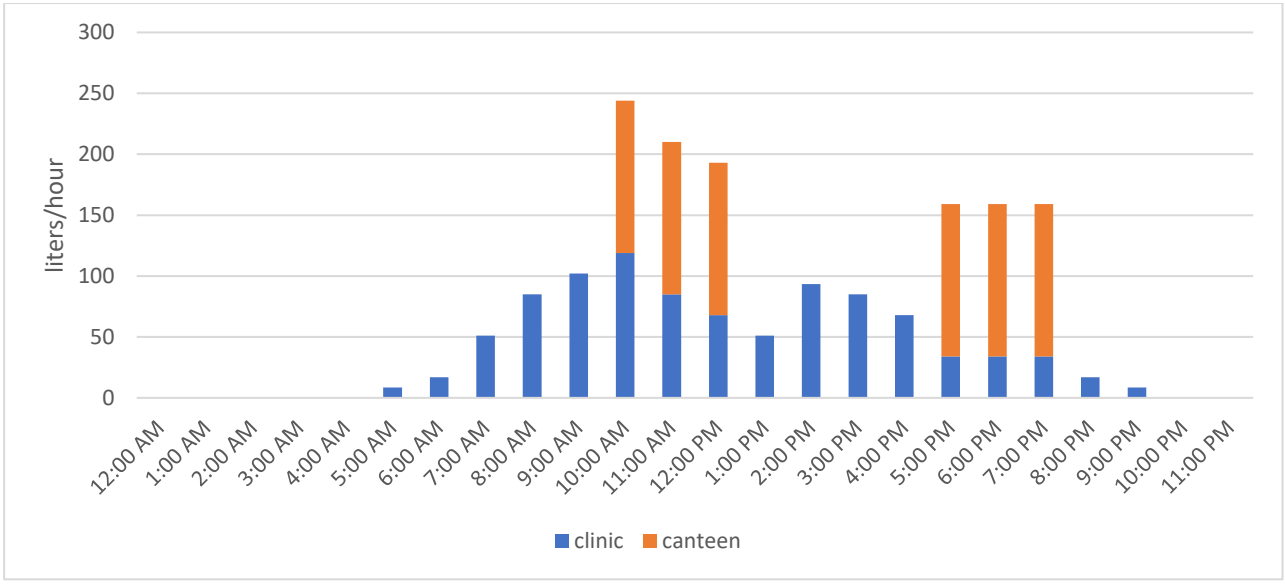

Figure 57 *ISPEMA hot water withdrawal daily profile*

4.3 ESTIMATION OF THE SYSTEM'S PERFORMANCE

Estimating the thermal performance of thermosyphon systems implies additional difficulties compared to forced circulation systems. The thermally driven circulation requires the simultaneous solution of energy and momentum transport equations[32]. Several approaches have been proposed for the analysis of performance of thermosyphon hot water systems, which can be divided in the categories of simplified models, performance correlations and rigorous simulation models[33].

Among the simplified models, the ΔT model estimates the daily system performance of a passive heater, exploiting the experimental observation that, for a multi-pass solar water heater, the difference in the fluid temperatures at the inlet and outlet of the collector is constant[33]. This model requires to assume that no water is withdrawn from the system during the insolation period, meaning that the system is intended to produce hot water for withdrawal either in the evening or early in the morning, as it is the case for common domestic hot water use profiles. Considering the pattern of the clinic's estimated load profile, this model is considered unsuitable. For the same reason, the monogram chart developed by Norton et al.[33] is considered unsuitable.

Being a detailed simulation of the system behind the purpose of this study, the estimation of the performance of the system is done with the approach explained in the following section. A suitable size for the system is found by the application of Life Cycle Solar Savings optimization criteria, processing the estimated solar fractions for different system' sizes.

The system efficiency for passive water heaters is influenced by the pattern of the hot water withdrawal[21]. In particular, the efficiency of the system when no load occurs is lower: due to water mixing inside the tank, water at the inlet of the collectors is at increasingly higher temperature during the day, as no cold-water replacement in the tank occurs. Being the fluid in the collector circulating at higher temperature, higher losses to the ambient are encountered; at the same time, higher losses occur from the tank.

On the contrary, when cold water replacement in the bottom of the tank occurs, lower losses are encountered, and the system's thermal efficiency is higher. Anyway, it must be noted that the system's thermal efficiency is not well representative of the whole system performance[34]. Considering that hot water must be delivered at a temperature above a certain value (above 40°C in this case), and considering that experimental investigation proved that an increment of approximatively 10°C occurs after a single pass of the water in the collector, to obtain useful heat from the system the whole mass of the water in the tank must pass several times through the collector, depending on the temperature in the tank at the beginning of the process. Depending on the application, accepting that the system is working under non-optimal efficiencies might be compulsory to obtain useful heat.

A possible simplified approach to estimate the useful gain from the system could consist in adopting a value of typical efficiencies for these installations, and multiplying this efficiency by the daily average radiation for the site investing the total collectors' surface; values found in the literature are in the range of 0,4 to 0,6[21]; in [7] is stated as the overall system efficiency for a domestic passive solar system are in the order of $\eta = 0{,}3 \div 0{,}4$. This approach would not allow any sight on the dynamic of the heat exchanges from the system to the load during the day, thus another approach is adopted, and these values of efficiency are then used to verify the results.

To estimate the useful heat delivered to the load during the day, it has been assumed that a constant temperature difference of 10°C between the outlet and the inlet of the collector occurs under every level of irradiance. This assumption is justified by experimental evidence in [32], where it was shown that the temperature difference between the outlet and the inlet ranges between 5 and 15°C depending on incident radiation.

Solar irradiance levels are discretized during the day, and it is assumed that within every hour irradiance level is constant and equal to the average value for that hour.

A temperature of 30°C is assumed for the water in the storage in the morning, when the sun starts to shine. This approximatively corresponds to the situation where 1 m^3 of water stored in a tank whose loss coefficient is 10 W/m^2K has been charged the day before until the temperature of 50°C, and be exposed to 10°C air temperature for 12 hours.

With these assumption, it is possible to calculate the thermosyphon flow rate for the first hour of sunshine, with the formula

$$\dot{m}_1 = \frac{A_C F_R [I - U_L(T_i - T_a)]}{c_p \Delta T_f}$$

, as it is reported in [35].

Under such conditions, the heat gain at the end of the first hour of sunshine is

$$\Delta Q_1 = \dot{m}\, \Delta T\, C_P$$

and the increment of temperature of the water in the tank, which is supposed to be fully mixed, at the end of the first hour of sunshine, is

$$T_f = T_i + \frac{\Delta Q_1}{M_T\, C_P}$$

Water withdrawal by the load is treated like if the total amount of water required were withdrawn at the end of the hour. Regardless of requirements on minimum temperature of delivery, water is withdrawn even if it is not hot yet; this corresponds to the situation where the tank is supplying hot water lines to the building, and is connected upstream to an auxiliary water heater which provides further heating when it is necessary.

The presence in the system of a tempering valve downstream the hot water outlet from the storage tank is modelized by limiting the amount of hot water withdrawn by the load, M_h, in the case that the average temperature of the storage tank is above the threshold of 43°. From an energy balance between inlets and outlet of the tempering valve, it follows that hot water withdrawn by the load is reduced by the quantity $M_h = M_L \cdot \frac{43-17}{T_t-17}$, where M_L is the total quantity of water required by the load at 43°C.

When water withdrawal occurs, the amount of hot water required by the load is replaced by the same amount of water from cold supply at the temperature of 17°C. Thus, the temperature in the storage decreases, and, supposing instantaneous mixing in the tank, the temperature in the tank after withdrawal is

$$T_z = T_f - \frac{M_h}{M_T} \cdot (T_f - T_{cold})$$

Then T_z represents the temperature at inlet of collectors for the following hour of sunshine; this value, jointly with solar irradiance, allows to calculate the value of thermosyphon flow rate for the next hour.

Heat provided by auxiliary heating at the end of the first hour can be calculated as

$$Q_{aux} = M_L c_p (T_L - T_f)$$

if $T_L > T_f$, $Q_{aux} = 0$ otherwise.

This procedure has been adopted to calculate the values of Q_{aux}, T_f, T_z, ΔQ,for every hour of sunshine. These calculations have been applied with the average daily irradiance profiles for every month in a year, for different collector's total area. The results are presented and discussed in the next section.

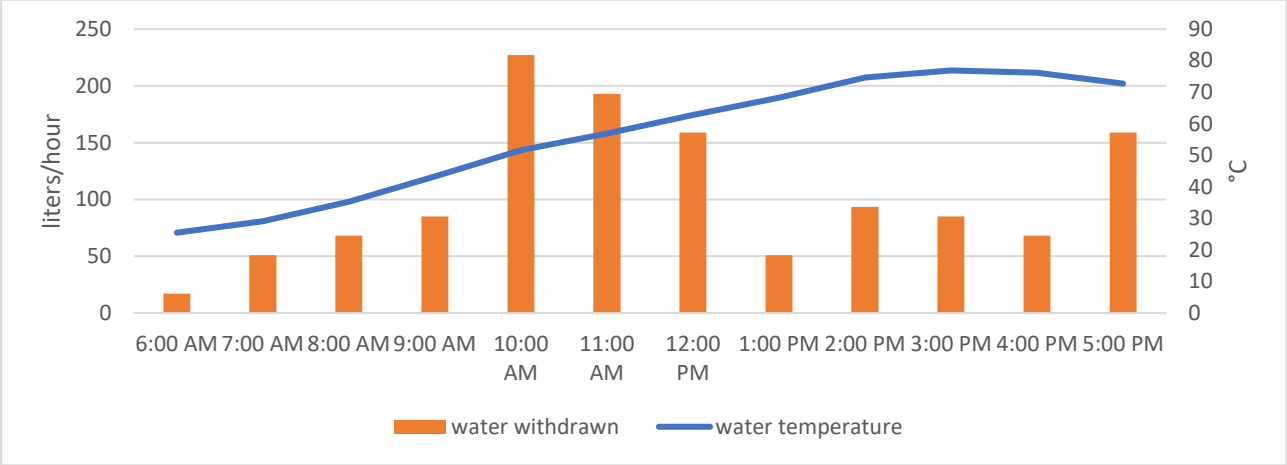

Figure 58 *Daily evolution of water temperature in the storage tank and hot water withdrawal by the load (February, 16 m^2 collectors, 1 m^3 storage)*

4.4 SIZING THE SYSTEM

Through the proceeding outlined in the previous section, the total heat provided by auxiliary heating was calculated for different total collector's area on a yearly basis. The annual solar fraction can be expressed as

$$F = 1 - \frac{Q_{aux}}{Q_{tot}}$$

The graph below represents the results obtained for different collector's total area.

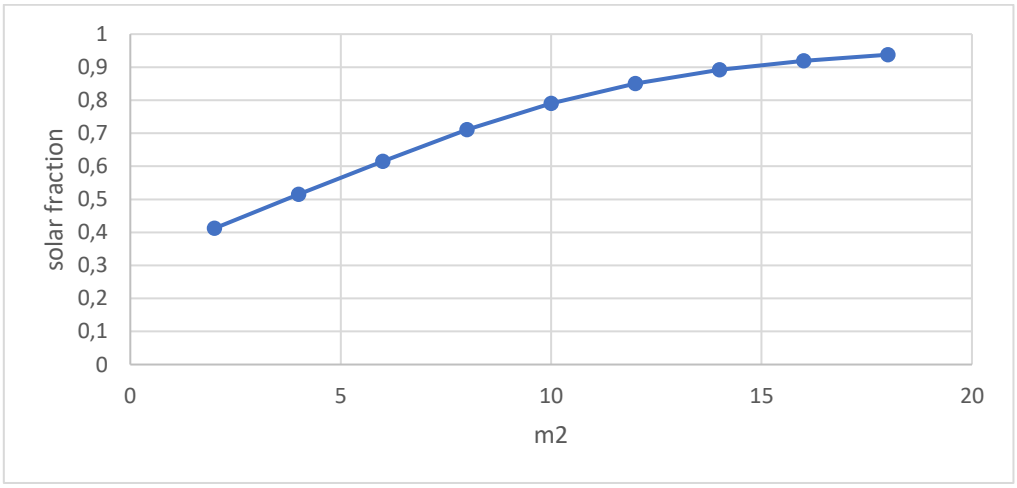

Figure 59 *Solar fraction for different collector's area*

To find the optimum size for the system, Life Cycle Solar Savings economic figure of merit was considered, and P_1P_2 method was used to maximize it; this method is described in the Appendix. The economical optimization criteria of Life Cycle Solar Savings requires to analyze the cost of the installation for different system sizes, hence, to carry on this evaluation, the cost of the installation must be categorized as fixed costs and area dependent costs. Estimating 140 $€/m^2$ for area dependent costs (collectors and storage tank), and 1000 € for area-independent costs (mounting structures, circulator, piping, thermostatic valve, stop valves), the application of P_1P_2 method shows that the optimum size is of 12 m^2; anyway, the range between 10 and 16 m^2 can be considered as optimal.

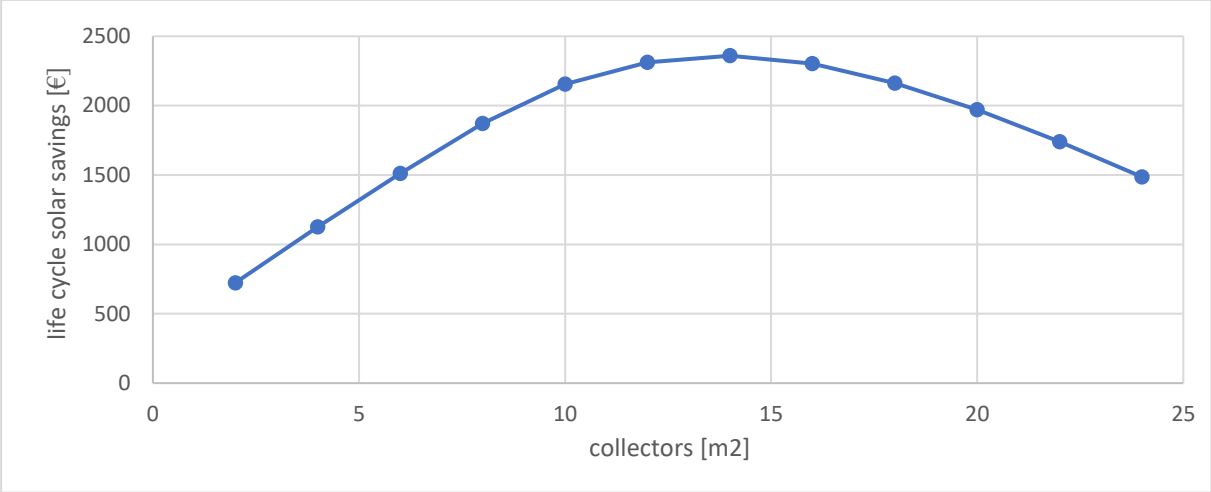

Figure 60 *Life cycle savings: results of the application of P_1 P_2 method*

As it will be discussed in section 4.6.3, the proceeding used to estimate the thermal performance of the system might have led to overestimate it, then the system is slightly oversized and the chosen total collector's area is 16 m^2. The calculation of the life cycle solar savings for a total area of 16 m^2 and a storage tank of 1 m^3, considering 10 years of useful life, leads to the value of 2161 €. The payback time of the installation, considering the method adopted in section 2.6, is 6,13 years.

4.5 PROPOSED LAYOUT OF THE INSTALLATION

The picture below represents a frontal view and a section view of the proposed layout of the installation.

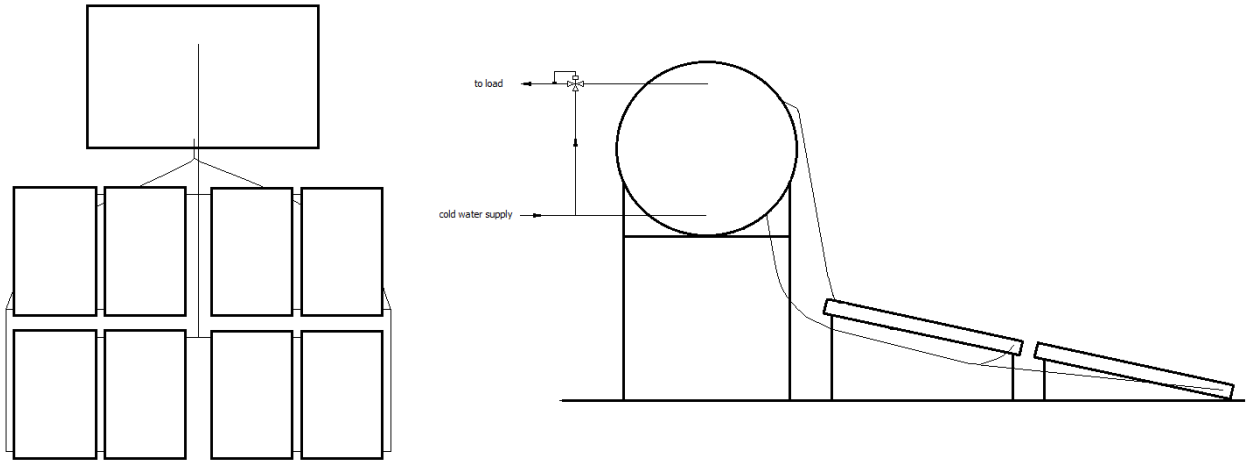

Figure 61 *Proposed layout of the installation*

Eight flat-plate harp absorber collectors are laid on a mounting structure and tilted at 14° towards south. All the collectors are parallel-connected; collectors are grouped in pairs: a pipe from the bottom of the tank serves cold water to the lower inlet of collectors; hot water rising through the collectors is gathered by a central pipe that convey it to the upper part of the storage tank. A storage tank of 1 m^3 is placed above a mounting structure; the tank is served by cold water main supply, and delivers how water to the load through a hot water outlet. A tempering valve is placed downstream the hot water outlet to prevent delivery of hot water at temperatures above 43-45°C, to prevent scalding of the users.

4.6 CONCLUSIONS

4.6.1 Summary of the chapter

First, it has been discussed which is the most suitable system configuration to meet the thermal load of ISPEMA Center. The load profile for hot water consumption was then calculated. An estimation of the system's performance has been undertaken, considering several methodologies proposed in the literature. The installation was then optimized by maximization of the life cycle solar savings; a layout for the system has been suggested.

4.6.2 Results

It is proposed to adopt a thermosyphon system configuration, to take advantage of its simple and economic installation. It has been estimated that the daily hot water requirements are of 1,7 m^3; by estimation of the performance of the system, carried on exploiting the practical evidence of a nearly constant temperature difference between the outlet and the inlet of the collectors, it has been calculated that 16 m^2 of collectors and a storage tank of 1 m^3 allows a solar fraction of 0,9. The estimated cost of the installation is of 3240 € for components only. The payback time is 6,13 years.

4.6.3 Discussion of the results

It has been assumed that the total flow rate is equal to the sum of the flow rate due to the single collectors, meaning that no additional friction and head losses occur due to the piping connecting several collectors in parallel. This assumption can lead to overestimation of the system's performance. To compensate this assumption the system was slightly oversized with respect to the optimal size from the economical point of view.

It is assumed that the temperature difference between the hot outlet and the cold inlet of the collectors is constant during all the insolation period. It has been experimentally verified [32][33] that the temperature difference between collector's outlet and inlet ranges between 5°C and 15°C; a constant value of 10°C has been chosen; this value is also adopted in [35].

5 FEASIBILITY STUDY OF AN ENERGY RECOVERY SYSTEM FROM THE WATER DISTRIBUTION NETWORK

As the campus is located on a decline, whose average slope is 11% from north towards south, there is a height difference up to 30 meters from the water reservoir (located in the uppermost side of the campus) to the furthest building towards south. Water in the distribution network has a pressure higher than it is necessary to supply the buildings, therefore the idea of recovering energy from water piping has been considered.

A practical way to operate this energy recovery would be the interception of a water pipe to deviate the flow towards a turbine, that extracts energy from it by converting surplus pressure into mechanical power. The connection of the turbine to a generator would allow the supply of electrical power to the grid of the campus. After pressure reduction, the flow is redirected to the water supply pipe.

5.1 INTRODUCTION ON PATS

Considering the modest producibility expected from this installation, the investment costs of an ad-hoc designed turbine would not be justified. The system can be realized with much lower investment costs by the adoption of a standard pump operated in reverse mode, both for fluid direction and direction of rotation. This kind of installations are referred as pumps-as-turbine (PATs). The major fields where PATs are used are energy recovery systems, and power supply to remote areas.

For what concerns energy recovery from water distribution systems, the adoption of PATs can substitute or integrate the adoption of pressure reducing valves. As water distribution systems have problems of leakage, the pressure control is fundamental for an optimized and sustainable system management[36]; the adoption of a PAT allows at the same time to recover energy and to keep pressure levels within acceptable limits.

Micro-hydropower systems are attractive solutions for electricity generation in remote area, as such systems can be installed even on small streams, without recognizable effects on the environment[37]. While the running cost of such plants is low, initial capital cost is instead relatively high, when a turbine is required. By reducing the equipment cost in micro hydropower projects, these can become more useful and easily accessible; PATs represent in these terms a valuable solution.

The main advantages of PATs over conventional turbines includes the availability for a wide range of heads and flows, great availability of standard sizes, low cost, easy availability of spare parts such as seals and bearings, and easy installation[37]. At the same time, the adoption of a PAT presents some issues, such as the difficulty to accurately predict the performance of the pump when operated as a turbine, low partial-load efficiency and no hydraulic control.

5.2 EVALUATION OF THE MOST SUITABLE LOCATION FOR THE INSTALLATION OF A PAT

The first step in this evaluation study has been the analysis of the water distribution system of the Campus, to identify the most suitable location for the eventual installation of a PAT.

The water distribution system is made up by HDPE pipes of pressure class PE16, in the diameters of 110, 75, 50 mm. A water reservoir of 70m^3, composed by seven tanks of 10m^3 is in the upmost side of the campus and is supplied by two sources: public water supply and water lines from two boreholes, located in the southern side of the Campus.

The elevation of the water reservoir is 2302 m asl. Assuming a constant value for the level of water in the reservoir of 2m above the bottom of the tank, the piezometric height is fixed at 2304 m asl.

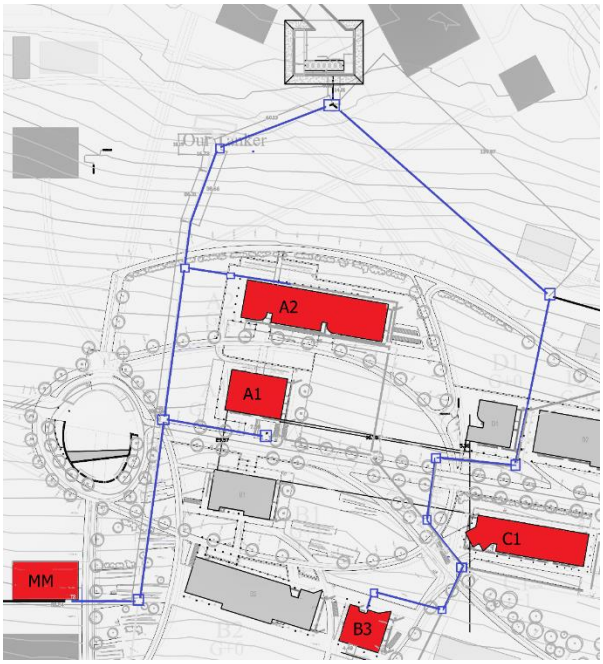

Figure 62 *Potable water distribution network of the Campus*

The elevations of the other buildings considered in this evaluation jointly with the altitude difference from the reservoir to the bottom of the buildings are resumed in Table 16 Resume of buildings' altitude differences from the main reservoir.

Building	Altitude	ΔH
A2	2292	12
A1	2284	20
MM	2273	31
C1	2279	25

Table 16 *Resume of buildings' altitude differences from the main reservoir*

The pipes that might offer considerable amount of pressure to recover are those supplying MM and C1 building (dormitory). However, it must be noted that C1 building is approximatively 8m height and there is a need to leave enough pressure to the fluid. Furthermore, increased head losses are encountered in the pipe supplying the dorm compared to that supplying the Clinic, due to longer piping and curvy path. The possibility to install a PAT at the bottom of the building is therefore discarded.

The feasibility of installing a PAT that intercepts the flow towards the Clinic (MM building) is instead further analyzed.

5.3 ESTIMATION OF THE PRODUCIBILITY

A preliminary calculation is done to estimate the maximum expected producibility of the PAT. The useful head, neglecting frictional losses in the pipe, is set to 16 m, considering that at least 15 m should be left to the fluid for serving the building with the minimum pressure required. Considering the potential energy of a mass of water of 3815 kg at 16 meters above the reference height value, we obtain

$$E_P = \frac{M \cdot g \cdot \Delta h}{3600} = 166{,}334\ [Wh]$$

Which is the maximum potential energy that could be converted into electrical energy neglecting losses. Such modest amount of energy is insignificant in terms of contribution to the energy supply of the campus. The evaluations are therefore carried on with the consciousness that such system could serve as a demonstrative installation on the operation of micro-hydroelectric plants.

5.3.1 Daily water consumption

A total daily water consumption of 3815 liters have been estimated for week days, while an amount of 1965 liters for Saturdays and Sundays. This values have been calculated assuming the daily water requirements per typology of user resumed in the chart below.

User	L/day	N. of users	
		Working day	Weekend
Resident staff	80	3	3
Students	15	30	0
Staff	25	5	0
Clinic patients (bed)	150	10	10
Clinic patients	10	100	10
Clinic staff	25	20	5
total liters		**3815**	**1965**

Table 17 *Daily water consumption of ISPEMA Center*

5.3.2 Load duration curve

To estimate the distribution during the day of water withdrawal, hourly data of water consumption for public hospitals found in the literature have been adopted. To consider a day-to-day variability the hourly values of flow rate have been multiplied by a randomly generated coefficient in the range of 0,8÷1,2. Figure 63 represents the duration curve obtained in this way.

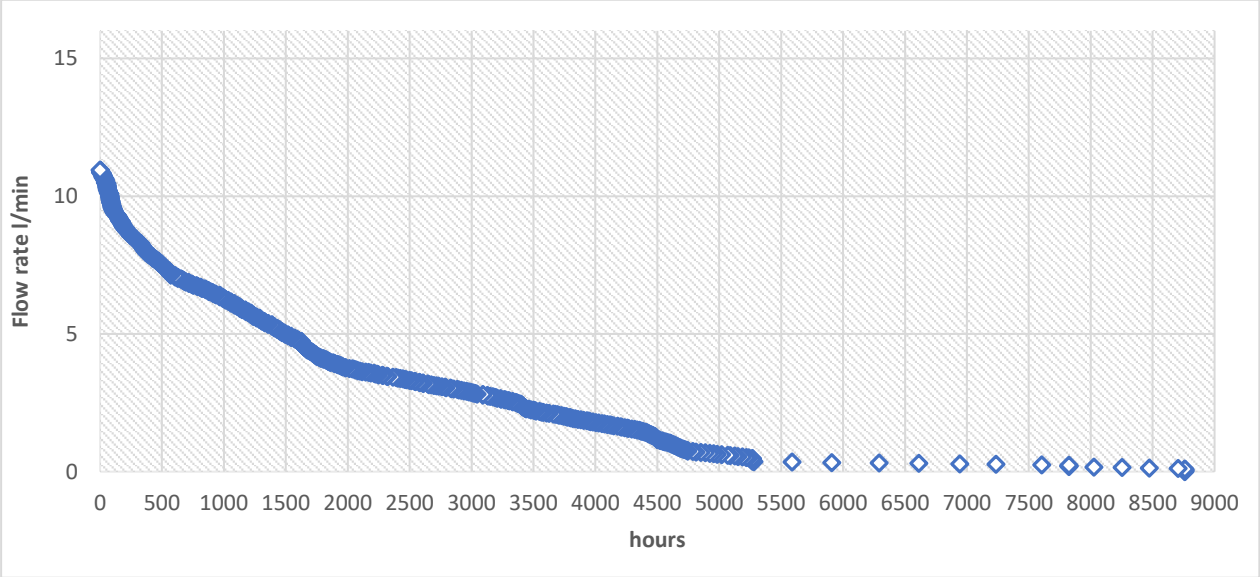

Figure 63 *Flow rate duration curve for ISPEMA Center*

5.4 ENERGY AND POWER EXTRACTED FROM THE MACHINE

The operation of the PAT would be greatly influenced by the way that water supply to the Clinic is managed. Two water reservoirs of 2,5 $m^3$are installed on the roof to supply cold water to the building. A first possibility in the management of water supply is to use the water from the tanks on the roof, and refill them through the main pipe when water level falls below a certain value. A second possibility is to consider the water tanks as auxiliary reservoirs and to supply the users directly through the pipe from main reservoir; if the water reservoirs on the roof are to be considered as auxiliary/emergency supply, then the flow in the pipe to the Clinic varies depending on demand. The typical flow rates (see load duration curve) in this case would be modest: below 5 liters/min for 7260 hours; the power extractable from the machine would then be approximatively 13W neglecting losses. This installation could eventually represent a charging point for a battery: the hydraulic machine could be connected to a dynamo which could charge the battery with DC current. The energy accumulated could then be used to supply a LED light in night time.

This section further analyses the behavior of the system in the hypothesis that the water reservoirs on the roof of the building are refilled once at the end of the day. In this case, the flow rate in the supply pipe, hence the flow rate of the turbine, is not depending on load requirements, and can be fixed at the optimal value for recovering energy from the fluid.

The net specific energy across the machine can be calculated [38] as

$$E = \frac{p_1 - p_2}{\rho} + \frac{v_1^2 - v_2^2}{2} + g(z_1 - z_2) \quad \left[\frac{J}{kg}\right]$$

Where subscripts 1 and 2 refer respectively to high and low pressure side.

The height difference between high and low pressure is neglected, thus the third term in the right side of the equation is null. Considering that the pipe upstream and downstream to the machine has the same diameter, velocities v_1 and v_2 are equal, thus also the second term in the equation is null. Pressure p_2 should not fall below the minimum pressure required at the basement of the building. Its value can therefore be fixed; no unknown terms are left in the equation and the energy gain through the machine can be calculated. Hazen-Williams formula can be used to calculate frictional losses occurring in the pipe, and reducing the available head. The formula is expressed in the form

$$f_H = \frac{10{,}67}{C^{1{,}85}} \cdot \frac{Q^{1{,}85}}{D^{4{,}87}} \cdot L \ \ [m]$$

Plotting head losses as function of the flow rate, considering:

- The internal diameter of the pipe $D = 0{,}0788\ m$
- The total length of the pipe $L = 228\ m$

the following graph is obtained.

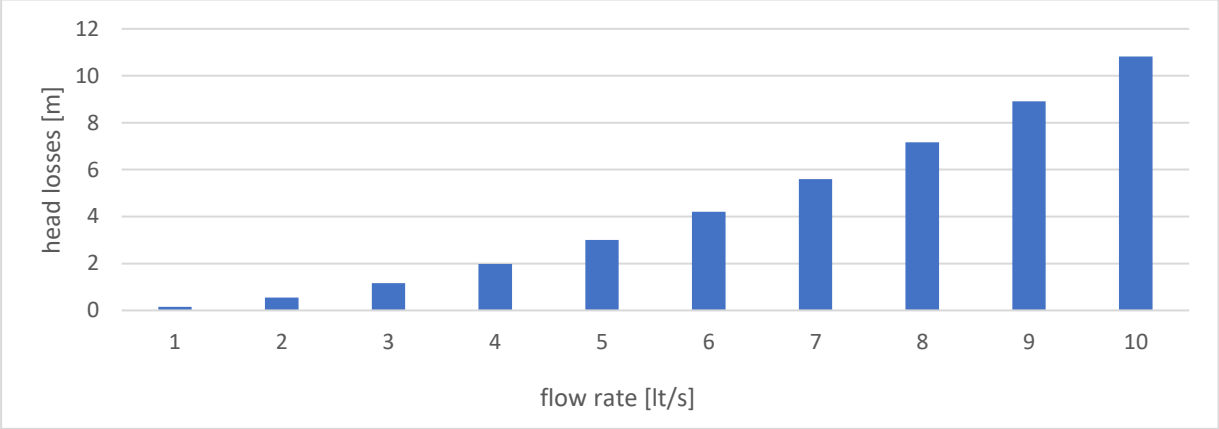

Figure 64 *Head losses in the water distribution pipe as a function of the flow rate*

Considering that a head of 15 meters must be residual at the low-pressure side of the PAT, the available specific energy of the fluid decreases as flow rate increases. Specific energy is calculated as follows:

$$E = \frac{p_1 - p_2}{\rho} - g f_H \ \ \left[\frac{J}{kg}\right]$$

While the theoretical power:

$$P = E \cdot \rho Q \ \ [W]$$

Assuming as global efficiency of the system $\eta = 0{,}7$ the corresponding values of electrical power and energy allowed by the system are presented in the graph below.

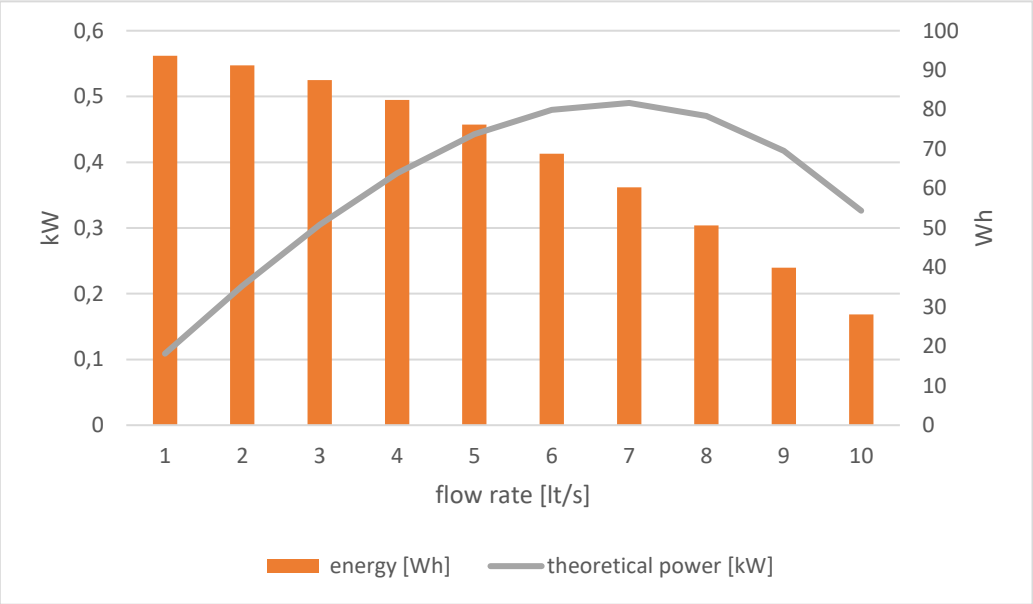

Figure 65 *Electrical energy and power output as a function of the flow rate*

5.4.1 Selection of the pump

The method of Sharma can be used to determine the required pump characteristics[38], exploiting the following formulas:

$$Q_t = \frac{N_t}{N_p} \frac{Q_{pBEP}}{\eta_{pBEP}^{0,8}}$$

$$H_t = \left(\frac{N_t}{N_p}\right)^2 \frac{H_{pBEP}}{\eta_{pBEP}^{1,2}}$$

The required turbine speed is related to the synchronous speed of the induction generator, which is in turn depending on the number of poles of the machine. Considering the frequency of the grid to be 50Hz, for a 2-poles machine the synchronous speed is 3000 rpm while for a 4-poles machine it is 1500 rpm.

5.4.2 Operation of the system

In most site installations, PATs are coupled with an induction generator. The direct coupling of an induction machine simplifies the installation and extends its life, since no gear nor belts are needed, the lateral forces are minimized and no shaft bearings are needed. This kind of machine is low cost, especially when compared to synchronous generators[39].

When the flow rate decreases, the turbine loses power. If the power input to the generator falls still more, the synchronous speed of the generator is reached, then no power is supplied to the grid. Further decrease of the flow rate makes the turbine to be driven by the generator: electrical power from the grid is converted to mechanical power by the induction machine, which is now operating as a motor. The turbine acts as a pump, as it gives energy to the fluid. To avoid this situation, a reverse power relay can be installed to protect the generator[39]; this device would open the circuit when power-withdrawal from the grid is sensed.

The opposite situation is when the flow rate rapidly increases and the impeller is accelerated. At approximatively 102% of the nominal speed the generator is at full capacity. Further increase of the speed occurred by excessive power input from the turbine would result in loss of stability of the generator.

5.5 CONCLUSIONS

From the analysis carried on in this Chapter, it resulted that the installation of a PAT in the water distribution network of the Campus could eventually represent a demonstrative installation; the contribution to the electrical system of the Campus, in terms of energy supplied, is neglectable. Nonetheless, the installation of a hydraulic machine that, through connection to a dynamo, could charge a battery and store energy for suppling a LED light can represent a valid didactical experience.

6 CONCLUSIONS

In Chapter 2, the design of solar thermal system to produce hot water for the showers of the dormitory of the Campus is presented. It has been estimated that the maximum monthly thermal load is of 2465 kWh_t, and occurs in December; considering that the presence of the students in the Dormitory varies during the year, it results the annual thermal load is of 22,265 MWh_t. From the comparison between the required investment costs for a forced circulation and natural circulation system, it resulted that a forced circulation solution is economically preferable for meeting a solar fraction higher than 50%. A forced circulation solution has therefore been recommended. An indirect drain-back configuration is suggested, to protect the system from overheating and ensure a longer operativity life of the plant. By application of the f-chart method and Life Cycle Savings optimization criteria, it was found that the optimal size of the system is of 24 m^2 of collectors. It was then verified that a total amount of 2 m^3 of storage is adequate to supply the peak period of the load. The percentage of the total thermal load, on a year basis, supplied by solar energy is 81%. The estimated investment cost of the system for components only is 8920 €. Considering the cost of the material only the payback time for the installation is 10,6 years.

In Chapter 3, a photovoltaic system with electrochemical storage is proposed. The actual disposition of the electrical plant of the building has been analyzed; several proposals to increase the safety and reliability level of the electrical system have been outlined. A commercial solution for off-grid systems is then described; it has been evaluated which area of the building it is feasible to protect from power outages with off-grid operation by adoption of sudden commercial solution. A layout for the battery bank was proposed, and how it is possible to integrate the PV system into the existing installation has been described.

From the load profile estimation, it resulted that the estimated daily electric energy consumption of the Center is 170 kWh, considering hot water to be produced with electrical water heaters; electrical water heaters are responsible of the consumption of 36,4 kWh each day. The most energivorous section of the building is the medical part (first floor) with 82 kWh out of 133kWh (if hot water is produced by the solar thermal plant). A three-phase system has been designed, composed by three battery inverters each rated 6 kW, two PV inverters one of 6 kW and one of 5 kW, 40 electrochemical storage units for a total capacity of 1925 Ah (C10). Through proper setting of the battery inverters and proper connection of the load disconnecting device it is possible to guarantee continuous power supply to the high-priority section of the building; a storage capacity of 21 kWh must be reserved to guarantee continuous supply to the high priority area. The annual energy yield of the PV plant is 17914 kWh; this energy supplies the 31% of the annual load. A layout for the battery bank has been proposed; the required ventilation air flow is 6,22 m^3/h. The investment cost of the system is 40500 €; the net present cost of the installation is 9884 €.

In Chapter 4, it has been discussed which is the most suitable system configuration to meet the thermal load of ISPEMA Center. The load profile for hot water consumption was then calculated. An estimation of the system's performance has been undertaken, considering several methodologies proposed in the literature. The installation was then optimized by maximization of the life cycle solar savings; a layout for the system has been suggested. It has been proposed to adopt a thermosyphon system configuration, to take advantage of its simple and economic installation. It has been estimated that the daily hot water requirements are of 1,7 m^3; by estimation of the performance of the system, it has been calculated that 16 $m^2$of collectors and a storage tank of 1 m^3 allows a solar fraction of 0,9. The estimated cost of the installation is of 3240 € for components only. The payback time is 6,13 years.

From the analysis carried on in Chapter 5, it resulted that the installation of a PAT in the water distribution network of the Campus could eventually represent a demonstrative installation, as the contribution to the energy supply of the Campus is neglectable. Nonetheless, the installation could offer valid didactical experiences.

6.1 FURTHER DEVELOPMENTS

Regarding the installations proposed in this work, several further verifications must be done before beginning executive design. It must be verified if ISPEMA Center's roof can sustain the extra load due to PV collectors; eventually, the structure of the roof has to be reinforced. When the electrical equipment of the Center will be installed, it is worth to verify the actual power and energy requirements of the Center by adoption of metering devices. For what concerns the solar thermal system for the dormitory, careful evaluation of the placement of the storage tanks on the soil of the floor must be done to distribute the weight on the highest number of structure-bearings elements.

ECUSTA's Campus offers many possibilities of renewable energies promotion that could not be developed in this study. As an instance, the Campus could become a test-field for a microgrid, to connect the power generating sources located in different areas; regarding the development of a microgrid within the Campus, it is suggested to contact the local branch of ABB, which could provide the necessary control equipment. A study could then be undertaken on the installation of solar-powered pumps, to operate the wells located in the southern side of the Campus.

7 REFERENCES

[1] W. E. Outlook, “Energy in Africa today,” pp. 1–20, 2014.

[2] P. G. Projects, “MINISTRY OF WATER , IRRIGATION AND,” 2015.

[3] T. Plan, I. I. Gtp, and A. Ababa, “Federal Democratic Republic of Ethiopia Volume I : Main Text,” vol. I, no. Gtp II, 2016.

[4] “ETHIOPIAN CATHOLIC UNIVERSITY OF ST . THOMAS AQUINAS,” no. October, 2011.

[5] V. Cararach, A. Kurjak, M. R. Carrapato, and F. Castella, “Program Life for Africa 1,” vol. 5, no. December, pp. 421–426, 2011.

[6] D. R. Tobergte and S. Curtis, “Solar heat worldwide,” *J. Chem. Inf. Model.*, vol. 53, no. 9, pp. 1689–1699, 2013.

[7] S. Kalogirou, “Thermal performance, economic and environmental life cycle analysis of thermosiphon solar water heaters,” *Sol. Energy*, vol. 83, no. 1, pp. 39–48, 2009.

[8] T. . Bokhoven, J. Van Dam, and P. Kratz, “Recent experience with large solar thermal systems in The Netherlands,” *Sol. Energy*, vol. 71, no. 5, pp. 347–352, 2001.

[9] R. Botpaev and K. Vajen, “Drainback Systems : Market Overview,” *Gleisd. Sol.*, pp. 84–92, 2014.

[10] R. Botpaev, J. Orozaliev, and K. Vajen, “Experimental investigation of the filling and draining processes of the drainback system (Part 1),” *Energy Procedia*, vol. 57, no. 561, pp. 2467–2476, 2014.

[11] AEE - Institute for Sustainable Technologies, “Thermal use of solar energy,” p. 121, 2009.

[12] S. A. Kalogirou, “Solar thermal collectors and applications,” *Progress in Energy and Combustion Science*, vol. 30, no. 3. pp. 231–295, 2004.

[13] S. Combisystems, “Stagnation behaviour of solar thermal systems,” no. November, 2002.

[14] S. Harrison and C. A. Cruickshank, “SHC 2012 A review of strategies for the control of high temperature stagnation in solar collectors and systems,” vol. 30, pp. 793–804, 2012.

[15] F. Mauthner and S. Fischer, “Overheating prevention and stagnation handling in solar process heat applications.,” *IEA SHC Task 49 Sol. Process heat Prod. Adv. Appl.*, p. 42, 2015.

[16] Z. Chen *et al.*, “(12) United States Patent,” vol. 2, no. 12, 2014.

[17] J. a. Duffie, W. a. Beckman, and W. M. Worek, *Solar Engineering of Thermal Processes, 4th ed.*, vol. 116. 2003.

[18] D. I. Acqua, C. Sanitaria, C. Tra, L. A. Normativa, and E. L. A. Pratica, “Ottimizzazione Di Sistemi Per La Generazione,” pp. 1–12.

[19] Y. M. Han, R. Z. Wang, and Y. J. Dai, “Thermal stratification within the water tank,” *Renew. Sustain. Energy Rev.*, vol. 13, no. 5, pp. 1014–1026, 2009.

[20] Berkeley; and E. F. King, “This is a reproduction of a library book that was digitized by Google

as part of an ongoing effort to preserve the information in books and make it universally accessible. http://books.google.com," *Oxford Univ.*, vol. XXX, p. 352, 1859.

[21] Y. M. Liu, K. M. Chung, K. C. Chang, and T. S. Lee, "Performance of thermosyphon solar water heaters in series," *Energies*, vol. 5, no. 9, pp. 3266–3278, 2012.

[22] D. I. Acqua *et al.*, "F-Chart Method for Designing Solar Thermal Water Heating Systems," *Sol. Energy*, vol. 83, no. 1, pp. 39–48, 2010.

[23] E. D. Tufte, "Impacts of Low Load Operation of Modern Four-Stroke Diesel Engines in Generator Configuration," no. June, p. 414, 2014.

[24] C. G. Sets, "Operation Residential / Commercial Generator Sets."

[25] "Inverter di rete ad isola SUNNY ISLAND 8.0H / 6.0H," pp. 1–156.

[26] "H + Line indice Guida pratica."

[27] R. Iea-pvps, *PV Systems for Rural Health Facilities in Developing Areas PHOTOVOLTAIC POWER SYSTEMS PROGRAMME PV Systems for Rural Health Facilities in Developing Areas*. 2014.

[28] SMA Solar Technology AG, "Designing PV Plants Optimised for Economic Efficiency," p. 12, 2013.

[29] S. M. A. Solar and T. Ag, "Planning Guidelines Design of Off-Grid Systems Table of Contents."

[30] B. S. En, "Safety requirements for secondary batteries and battery installations," 2001.

[31] M. Report, C. Public, U. Commission, and E. Division, "CALMAC Study ID CPU0052 Main Report Embedded Energy in Water Studies Study 3 : End-use Water Demand Profiles Prepared by Prepared for the California Public Utilities Commission Energy Division Managed by California Institute for Energy and Environment," *Main*, vol. 1, 2011.

[32] V. Belessiotis and E. Mathioulakis, "Analytical approach of thermosyphon solar domestic hot water system performance," *Sol. Energy*, vol. 72, no. 4, pp. 307–315, 2002.

[33] B. Norton, P. C. Eames, and S. N. G. Lo, "Alternative approaches to thermosyphon solar-energy water heater performance analysis and characterisation," *Renew. Sustain. energy Rev.*, vol. 5, no. 1, pp. 79–96, 2001.

[34] A. Hasan, "THERMOSYPHON SOLAR WATER HEATERS : EFFECT OF STORAGE TANK VOLUME AND CONFIGURATION ON EFFICIENCY," vol. 38, no. 9, pp. 847–854, 1997.

[35] D. Carbonell, J. Cadafalch, and R. Consul, "Dynamic modelling of flat plate solar collectors: Analysis and validation under thermosyphon conditions," *Sol. Energy*, vol. 89, pp. 100–112, 2013.

[36] H. Ramos, D. Covas, L. Araujo, and M. Mello, "Available energy assessment in water supply systems," *XXXI IAHR Congr. Seoul, …*, pp. 1050–1060, 2005.

[37] T. Agarwal, "Review of pump as turbine (PAT) for micro-hydropower," *Int. J. Emerg. Technol. Adv. Eng.*, vol. 2, no. 11, pp. 163–169, 2012.

[38] D. R. Giosio, A. D. Henderson, J. M. Walker, P. A. Brandner, J. E. Sargison, and P. Gautam, "Design and performance evaluation of a pump-as-turbine micro-hydro test facility with incorporated inlet flow control," *Renew. Energy*, vol. 78, pp. 1–6, 2015.

[39] “Q&Aturbine6.pdf.” .

[40] International Energy Agency, “Africa Energy Outlook. A focus on the energy prospects in sub-Saharan Africa,” *World Energy Outlook Spec. Report, Int. Energy Agency Publ.*, pp. 1–237, 2014.

8 APPENDIX

8.1 PAYBACK TIMES FOR SOLAR THERMAL INSTALLATIONS IN ADDIS AREA

The typical household appliances for urban areas in sub-Saharan Africa consist of television, refrigerator and mobile phones and, in a minor share, electrical water heaters. It must be considered that electrical water heaters are high energy-consuming devices: the energy of 1,5 kWh is required to heat water for a single shower, almost equivalent to the functioning of a refrigerator for a whole day[9].

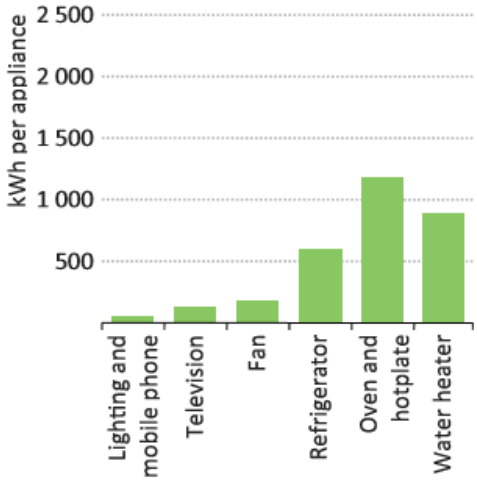

Figure 66 *Indicative electricity consumption levels by appliance per household in sub-Saharan Africa, urban areas. From* [40]

Usage of electricity for water heating in sunny regions is senseless, especially where power outages are due to insufficient production for meeting the load. A convenient alternative is to adopt solar water heaters, exploiting the high level of available solar energy (average 5,5 $kWh/day \cdot \mathrm{m}^2$ for Ethiopia). This fact is considered in several country's energy policies[40]: as instances, Kenya requires the installation of solar water heaters for buildings served by the grid; Mozambique has the target to install 100000 solar water heaters by 2025.

This section analyzes the convenience of installing a solar water heater in Addis Area, considering the local prices of solar equipment, and the local price of electricity

8.1.1 Economic analysis

This analysis is done considering a commercial system which is suitable for supplying hot water to a household of 5 people, where hot water can be used for sanitary purposes and for water pre-heating for cooking. The system is the UltraSun 150L Direct, commercialized by Davis&Shirtliff and sold in Ethiopia and Kenya for the equivalent of 720 €. The system is composed of a flat plate collector whose aperture area is nearly 2 m^2 and a storage tank

[9] Electrical water heater: $\eta_{boil} = 0{,}85$; 50 liters; $t_{shower} = 39°C$; $t_{cold} = 17°C$. Refrigerator: based on power consumption of 500kWh/year

of 150 liters, closed-coupled with the collector. The system is of direct type; a 2kW electric heater is integrated in the storage, which presents also a sacrificial anode to protect against corrosion.

The useful heat output from the system is calculated as per the proceeding outlined in section 4.3. Considering an average solar radiation on a year of 6047 $Wh/day \cdot m^2$ for an optimally-tilted surface (14° towards south), the average heat output from the system is of 7185 Wh/day (corresponding efficiency $\eta = \frac{Q_U}{Q_{IRR}}$ = 0,59 consistent with typical values of thermosyphon units from the literature).

From the financial point of view, the convenience of installing a solar water heater is obtained when the cumulative fuel savings during the lifetime of the solar water heater exceeds the initial investment.

Payback times can be defined in different ways; the most common way to define payback time is *the time needed for the cumulative fuel savings to equal the total initial investment, that is, how long it takes to get an investment back by savings in fuel* [17].

Payback times have been calculated for different percentages of solar fraction, which are related to the consumption habits of the household. Three different scenarios are presented: first, the actual price of electricity for end-users in Ethiopia (residential tariff); a scenario that considers what would happen if electricity were sold at the cost of production; a scenario that considers typical European tariffs.

It can be seen from the graph below that return on investment is hardly obtained with the actual price of electricity: considering 10 year of useful life of the plant, as it is suggested in [6], return on investment is obtained only if the solar fraction of the load is greater than 0,9.

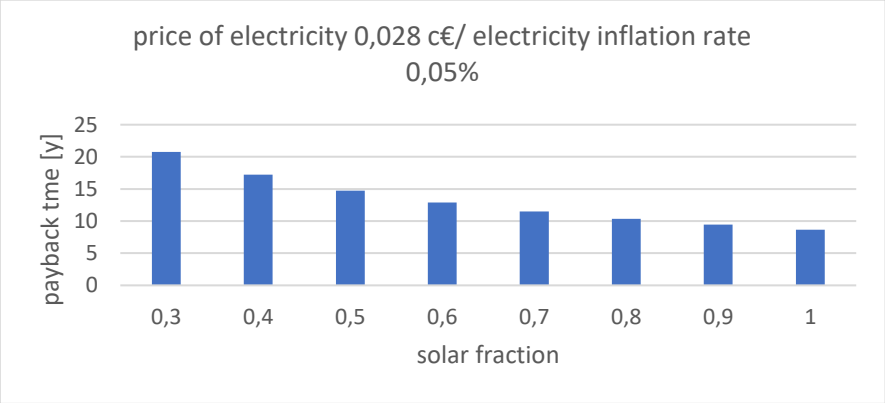

On the contrary if electricity were sold at the price of production, thus without subsidizing it, payback time would be much shorter: with a modest solar fraction of 0,3, ROI would already be within the useful life of the plant.

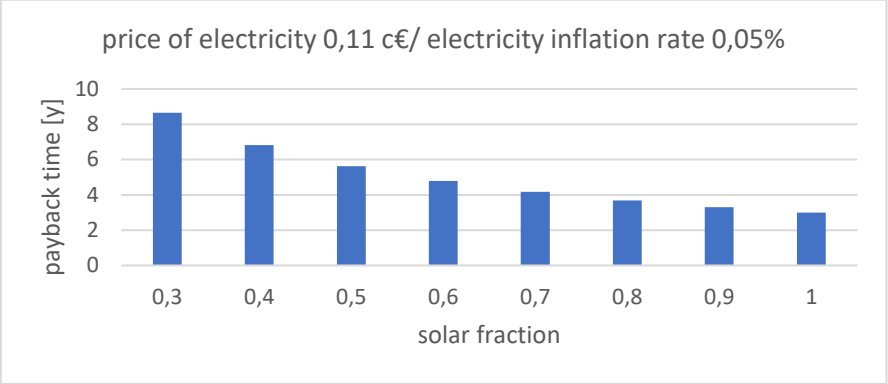

Finally, if electricity were sold at a typical European tariff, then the high levels of solar radiation typical of sub-Saharan regions would allow a return on investment shorter than 3 years for solar fractions higher than 0,4.

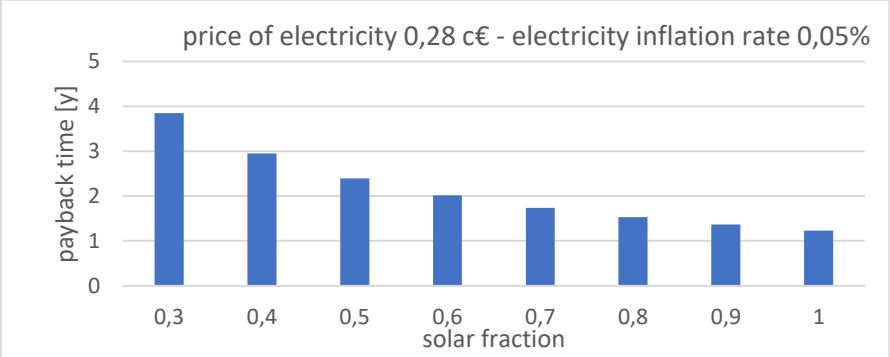

Optimum optimization of the system means reducing at minimum electricity consumption. This can be achieved by load shifting.

1. Size the system based on demand. In this way, no unnecessary investments are encountered.
2. Optimal utilization of the system: large amounts of hot water should be fetched exclusively in the evenings, when the system is charged; otherwise, auxiliary heater must provide further heating and this would result in a decreased solar fraction. Tapping little water during the day does not compromise the possibility to withdraw large amounts in the evening as the efficiency of the solar heater is higher after water withdrawn.

8.2 DESCRIPTION OF THE ANALYSIS TOOLS

8.2.1 Introduction to f-chart method

The f-chat design method has been extensively used for this work. This section is intended to introduce the reader to the method.

The f-chart method has been developed by Klein et al. (1976, 1977) and Beckman et al. (1977) for estimating the annual thermal performance of active heating systems for buildings. To develop this method, the results of hundreds of numerical simulations have been correlated by the authors in terms of dimensionless groups, X and Y, where these groups represents the following ratios:

$$X = \frac{collector\ energy\ losses\ during\ a\ month}{total\ heating\ load\ during\ a\ month}$$

$$Y = \frac{total\ energy\ absorbed\ by\ collector\ plate\ during\ a\ month}{total\ heating\ load\ during\ a\ month}$$

The correlation found by the authors between such groups gives f, which is the monthly fraction of loads carried by solar energy.

Groups X and Y are defined as follows:

$$X = \frac{A_c F_R' U_L \left(T_{ref} - \bar{T}_a\right) \Delta t}{L}$$

$$Y = \frac{A_c\ F_R'\ (\overline{\tau\alpha}) \bar{H}_T N}{L}$$

In the equations above,

A_c = collector's area $[m^2]$

F_R' = collector heat exchanger efficiency factor

U_L = collector overall loss coefficient $[W/m^2°C]$

T_{ref} = empirically derived reference temperature (100°C)

$\bar{T}_a$ = monthly average ambient temperature

Δt = total number of seconds in a month

L = monthly total heating load for space heating and hot water $[J]$

$(\overline{\tau\alpha})$ = monthly average transmittance-absorptance product

$\bar{H}_T$ = monthly average daily radiation incident on collector surface per unit area $[\ J/m^2]$

N = days in month

When considering a solar thermal system, whose purpose is only service water heating (space heating is excluded), group X must be modified as follows:

$$\frac{X_C}{X} = \frac{11.6 * 1.18\ T_W + 3.86\ T_M - 2.32\ \bar{T}_a}{100 - \bar{T}_a}$$

As f-chart method has been created considering a standard storage capacity of 75 liters of stored water per square meter of collector area, another modification occurs when considering a different ratio. X group must be modified as per:

$$\frac{X_C}{X} = \left(\frac{actual\ storage\ capacity}{standard\ storage\ capacity}\right)^{-0.25}$$

The relationship between X, Y and f in the equation form is

$$f = 1.029Y - 0.065X - 0.245Y^2 + 0.0018X^2 + 0.0215Y^3$$

An alternative expression of groups X, Y that allows to calculate them in a simpler way considering the values obtained from testing the collectors and generally provided by constructors is the following:

$$X = F_R U_L * \frac{F'_R}{F_R} * \left(T_{ref} - \bar{T}_a\right) * \Delta t * \frac{A_c}{L}$$

$$Y = F_R(\tau\alpha)_n * \frac{F'_R}{F_R} * \frac{(\overline{\tau\alpha})}{(\tau\alpha)_n} * \bar{H}_T N * \frac{A_c}{L}$$

Constraints

Ranges of design parameters used in developing f-charts for liquid systems are the followings:

$0{,}6 \leq (\tau\alpha)_n \leq 0{,}9$

$5 \leq F'_R A_c \leq 120\ m^2$

$2{,}1 \leq U_L \leq 8.3 \frac{W}{m^{2\circ}C}$

$30 \leq \beta \leq 90°$

$83 \leq (UA)_h \leq 667 \frac{W}{^\circ C}$

$0.5 \leq \left(\frac{actual\ storage\ capacity}{standard\ storage\ capacity}\right) \leq 4$

8.2.1.1 Proceeding for converting values of η_0, a_1, a_2 to $F_R(\tau\alpha), F_R U_L$

Collectors' efficiency can be expressed as a function of ΔT_m in different ways, considering collectors' efficiency having either a linear or quadratic dependence on ΔT_m.

As the f-chart method uses the first equation found below, while information found in collectors' datasheet is expressed as per the second equation, it is necessary to convert one form to the other to use datasheet information in f-chart design.

$$\eta_i = F'(\tau\alpha)_n - F'U_L \frac{\Delta T_m}{G_T}$$

$$\eta_i = \eta_0 - a_1 \frac{\Delta T_m}{G_T} - a_2 \frac{\Delta T_m^2}{G_T}$$

Sudden conversion has been done as per the proceeding described below:

1. If values are relative to aperture area, calculate those values based on gross area by multiplying the given values by the ratio of aperture to gross area;
2. Choice of two values of $\frac{\Delta T}{G}$ where the curves of linear and second order fit intersect (0,05 and 0,012 are a reasonable choice citdb) and a value of incident radiation ($G = 1000\ W/m^2$ considering the high irradiance of the latitude);

3. Resolution of the two equations – two variables system:
4.

$$\begin{cases} F'(\tau\alpha)_n - F'U_L\left(\frac{\Delta T}{G}\right)_1 = \eta_0 \; - \mathrm{a}_{1\mathrm{g}}\left(\frac{\Delta T}{G}\right)_1 - \mathrm{a}_{2\mathrm{g}}\,\mathrm{G}\,\left(\frac{\Delta T}{G}\right)^2_1 \\ F'(\tau\alpha)_n - F'U_L\left(\frac{\Delta T}{G}\right)_2 = \eta_0 - \mathrm{a}_{1\mathrm{g}}\left(\frac{\Delta T}{G}\right)_2 - \mathrm{a}_{2\mathrm{g}}\,\mathrm{G}\,\left(\frac{\Delta T}{G}\right)^2_2 \end{cases}$$

to find $F'(\tau\alpha)_n$ and $F'U_L$;

5. It is then possible to obtain the desired $F_R(\tau\alpha)_n$ and $F_R U_L$ with the formulas below [17] :

$$F_R(\tau\alpha)_n = F'(\tau\alpha)_n\left(1 + \frac{A_c F'U_L}{2\dot{m}C_p}\right)^{-1}$$

$$F_R U_L = F'U_L\left(1 + \frac{A_c F'U_L}{2\dot{m}C_p}\right)^{-1}$$

8.2.2 Introduction to P_1P_2 method

P_1P_2 method have been used in this work to obtain the life-cycle solar savings for the renewable energy installations. This method has been developed by Brandemuehl and Beckman (1979); it allows the calculation of life-cycle solar savings in a simple form, expressing them as per the equation below:

$$LCS = P_1 C_{F1} F - P_2(C_A A_C + C_E)$$

Where

- P_1 is the ratio of the life-cycle fuel cost savings to the first-year fuel cost savings
- C_{F1} is the fuel cost (€/MWh)
- L is the total thermal load for a year (MWh)
- F is the solar fraction
- P_2 is the ratio of the life-cycle expenditures incurred because of the additional capital investment to the initial investment
- C_A are the total area-dependent costs (€/m^2)
- A_C collector area (m^2)
- C_E is the total cost of equipment which is independent of collector area (€)

Coefficients P_1 and P_2 are expressed as

$$P_1 = (1 - C_t)\; PWF\;(N_e, i_F, d)$$

$$P_2 = P_2^1 + P_2^2 + P_2^3 + P_2^4 + P_2^5 + P_2^6 + P_2^7$$

Where

$P_2^1 = D$ down payment;

$P_2^2 = (1 - D) * \frac{PWF(N_{min},0,d)}{PWF(N_L,0,m)}$ life cycle-cost of the mortgage principal and interest;

$P_2^3 = -t\,(1-D)[PWF\,(N_{min}, m, d)\left(m - \frac{1}{PWF(N_L,0,m)}\right)$	income tax deductions of the interest;
$P_2^4 = M_S(1-Ct\,)PWF(N_e, i, d)$	miscellaneous costs: insurance and maintenance;
$P_2^5 = tV(1-t)PWF(N_e, i, d)$	net property tax costs;
$P_2^6 = -\frac{Ct}{N_D}\,PWF(N'_{min}, 0, d)$	straight line depreciation tax deduction;
$P_2^7 = -\frac{R_v}{(1+d)^{N_e}}(1-Ct)$	present worth of resale value at the end of the period of the economic analysis.

Present-Worth Factor

N is the number of periods taken into consideration, *i* is the inflation rate per period, *d* is the discount rate. Multiplying the first of a series of N payments that are made at the end of the periods, we obtain the sum of N payments discounted to the present with a discount rate d.

```
Function PWF(N As Integer, i As Single, d As Single)

Dim value As Single

If d = i Then

value = N / (i + 1)

Else: value = (1 / (d - i)) * (1 - (((1 + i) / (1 + d)) ^ N))

End If

PWF = value

End Function
```

Figure 67 *Simple VBA code implementing a function to calculate Present Worth Factors*

8.3 MEASUREMENTS OF WIND SPEED VELOCITY IN THE CAMPUS

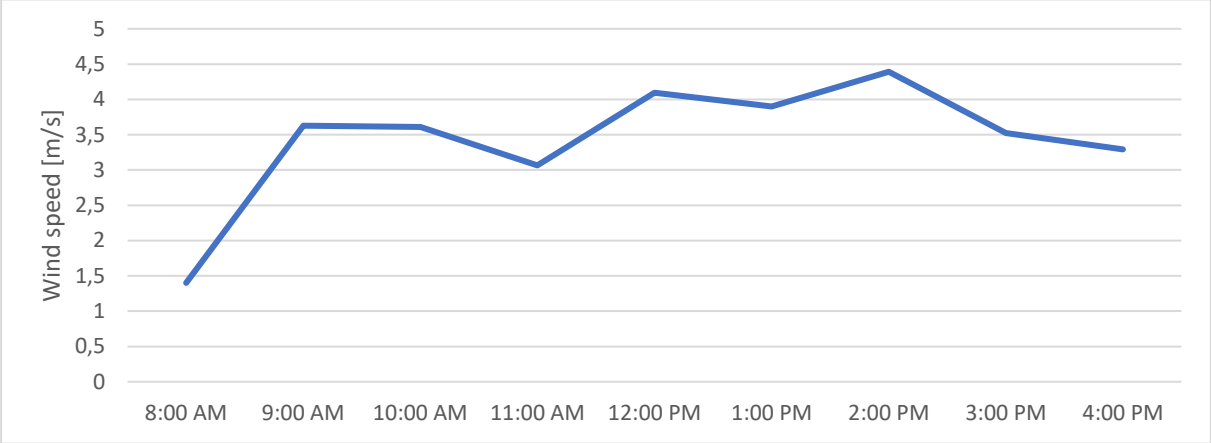

Figure 68 *Average wind speed data in the site of the campus*

Figure 67 reports the average hourly speed registered in the site of the campus from November 2016 to March 2017.

8.4 SOLAR MAP OF ETHIOPIA

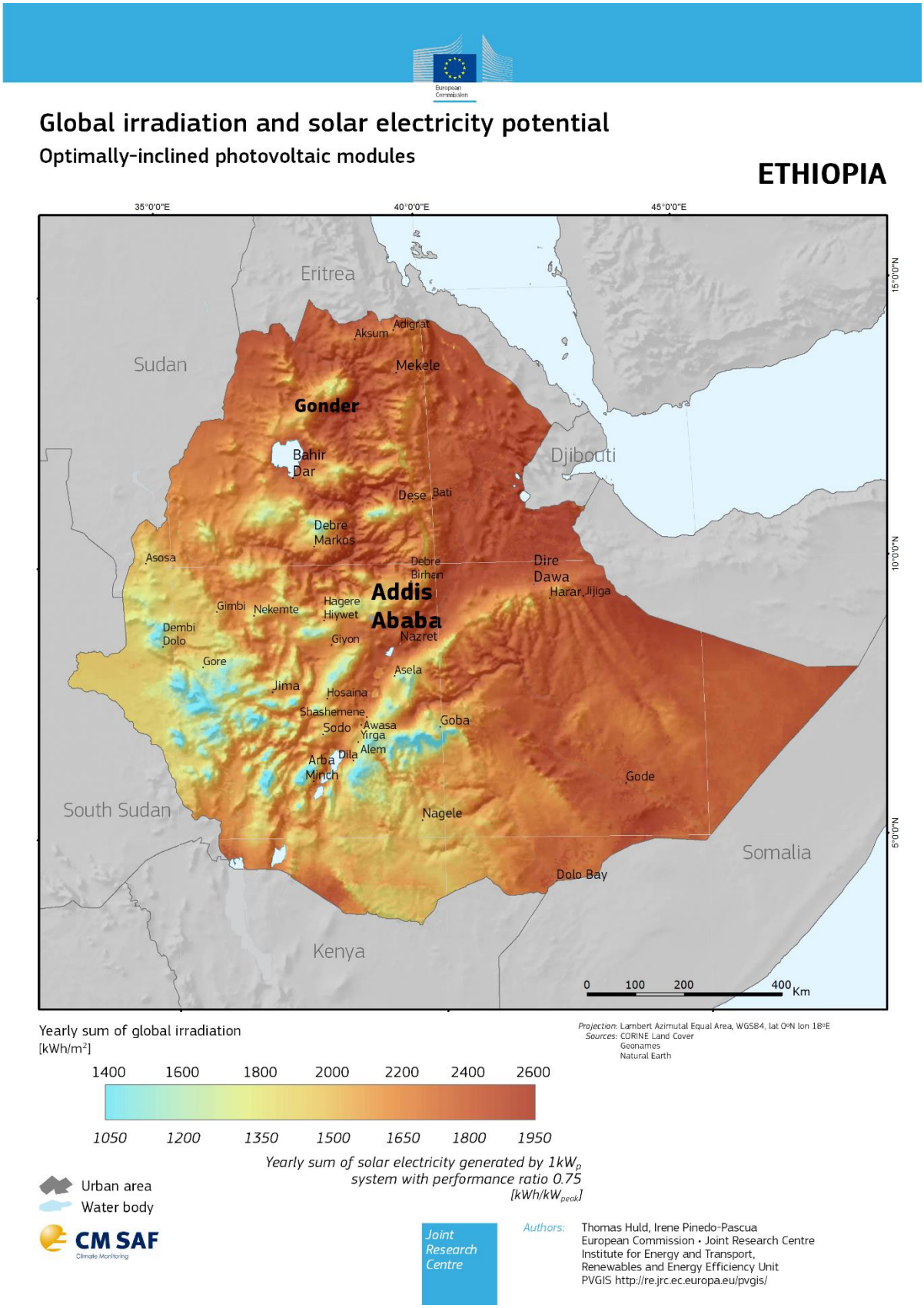

8.5 DATASHEETS OF THE COMPONENTS

8.5.1 Generator

ENGINE SPECIFICATIONS

STANDARD FEATURES	Manufacturer / Model	JOHN DEERE 6068HF120-153 , 4-strokes, Turbo , Air/Air DC 6 X
	Cylinder Arrangement	L
	Displacement	6.72L [410.1C.I.]
	Bore and Stroke	106mm [4.2in.] X 127mm [5.0in.]
	Compression ratio	17 : 1
	Rated RPM	1500 Rpm
	Piston Speed	6.35m/s [20.8ft./s]
	Max. stand by Power at rated RPM	150kW [201BHP]
	Frequency regulation, steady state	+/- 2.5%
	BMEP	16.3bar [236psi]
	Governor : type	MECA
EXHAUST SYSTEM	Exhaust temperature	555°C [1031°F]
	Exhaust gas flow	385L/s [816cfm]
	Max back pressure	750mm CE [30in. WG]
FUEL SYSTEM	110% (Stand By power)	36.5L/h [9.6gal/hr]
	100% (of the Prime Power)	33.5L/h [8.9gal/hr]
	75% (of the Prime Power)	25L/h [6.6gal/hr]
	50% (of the Prime Power)	17L/h [4.5gal/hr]
	Max. fuel pump flow	108L/h [28.5gal/hr]
OIL SYSTEM	Total oil capacity w/filters	21.5L [5.7gal]
	Oil Pressure low idle	1bar [14.5psi]
	Oil Pressure rated RPM	5bar [72.5psi]
	Oil consumption 100% load	0.037L/h [0.010gal/hr]
	Oil capacity carter	20.6L [5.4gal]
THERMAL BALANCE	Heat rejection to exhaust	99kW [5629Btu/mn]
	Radiated heat to ambiant	16kW [910Btu/mn]
	Heat rejection to coolant	55kW [3127Btu/mn]
AIR INTAKE	Max. intake restriction	625mm CE [25in. WG]
	Engine air flow	170L/s [360cfm]
COOLANT SYSTEM	Radiator & engine capacity	25.8L [6.8gal]
	Max water temperature	105°C [221°F]
	Outlet water temperature	93°C [199°F]
	Fan power	3 kW
	Fan air flow w/o restriction	4.44m3/s [9409cfm]
	Available restriction on air flow	20mm CE [0.8in. WG]
	Type of coolant	Gencool
	Thermostat	82-94 °C
EMISSIONS LEVEL	PM	80 mg/Nm3
	CO	150 mg/Nm3
	Nox	2800 mg/Nm3
	HC	35 mg/Nm3

ALTERNATOR SPECIFICATIONS

GENERAL DATAS	Manufacturer	LEROY SOMER
	Type	LSA442M95
	Number of phase	3
	Power factor (Cos Phi)	0.8
	Altitude	< 1000 m
	Overspeed	2250 rpm
	Pole : number	4
	Exciter type	SHUNT
	Insulation : class, temperature rise	H / H
	Voltage regulator	R230
	Total harmonics (TGH/THC)	< 2%
	Wave form : NEMA = TIF – TGH/THC	< 50
	Wave form : CEI = FHT – TGH/THC	< 2%
	Bearing : number	1
	Coupling	Direct
	Voltage regulation 0 to 100% load	+/- 0.5%
	Recovery time (20% Volt dip) ms	500 ms
	SkVA with 90% of nominal sustained voltage (at 0.4PF)	N/A
OTHER DATAS	Continuous nominal rating @ 40°C	150 kVA
	Standby rating @ 27°C	165 kVA
	Efficiencies @ 4/4 load	92.2 %
	Air flow	0.37m3/s [783.98cfm]
	Short circuit ratio;50 (Kcc)	0.42
	Direct axis synchro reactance unsaturated (Xd)	317 %
	Quadra axis synchro reactance unsaturated (Xq)	190 %
	Open circuit time constant;50 (T'do)	2865 ms
	Direct axis transient reactance saturated (X'd)	11 %
	Short circuit transient time constant (T'd)	100 ms
	Direct axis subtransient reactance saturated (X"d)	6.6 %
	Subtransient time constant (T"d)	10 ms
	Quadra axis subtransient reactance saturated (X"q)	7.8 %
	Zero sequence reactance unsaturated (Xo)	0.1 %
	Negative sequence reactance saturated (X2)	7.3 %
	Armature time constant (Ta)	15 ms
	No load excitation current (io)	0.6 A
	Full load excitation current (ic)	2 A
	Full load excitation voltage (uc)	36 V
	Recovery time (Delta U = 20% transitoire)	500 ms
	Motor start (Delta = 20% perm. Or 50% trans.)	284.2 kVA
	Transient dip (4/4 charge) – PF : 1.8 AR	14.7 %
	No load losses	2.62kW [2.62Kw]
	Heat rejection	10.15 kW

9 ACKNOWLEDGEMENTS

I would like to express my gratitude to all the staff of ECUSTA for their smiles and welcoming ways. I would have loved to stay longer to have known you better. A big thank you to Prof. Getachew Bekele for having spent part of his time to help me in this project, and for having introduced me to his culture. It has been a great pleasure to spend time with you.

Grazie al Prof. Lorenzoni ed al Prof. Sonato per la loro disponibilità. Grazie a Walter, lavorare con te è stata un'esperienza, e grazie per le chiacchierate alla sera. Un grazie ad Henos per il tempo passato assieme in Addis.

I più sentiti ringraziamente a mia madre. Agli amici tutti, soprattutto alle Rocce, a cui non devo una cena di pesce. A Francesca.

Fornac, sei un grande.